Master's Degree Thesis

Master's Degree course in INGEGNERIA MECCANICA (MECHANICAL ENGINEERING)

Techno-economic optimization of the RES portfolio for the electrification of transportation in remote communities: integrated energy system modeling.

Supervisor:

Dr. Fabio Carapellese

Co-supervisors:

Dr. Edoardo Pasta

Prof. Pedro Cabrera

Dr. Filippo Giorcelli

Viola De Clerck

Candidate:

Tommaso Terzaghi

Student ID: 332077

A.Y. 2025-2026

Abstract

The diffusion of electric vehicles (EVs) increases electricity demand and makes charging management increasingly relevant, especially in isolated networks where energy costs, renewables integration, and system flexibility are critical. In such contexts, transport electrification and renewable energy penetration should be assessed jointly to support more effective energy system configurations.

This thesis investigates the case of the island of La Gomera, by linking smart charging with island-scale energy system simulations through the integration of optimized charging profiles. The research examines whether smart charging can reduce the additional energy costs of EV demand and how its effects propagate when the resulting charging profiles are integrated into the island's energy system analysis.

A MATLAB-based model was developed to allocate charging power among vehicles under limited station capacity, charging constraints, and time-varying electricity prices. The optimized strategy was compared with a First-In-First-Served (FIFS) baseline in order to evaluate its effect on charging costs and demand distribution. The model was then extended to annual simulations calibrated to the La Gomera case, generating hourly EV charging profiles consistent with the island's mobility demand assumptions.

The profiles were subsequently integrated into EnergyPlan through the MATLAB Toolbox for EnergyPlan to analyze the interaction between electric-vehicle penetration and renewable-system design. A multi-objective framework was used to explore the trade-off between a demand-production mismatch indicator and CO2 emissions under different renewable mixes and EV penetration levels.

The results indicate that a higher presence of electric vehicles generally improves the best achievable system performance and is associated with the lowest CO2 levels, while intermediate and lower penetration levels, when combined with optimal charg-

ing schedules, can still provide competitive low-mismatch solutions and charging-cost savings.

The main contribution of this study is the development of a methodological bridge between detailed EV smart charging modeling and island-scale energy system planning, thus providing a structured, extendable, and replicable framework for the analysis of transport electrification in isolated contexts.

Acknowledgements

I would like to express my sincere gratitude to Dr. Edoardo Pasta, who originally supervised this thesis, for his continuous support and for his trust in my ability to take on this project.

My deepest gratitude goes to Dr. Filippo Giorcelli, co-supervisor, for his constant guidance and invaluable assistance. His contribution extended far beyond the academic dimension, offering steady and essential support in managing the challenges I faced before, during, and after my stay abroad. His continuous encouragement, thoughtful advice, and meticulous attention have been fundamental to my personal and scientific development.

I am also profoundly grateful to Prof. Pedro J. Cabrera Santana for his guidance, collaboration, and immense support during my research period in Spain. From the very beginning, he wholeheartedly welcomed me into his research group, consistently showing a genuine interest in the project and a strong commitment to finding solutions together. His ever-supportive attitude, along with that of the entire research team in Las Palmas, was crucial to the successful completion of this work. Within the group, a special mention goes to Dr. Carlos Matos Sánchez for his warm companionship in the office and his indispensable logistical help, which allowed me to seamlessly continue my work remotely from Italy.

I would also like to thank Dr. Fabio Carapellese, the official supervisor of this thesis, for his willingness to step in and for his support in concluding this project.

My sincere appreciation goes to Viola De Clerck for her valuable guidance and help, especially throughout the final drafting stages of this work.

A special thanks goes to Luca Ambrosino for his remarkable availability and for kindly sharing and explaining a portion of the original code from his research. His insights were incredibly helpful during the early stages of developing the optimization model.

Finally, I wish to thank Politecnico di Torino for providing an engaging academic environment and the financial support that made my research abroad possible. I am equally grateful to the Universidad de Las Palmas de Gran Canaria (ULPGC) for offering me the opportunity to work in a highly stimulating and international research context.

Table of Contents

List of Figures

List of Tables

List of Symbols

Symbols

$A(t,i)$: Availability matrix, equal to 1 if vehicle i is present at time step t, and 0 otherwise.
C_t [kW]: Total charging capacity available at time step t.
e_i [kWh]: Unmet energy demand associated with vehicle i.
$E(t)$ [kWh]: Total energy delivered during time step t.
$E_{\mathrm{EV,ann}}$ [GWh/y]: Annual electricity demand associated with electric vehicles.
L_i [kWh]: Energy demand associated with vehicle i.
$\bar{L}$ [kWh]: Maximum theoretical energy deliverable during the vehicle stay.
N: Number of vehicles.
n_{ports}: Equivalent number of charging ports.
$\bar{p}$ [kW]: Maximum charging power assignable to a single vehicle.
s: Electric vehicle penetration share.
T: Number of time steps in the optimization horizon.
$Y(t,i)$ [kW]: Charging power assigned to vehicle i at time step t.
a_i: Arrival time step of vehicle i.
d_i: Departure time step of vehicle i.
Δ [h]: Duration of the time step.
γ [EUR/kWh]: Penalty coefficient for unmet energy demand.
η_{BESS}: Battery-related performance indicator used in preliminary formulations.
ϕ [MWh]: Root Mean Squared Error mismatch indicator used in the EnergyPLAN multi-objective analysis.
π_t [EUR/MWh]: Electricity price at time step t.

Abbreviations

AC: Alternating Current.

BESS: Battery Energy Storage System.

CVX: Convex optimization package used in MATLAB.

EV: Electric Vehicle.

FIFS: First-In-First-Served.

GA: Genetic Algorithm.

LP: Linear Programming.

NSGA-II: Non-dominated Sorting Genetic Algorithm (II).

OWT: Offshore Wind Turbine.

PV: Photovoltaic.

RES: Renewable Energy Sources.

RMSE: Root Mean Squared Error.

UTC: Coordinated Universal Time.

V2G: Vehicle-To-Grid.

WT: Wind Turbine.

Chapter 1

Introduction

The energy transition in remote communities poses challenges that are difficult to address from a single sectoral perspective [4, 17]. In such contexts, electricity generation, end-use demand, the role of conventional fuels, and the electrification of transportation are closely intertwined [3, 16]. The introduction of electric vehicles (EVs) represents not only a change in the mobility sector, but also alters the shape of electricity demand, the way renewable generation is absorbed by the system, and, more generally, the operating conditions of the entire local energy system [21].

This aspect becomes particularly relevant in the case of non-interconnected or weakly-interconnected communities, such as insular systems, where the small scale of the system, dependence on imported fuels, and limited structural flexibility highlight both the critical issues and the opportunities of the transition [18, 16]. In an isolated system, the adoption of electric vehicles can help reduce fossil fuel consumption in the transport sector, but at the same time introduces a new component of electricity demand that, if managed rigidly, risks exacerbating the challenges of balancing generation and consumption [22, 26]. Conversely, if this demand is treated as a flexible load, it can become a useful tool for improving the integration of renewable energy sources [1, 19].

This thesis fits within this framework and analyzes the role of smart charging of electric vehicles in the case study of the island of La Gomera, in the Canary Islands. The underlying premise of this work is that the impact of electric vehicles cannot be assessed simply in terms of the additional annual required, but must also be studied by considering the temporal distribution of charging and its consequences for the island's energy system. For this reason, the thesis links two distinct yet complementary levels of analysis: a modeling level of the energy demand, developed in MATLAB, and a simulation level of the energy system, developed in EnergyPLAN.

Therefore, the work is not limited to describing a charging optimization model or presenting a set of independent energy simulations. The methodological contribution of the thesis lies primarily in the link between these two levels. On the one hand, a smart charging model is developed capable of generating annual hourly charging profiles consistent with capacity constraints, vehicle availability, and real-time electricity prices. On the other hand, these profiles are fed into an energy system model of La Gomera to assess their impact in combination with different levels of electric vehicle penetration and various renewable energy system configurations and allocated capacities.

1.1 Background and motivation

In recent years, the growth of electric mobility has made it increasingly clear that the spread of electric vehicles is not just a transport issue, but also an energy planning issue [3]. Electric vehicles are, in fact, changing the relationship between sectors that were traditionally analyzed separately. From a mobility perspective, they contribute to reducing the direct use of fossil fuels. From the perspective of the electric energy system, they introduce new demand that can be concentrated during certain hours or distributed more flexibly throughout the day. This implies that the ultimate impact of their adoption depends not only on how many vehicles are introduced, but also on how and when those vehicles are charged.

This observation is particularly important in island systems. In a large, interconnected continental system, the additional demand associated with electric vehicles can be partially absorbed through greater diversification of generation, grids, and markets. On an island, however, the smaller size of the system makes the link between each new electrical load and the available generation mix more evident [25]. This means that electric vehicle charging can either exacerbate or mitigate the challenges of integrating renewables, depending on how it is distributed over time.

In this sense, smart charging plays a role that goes beyond simply minimizing costs for the user or the charging station operator [6]. It can be seen as a tool for coordinating the mobility sector with the energy system. If EV demand is shifted to times when energy is less expensive or more abundant from renewable sources, it can help reduce relative dependence on conventional generation and improve the alignment between demand and production [23]. If, on the other hand, charging occurs in a rigid and uncoordinated manner, electric mobility risks amounting to a mere transfer of energy consumption from fuels to the electricity grid, without leveraging its potential for flexibility.

Another point of interest is that island systems are often used as natural laboratories for the energy transition [4, 14]. Their small scale makes the effects of planning decisions more immediate, and their heavy reliance on imported fuels increases the interest in greater self-sufficiency based on renewable sources. In this context, electric vehicles are not only an option for decarbonizing transportation, but also a possible way to adapt the electric grid to new renewable energy configurations.

In the case of La Gomera, these considerations take on even greater relevance in light of recent changes in the island's energy system. The presence of new renewable capacity and the growing interest in more advanced energy transition pathways make it particularly useful to conduct an assessment that integrates both the EV demand side and the system configuration side. This study therefore falls within a research framework in which charging flexibility is interpreted not as an operational detail, but as a variable that is potentially relevant for energy planning.

1.2 The case study of La Gomera

The choice of La Gomera as a case study is based on a number of scientific and methodological reasons. First, it is an island context where the small scale of the system makes it easy to see the connection between new electricity demand, the generation mix, and the residual use of fossil fuels. Second, La Gomera is part of the broader context of the Canary Islands (Figure 1.1), an archipelago where the energy transition is of particular importance for both structural and political-strategic reasons [10, 11].

Another important reason for interest is that La Gomera has already been the subject, in recent years, of studies analyzing its energy system and the potential for integrating renewables [4, 7, 8, 14, 15]. This allows us to situate the present work within an existing line of research, while also highlighting its unique aspects. In particular, compared to studies more focused on the general configuration of the

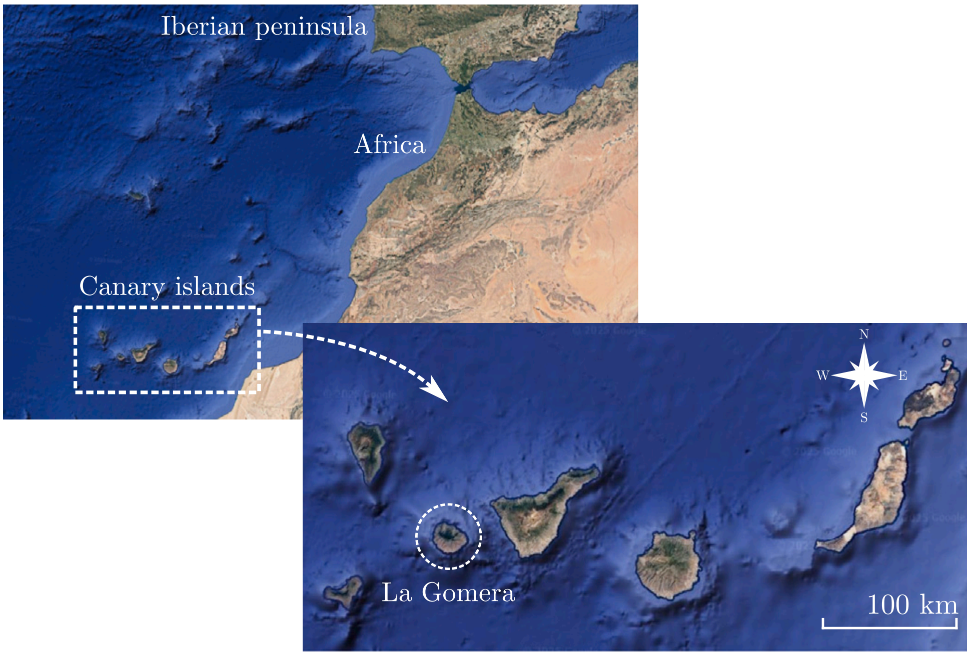

Figure 1.1: Geographical location of La Gomera island in the Canary Islands archipelago [14].

system, this thesis introduces a specific focus on the hourly pattern of EV demand and its connection to an externally developed charging model.

From a temporal perspective, this study focuses on the period from April 2023 to March 2024, consistent with the analytical framework already used in the system study to which this thesis is linked [14, 15]. This choice ensures consistency between the price data used in the smart charging model, the annual profiles imported into EnergyPLAN, and the island's energy context during the period under consideration.

La Gomera is therefore a suitable case study not only because it is an island, but also because it allows for a clear analysis of the thesis's central problem: to what extent the distribution of EV demand over time can influence the system-level energy assessment of an island context.

1.3 Research objectives and questions

The overall objective of this thesis is to evaluate the role of smart charging of electric vehicles within La Gomera's energy system, by combining a smart charging model developed in MATLAB with an annual simulation of the energy system run in EnergyPLAN (a deterministic, hourly-resolution energy system simulation tool [13, 14], which will be described in detail in Section 4.2).

Based on this overall objective, the work is divided into three specific objectives.

The first objective is to develop a charging model flexible enough to represent, in a concise yet consistent manner, the behavior of a fleet of electric vehicles subject to constraints on capacity, temporal availability, and hourly electricity prices. In this phase, the focus is on comparing a simple First-In-First-Served (FIFS) strategy with a price-optimized strategy based on linear programming (LP).

The second objective is to extend this model to an annual time horizon consistent with the La Gomera case, by introducing a calibrated EV demand, a seasonality component, and real hourly prices for Spain for the period April 2023–March 2024 [9]. The objective of this phase is not only to generate annual profiles but also to make these profiles usable in a subsequent system simulation.

The third objective is to integrate the annual profiles obtained into an EnergyPLAN model for La Gomera and analyze, through a multi-objective exploration, the trade-off between the mismatch between energy production and energy demand and CO_2 emissions, for different levels of EV penetration and different renewable capacity configurations.

These objectives give rise to the main research questions of this study:

- To what extent does a price-driven smart charging strategy reduce charging costs compared to a FIFS baseline?
- How does the integration of optimized EV charging profiles affect the energy system of an island, particularly concerning renewable energy integration, demand flexibility, and CO_2 emissions reduction?
- Which combinations of EV penetration and renewable capacity are most favorable in the trade-off between mismatch and emissions?

These questions reflect the multi-layered nature of the work. The thesis does not merely ask whether smart charging "works", but seeks to understand how it alters the systemic implications of electric vehicle adoption in isolated energy systems, specifically for the case of La Gomera.

1.4 Methodological overview

The method adopted in this thesis can be viewed as a sequence of steps across different levels of analysis, as conceptually summarized in Figure 1.2. In the first phase, the problem is addressed at the demand modeling level by constructing an EV charging model with discrete time granularity, capacity constraints, and a comparison of allocation strategies. In a second phase, this model is extended to an annual horizon and calibrated to the case study. In a third phase, the annual profiles thus obtained are integrated into La Gomera's EnergyPLAN model. In a fourth and final phase, the results are organized and interpreted in terms of model behavior and system-level energy-environmental trade-offs.

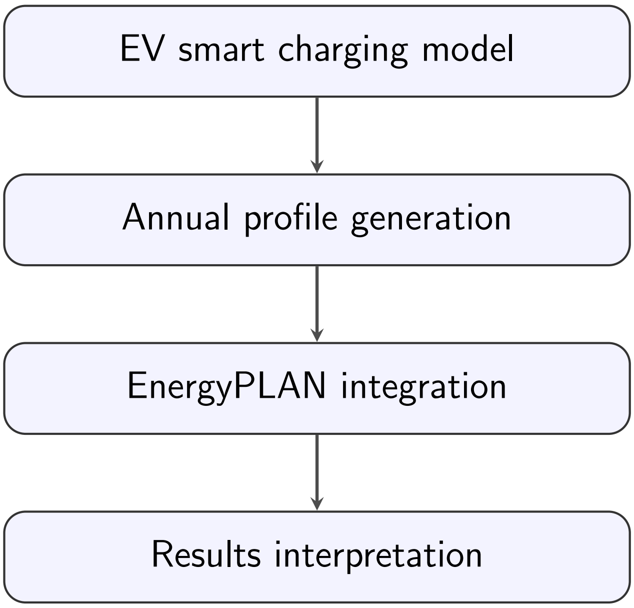

Figure 1.2: Conceptual map of the thesis methodology.

This methodological framework reflects a deliberate choice: to avoid both a purely micro-level analysis, focused solely on the charging scheduler, and a purely macro-level analysis, in which EV demand is introduced as an unmotivated exogenous profile. Instead, the study seeks to establish an explicit link between the local level of charging and the systemic level of energy planning.

An important aspect of the method is that the transition between the different levels is not automatic. Each phase required verification, calibration, and interpretation. In the charging model, for example, it was necessary to clarify the relationship between power and energy, properly handle time discretization, and reformulate certain constraints to avoid distorted results in the presence of zero or negative prices. In the transition to EnergyPLAN, it was necessary to build a workflow capable of transferring EV profiles into the energy system while maintaining consistency with the annual values of the transport sector. This focus on the workflow constitutes an important part of the overall methodological value of the work.

1.5 Structure of the thesis

The thesis is organized into six chapters, as illustrated in Figure 1.3.

Chapter 2 presents the literature review and situates the work within the main relevant research areas: the optimization of electric vehicle charging, studies on island energy systems, and work based on EnergyPLAN applied to similar contexts or directly related to La Gomera.

Chapter 3 describes the development of the charging model built in MATLAB. Specifically, it presents the logic of the daily model, a comparison between the FIFS baseline and linear optimization, the annual extension, the use of real-world prices, the seasonality of demand, and the infrastructure sizing study.

Chapter 4 illustrates the integration of the model into EnergyPLAN. It explains how the MATLAB-generated annual profiles are introduced into EnergyPLAN, the management of inputs and outputs, the implementation of EV penetration levels, and the construction of the multi-objective simulation and optimization environment.

Chapter 5 presents and interprets the final results of the system simulation. In particular, the chapter focuses on the Pareto fronts obtained using a genetic algorithm (GA), the comparison of different levels of electric vehicle penetration, and the composition of the renewable energy mix across the non-dominated solutions.

Chapter 6 concludes the thesis by discussing the most important results, the main limitations of the work, and possible future extensions.

Overall, the structure of the thesis reflects the logic of the entire project: starting with a local demand management problem, extending it to an annual scale, and finally linking it to a systemic assessment of the case of La Gomera.

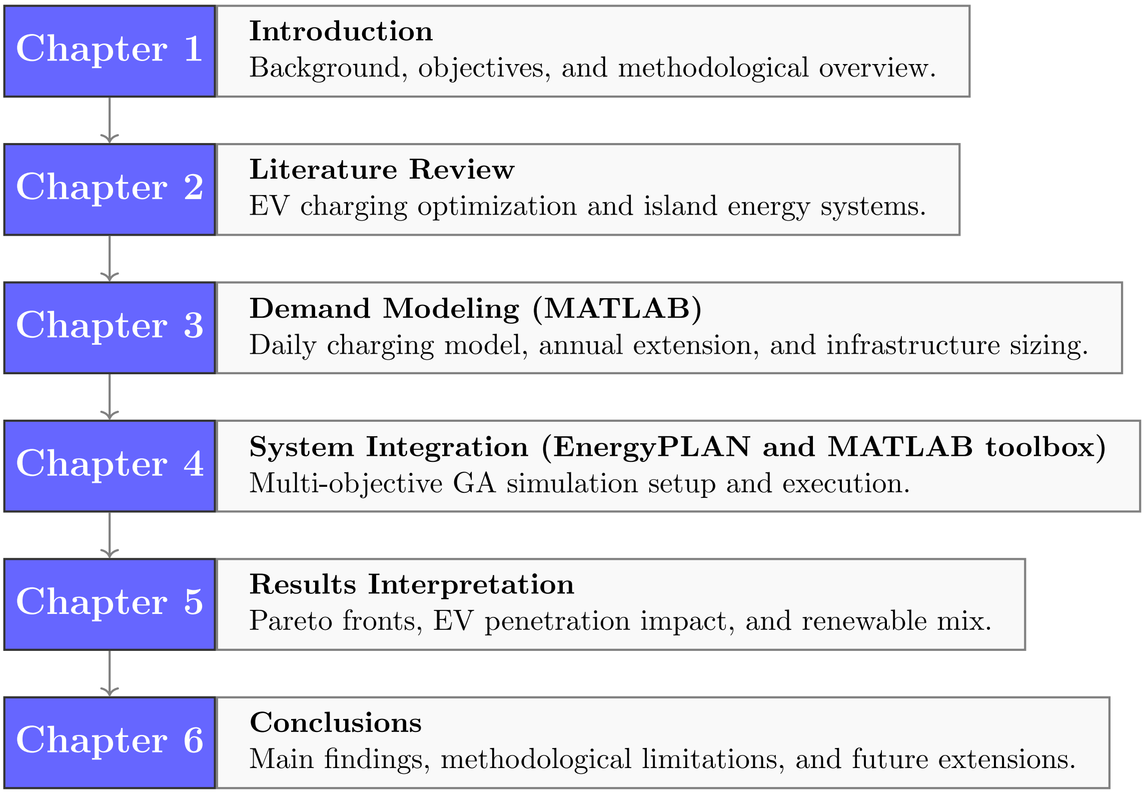

Figure 1.3: Overview of the thesis structure and chapter contents.

Chapter 2

Literature Review

This thesis lies at the intersection of at least three distinct lines of research. The first concerns the optimization of electric vehicle charging, with a particular focus on time-based demand management, capacity constraints, and a comparison between simple and optimized scheduling strategies. The second concerns energy system studies, especially those that use annual simulation tools to assess the role of electric vehicles within transition scenarios. The third strand more specifically includes work dedicated to island systems and, in particular, studies that have examined the case of La Gomera.

Since the work developed in this thesis links a smart charging model developed in MATLAB with an EnergyPLAN model of La Gomera's energy system, the literature review cannot be limited to a single disciplinary field. Instead, it is necessary to systematically summarize the main contributions of the three strands mentioned above, while highlighting which aspects have already been addressed in the literature and which remain less explored. From this perspective, the purpose of the review is not merely to summarize previous work, but to establish the context for the present study.

2.1 Electric vehicle charging optimization

One of the most extensively studied areas in recent literature concerns the intelligent management of electric vehicle charging. In this context, the focus is primarily on how charging demand can be distributed over time in the presence of technical constraints and price signals, in order to reduce charging costs, improve the utilization of available capacity, or avoid grid overloads [24].

For this thesis, a direct reference is the paper *Robust Power Scheduling for Smart Charging of Electric Vehicles* [1]. In that paper, the charging problem is addressed as a power allocation problem among connected vehicles, subject to capacity limits and electricity prices that vary over time. The value of this paper lies not only in its mathematical formulation but also in its conceptual framework: EV demand is treated as a flexible load, and the comparison with a FIFS strategy allows us to quantify the benefits of optimized charging management.

A second important reference is the paper *A Cohort-Based Optimization Model for Electric Vehicles Charging* [2]. This paper proposes a different formulation, in which vehicles are aggregated into cohorts rather than treated individually. From a methodological standpoint, the paper demonstrates how the charging optimization problem can be made more scalable through an aggregated representation. However, precisely because of this increased complexity and the different level of abstraction, this approach was not directly adopted in the present work, which instead opted to maintain a structure closer to the single-vehicle model, more transparent and easier to interpret.

Alongside these two works, the paper *Optimizing electric vehicles charging through smart energy allocation and cost-saving* [6] was particularly useful for its focus on comparing optimized power allocation with a FIFS benchmark. Again, the main point of interest for this thesis is not so much the formal details of the problem as the confirmation that the value of smart charging lies primarily in the temporal reallocation of demand while keeping the total energy required constant.

Taken together, these studies share a common approach. First, they treat EV charging as a scheduling problem. Second, they assign a central role to capacity constraints. Third, they show that the price signal can be used as a criterion for distributing charging in a more economically efficient manner. The model developed in Chapter 3 of this thesis falls precisely within this framework.

It should be emphasized, however, that these contributions focus primarily on the local or station level. They therefore provide a very useful basis for constructing a charging optimization model, but they do not directly address the subsequent problem, namely, the transfer of the obtained charging profiles to the level of energy system analysis.

While the core focus of the aforementioned literature remains on unidirectional scheduling, it is worth acknowledging broader related approaches. For example, Akbari-Dibavar et al. [5] explore hybrid charging stations integrated with local photovoltaic systems using two-stage robust management. Furthermore, when shifting towards bidirectional frameworks, Vehicle-to-Grid (V2G) technologies offer additional flexibility by allowing EVs to discharge power back to the grid, profoundly impacting sector-coupled systems [19]. However, these approaches address either self-sufficient micro-systems or advanced bidirectional hardware configurations. The present work instead occupies an intermediate position: it focuses on unidirectional smart charging but maintains a sufficient level of detail to generate plausible EV profiles designed specifically for subsequent macroscopic energy system analysis.

2.2 Island energy systems and EnergyPLAN-based studies

A second major line of literature relevant to this thesis concerns energy system studies, particularly those that analyze the integration of electric vehicles into island systems using annual simulation tools. In this context, EnergyPLAN plays an important role as a deterministic simulation tool with hourly resolution, capable of integrating the electricity, heating, and transport sectors.

An important reference is the paper *Smart energy system approach validated by electrical analysis for electric vehicle integration in islands* [3]. This work demonstrates that the integration of electric vehicles into island systems requires a "smart energy system" approach, that is, an assessment that considers electrical aspects, temporal profiles, and interactions among different sectors of the system. For the present work, the paper is important not only for its use of EnergyPLAN but also for its underlying message: electric mobility must be evaluated as part of a system and not simply as an additive demand.

A fundamental methodological reference for this work is the paper by Cabrera et al. on the *MATLAB Toolbox for EnergyPLAN* [13]. This paper describes a tool developed to manage EnergyPLAN directly from MATLAB, automatically modifying input files, running repeated simulations, and reading the results produced by the software within the same computing environment. The relevance of this paper lies in the methodological principle underlying the workflow: EnergyPLAN is used as the simulation engine, while MATLAB enables the automation of scenario exploration, parameter modification, file management, and post-processing of results.

This tool is directly relevant to the EnergyPLAN section of the thesis. The workflow developed in Chapter 4 uses MATLAB, and specifically the toolbox conceived by Cabrera et al., as an external control layer for the EnergyPLAN model, with the goal of transferring the EV profiles generated in Chapter 3 into the simulator, consistently modifying the transport sector parameters, and evaluating multiple system configurations. In this regard, the work by Cabrera et al. serves as the most direct technical and methodological reference for understanding the MATLAB–EnergyPLAN coupling logic adopted in this thesis.

Alongside Cabrera's contribution, the recent work by Giorcelli and co-authors represents a key reference for the EnergyPLAN model of La Gomera and for the interpretation of the system-level results [14]. In their work on energy co-design for the optimization of a Wave Energy Converter, Giorcelli et al. apply EnergyPLAN to the island system of La Gomera, coupling it with a multi-objective genetic algorithm and evaluating the resulting configurations in terms of CO_2 emissions and the mismatch between renewable generation and demand. This contribution is particularly significant because it demonstrates how an EnergyPLAN model of the island can be constructed, validated using real-world data, and used as a basis for exploring alternative renewable energy scenarios.

Although the technology analyzed by Giorcelli et al. differs from that addressed in this thesis, the methodological approach is very similar. In both cases, a technology or system component is incorporated into the island's energy model and evaluated not only for its isolated performance but also for its overall effect on the system. Their focus is on the integration of wave energy and the role of co-design between technology and the system, but the underlying system-level logic is directly relevant to the present work.

Another significant contribution is the work by Giorcelli, De Clerck, and Pasta on robust optimization applied to energy planning for La Gomera [15]. This study extends the EnergyPLAN model for the island by incorporating interannual variability in meteorological and oceanographic data and evaluating multi-technology renewable energy portfolios using an Non-dominated Sorting Genetic Algorithm (NSGA-II) framework in MATLAB. The paper is useful for the present work because it confirms three important methodological aspects: the centrality of La Gomera as a case study for non-interconnected island systems, the need to use consistent and validated time-series data, and the usefulness of system indicators for evaluating energy configurations.

Another interesting work is *Assessment of sustainable energy system configuration for a small Canary island in 2030* [4]. This study addresses the case of the Canary Islands and shows how the optimal configuration of an island system depends on a complex balance between renewable resources, storage, final demand, and system objectives. Although it does not focus on smart charging in the strict sense used in this thesis, the work is useful for understanding the systemic framework within which electric vehicles can be evaluated.

The paper *On the impact of probabilistic weather data on the economically optimal design of renewable energy systems – a case study of La Gomera island* [7] follows a similar line of inquiry. The value of this contribution is twofold. On the one hand, it confirms the relevance of La Gomera as a case study for energy modeling. On the other hand, it shows that planning results can depend significantly on the quality and temporal structure of the input data. This aspect is methodologically aligned with the central theme of this thesis, where the EV demand profile is also treated as a structured temporal input rather than a simple annual aggregate.

Adding to this methodological landscape, the coupling of EnergyPLAN with external optimization routines (such as genetic algorithms or Pareto-based approaches) has become a mature practice for island energy planning [20]. For instance, Groppi et al. [17] developed the EPLANopt model to explore Pareto-optimal technology configurations for the island of Favignana, while Rivera-Durán et al. [18] assessed fully renewable generation systems with storage across the Canary archipelago. While these works demonstrate the effectiveness of multi-objective optimization for island systems, they typically treat EV charging profiles as predefined macro-level inputs rather than actively integrating a dedicated, micro-level smart charging optimization step.

Taken together, these studies show that the challenge of the island energy transition requires tools capable of representing the temporal structure of supply and demand. Precisely for this reason, this thesis adopts EnergyPLAN as the simulation environment for La Gomera's energy system, but incorporates EV profiles generated externally by a smart charging model.

2.3 Previous studies on the data context of La Gomera and the Canary Islands

The literature on La Gomera and, more generally, the official documents on the Canary Islands' energy system, constitute another essential reference for this study. In particular, their purpose is not only to provide a contextual framework but also to offer quantitative data and planning guidelines useful for calibrating the case study.

Among academic works, the thesis *Technical Feasibility of Integrating Renewable Energy Generation on the Island of La Gomera* [8] is a useful source of technical and historical background. Despite being older than the most recent developments in the island's energy system, it offers a clear picture of the challenges associated with integrating renewables in an island context such as La Gomera.

In terms of institutional documents, the *Canary Islands Energy Transition Plan (PTECan)* [10] provides the broader strategic framework within which to situate the case study. It is useful for understanding the transformation trajectories of the regional energy system and the role assigned to the energy transition in the Canary Islands. Complementarily, the *Anuario Energético de Canarias 2023* [11] serves as an important source for the observed data used in this study, including indicators of production, consumption, and the energy mix in the Canary Islands.

These documents do not replace the scientific literature, but they play a crucial role in ensuring that the case study is quantitatively founded. In an applied thesis such as this one, their use is particularly important because it allows the methodological work to be situated within a real and updated framework.

In addition to these institutional references, the recent EnergyPLAN-based studies on La Gomera by Giorcelli and co-authors are also relevant [14, 15]. These studies, already discussed in the previous section, are important because they construct a true energy model of the island's system, based on official data, hourly profiles, sectoral consumption, and validation against observed values.

Adding to this specific geographical context, recent research by Iacono et al. [16] developed a sector-coupled optimization framework for La Gomera, progressively expanding the system from a standalone configuration to an interconnected one with Tenerife. Their work highlights the crucial role of cross-sectoral coordination and subsea interconnection in achieving high renewable penetration. The present thesis aligns with this line of research but approaches the problem from a complementary angle: rather than focusing on the macro-level impact of inter-island cables and broad sector coupling (such as waste-to-energy), this work deeply investigates the micro-dynamics of EV smart charging.

Ultimately, the contribution of all these works is to complement the smart charging literature reviewed above: while the optimization algorithms govern the construction of the EV profiles, the institutional data and recent EnergyPLAN-based analyses of La Gomera provide the solid modeling framework into which those profiles are subsequently integrated.

2.4 Research gap and positioning of the thesis

A review of previous works clearly reveals at least two findings. The first is that the literature on smart charging optimization is already sufficiently mature to offer useful models for managing EV demand at the charging station or local aggregate level. The second is that the literature on isolated power systems has already demonstrated the importance of carefully evaluating the temporal structure of demand and generation, especially in contexts with high renewable energy penetration.

What appears less developed is the explicit link between these two levels. Research on charging optimization tends to stop at the level of charging management. System-level studies, on the other hand, often treat electric vehicles as exogenous demand without detailing the process by which the charging profile was generated. This leaves an important gap in research, especially when the context under study is a specific island rather than an abstract system.

This gap becomes particularly clear when considering the two main sets of references on which this thesis is based. On the one hand, the work of Calafiore and Ambrosino [1, 2, 6] provides a solid foundation for the mathematical modeling of smart charging, for defining availability and capacity constraints, and for comparing charging strategies. On the other hand, the work of Cabrera, Giorcelli, and De Clerck [13, 14, 15] provides a solid foundation for EnergyPLAN modeling, for MATLAB-EnergyPLAN automation, for the validation of the La Gomera energy system, and for the use of reference indicators in the optimization process.

However, these two components are not typically integrated into a single workflow that starts with the generation of the EV profile and ends with the assessment of its effect on the island's energy system. Charging optimization studies tend to stop at the level of charging management, while system-level studies often introduce electric vehicles as an exogenous demand without explicitly reconstructing how the corresponding hourly charging profile is generated.

This thesis fits precisely into this gap. Its contribution does not lie in introducing a radically new optimization formulation, nor in developing a new energy simulation software. Rather, it lies in establishing an explicit methodological link between a smart charging model developed in MATLAB and an EnergyPLAN model of La Gomera's energy system. In this way, the work seeks to demonstrate how the hourly pattern of EV demand can affect the overall assessment of the system.

Chapter 3

Modeling of the charging of electric vehicles

The objective of this chapter is to describe the development of the MATLAB-based model employed to optimize the electric vehicle charging strategy. The optimization aims to minimize the cost of recharging by scheduling the vehicle's charge when the prices are favorable. The charging simulations were driven by the historical hourly Spanish wholesale electricity prices reported by Ember for the period from April 2023 to March 2024, as shown in Figure 3.1. More specifically, the series corresponds to Spain's day-ahead wholesale prices [9].

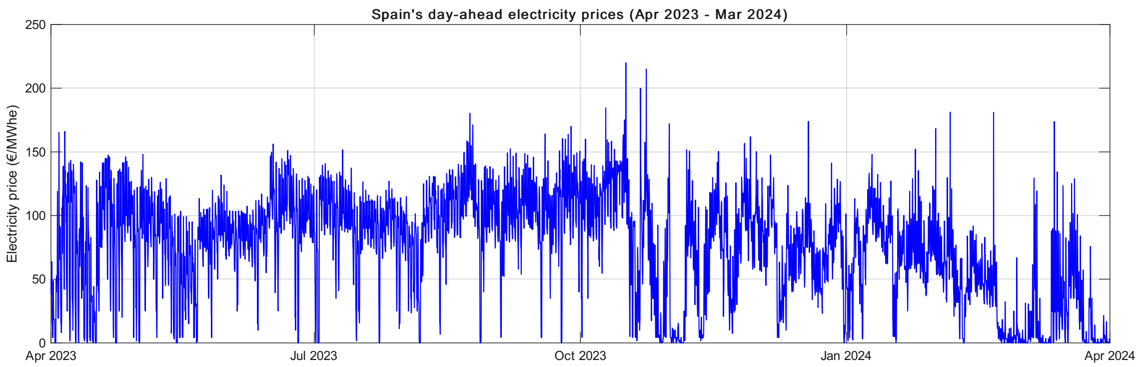

Figure 3.1: MATLAB-generated graph of Spain's day-ahead wholesale electricity prices for the April 2023 - March 2024 period.

This chapter describes in detail the smart-charging model developed in MATLAB to optimize the electric vehicle charging in a charging station. The objective is not only to present a series of implemented choices, but rather to reconstruct the reasoning that led from the reproduction of a reference model, the one proposed in [1], to the development of a simulation instrument sufficiently robust to be used, in a further phase, as a source of EV demand profiles for the energetic analysis of the case study of La Gomera.

3.1 Model scope and chapter structure

This work places itself on an intermediate scale between the single point of charge and the whole energetic system. On one hand, the model preserves a relatively detailed description of the vehicles' behavior: time of arrival, duration of the stop, energy demand, charging availability, and power limits for individual users and outlets. On the other hand, it is not designed as a real-time control model but rather as a planning and simulation instrument able to produce aggregated demand profiles coherent with realistic hypotheses over electricity prices and capacity restraints of the station.

This dual nature is important to understand both the potential and the limits (that will be recalled in the final chapter of the present thesis) of this model. The basic concept is that the recharge of the vehicles should not be treated as a passive load, rigidly assigned to the connection hours, but as a process managed between a time window defined by the permanence of the vehicle and regulated by three main elements: the total available capacity of the infrastructure, the power limit of the single outlet, and the temporal profile of the energy prices. From these elements, a systematic comparison is built between a simple FIFS policy and an optimized policy based on linear programming.

The interest in this comparison is not purely algorithmic. In the context of the present work, the FIFS strategy represents an intuitive benchmark, easily recognizable and close to an ingenuous logic of service: the vehicles are served according to their arrival order, in accordance with the available capacity, without any awareness of the price volatility. The optimized strategy, on the contrary, takes advantage of all the temporal flexibility allowed by the problem to reduce the recharging cost, while adhering to the physical constraints and the vehicles' availability. The interest of the comparison then lies in the quantification of the achievable added value obtained not by changing the energy demand but by modifying the way it is distributed in time.

The development of the model was not linear. A substantial part of the work involved verifying the physical consistency of the quantities, correcting conceptual errors related to time discretization, correctly interpreting the relationship between power and energy, and gradually transforming initially exploratory scripts into a more structured, parametric, and reproducible workflow. In this sense, the chapter also serves a methodological purpose: showing how a formally simple formulation can produce misleading results if not implemented in a totally coherent way, and how the debugging process represents an integrating part of the model's construction.

The chapter is organized as follows: Section 3.2 introduces the general architecture of the problem and the fundamental variables. Section 3.3 describes the daily model: time frame, synthetic generation of the vehicles' behavior, construction of the availability matrix, and definition of the energy demand. Section 3.4 presents the formulation of the two charging strategies, respectively the FIFS baseline and the optimized model. Section 3.5 is dedicated to the price data, its preparation, and the passage from an average daily profile to a real hourly series. Section 3.6 describes the model's extension from day to year, with particular attention to the calibration of La Gomera's case, the EV demand's seasonality, and the simulation time frame's choice. Section 3.7 discusses the computational aspects, including the solver selection and the problem of scalability for elevated numbers of vehicles. Finally, Section 3.8 presents the logic of the infrastructure's sizing, which serves as the natural conclusion to the level of analysis developed in this chapter and as a bridge to the subsequent integration of the EV charging strategy into the model of the island's energy system. The workflow of this chapter is illustrated in Figure 3.2, as well as the structure of the charging problem in Figure 3.3.

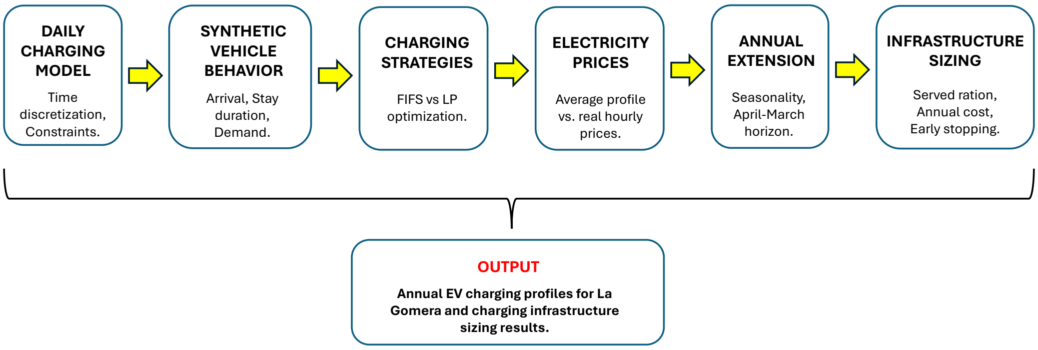

Figure 3.2: General workflow of the Chapter 3 modelling process.

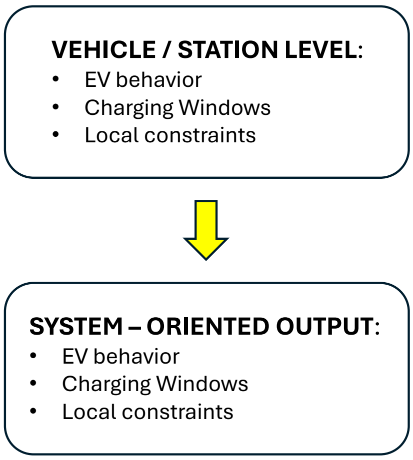

Figure 3.3: Conceptual structure of the charging problem.

3.2 Problem framework and modeling logic

The problem addressed in this chapter involves generating and managing an EV charging demand profile subject to capacity constraints and hourly electricity prices that vary over time. Conceptually, consider N electric vehicles that, over the course of a day, arrive at a shared charging station, remain there for a certain period of time, and consume a certain amount of energy. The infrastructure has a maximum total capacity of C_t, and each vehicle is subject to an individual power limit of $\bar{p}$.

The difference between the two recharging strategies considered in this study lies in how this total capacity is allocated over time to individual vehicles.

The choice of using an aggregated infrastructure, rather than a detailed representation of the individual physical charging points, derives from the purpose of the model. The objective is not to replicate the exact operations of a real-world station with a finite number of strictly separated charging ports, but to develop a planning model that is simple enough to capture the effect of price-based demand shifting. In this framework, C_t represents the total capacity made available to the charging system, while $\bar{p}$ represents the maximum charging rate that can be assigned to each vehicle in each time interval.

The daily model covers a 24-hour period divided into T intervals of duration Δ. In the initial stages of work, different values of the discretization were evaluated, but, in the final formulation of the annual workflow, hourly intervals were adopted in order to adapt to the dataset of prices, to create a less intensive computation problem, and, more importantly, to adapt to the functioning of the energy system model, which receives as inputs normalized hourly distributions.

Each vehicle is characterized by three key pieces of information: the arrival time a_i, the departure time d_i, and the energy demand L_i. The first two variables are not treated as continuous but as discrete indices of the time steps. This seemingly trivial point turned out to be one of the most conceptually important steps in the development of the model, because it required a proper reformulation of the relationships between parking duration, maximum power, and energy demand. In the absence of this clarification, the change in Δ produced incompatible energy demands and therefore unparalleled results.

From the applicative point of view, the model was gradually shifted from a purely abstract context to one referring to the case study of La Gomera. This passage did not aim to provide a statistically precise description of the actual behavior of the island's users, but it did set a benchmark for the average daily consumption per vehicle, based on data from statistical studies on the Canary Islands, as well as, in a subsequent phase, a seasonal modulation on a weekly and monthly basis [10, 11]. In this way, the model kept the simplicity of the arrivals and departures' generation, but it acquired an energetic scale consistent with the analyzed context.

3.3 Daily charging model

3.3.1 Time horizon and discretization

As discussed, the starting point of the model is a 24-hour time horizon. This decision follows the logic of the reference works that served as the inspiration for the development of the smart charging system [1, 2, 6] and responds to the idea that scheduling decisions can be made on a day-by-day basis, assuming that arrival times, vehicle availability, and prices are known for the day in question. Therefore, the daily horizon is the basic unit of the simulation, and once its behavior is validated, it can be replicated throughout the entire year.

In the early stages of the work, two choices of discretization were applied: a coarser one with $\Delta = 1$ h and a finer one with $\Delta = 5$ min. The first one entails $T = 24$ intervals, while $T = 288$ for the second one. The comparison between the two configurations was not carried out to evaluate the graphic quality of the charging profiles, but mainly to understand the effect of the temporal aggregation on the problem's structure. Given the same physical system, reducing Δ does not change the actual constraints, but it does change the way the arrival, departure, and power allocation events are observed and represented in the model.

Referring to the plots in Figures 3.4, 3.5, 3.6, and 3.7, with $\Delta = 1$ h the charging profiles appear more aggregated, because more events are compressed within the same hourly interval. With $\Delta = 5$ min, the same events are distributed over a larger number of intervals, which makes the profile temporally more resolved but also visually more jagged. This difference should be interpreted exclusively as an effect of the adopted time discretization, rather than as a comparison between the two charging strategies themselves. In particular, the plots related to the energy consumption and costs are included here only to illustrate the different graphical resolution associated with the two values of Δ; a substantive comparison between FIFS and optimized charging is presented in Section 3.4.

The discretization also affects the computational cost. Since the number of variables of the optimized problem grows proportionally to $T \times N$, the shift from 24 to 288 daily intervals results in a significant increase in the problem size, especially when it is then run for a whole year. More importantly, the subsequent use of the energy system model was taken into account. The program runs on hourly energy distributions over a 366-day year: creating more refined time intervals would have been impractical

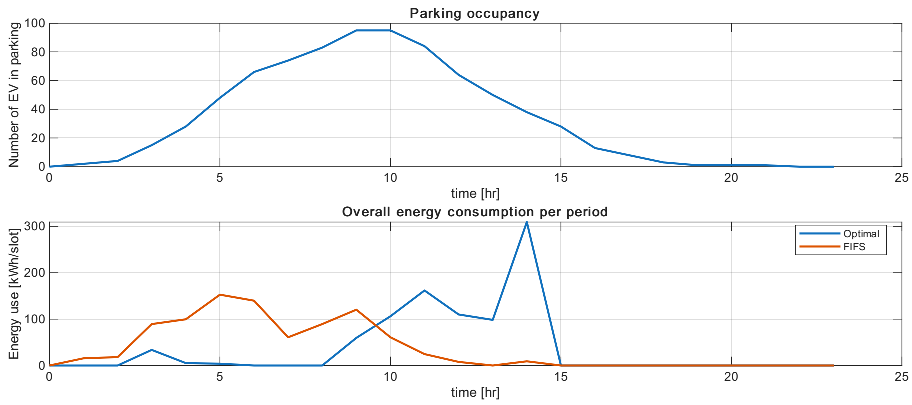

Figure 3.4: MATLAB-generated graphs of parking occupancy and energy demand, for $\Delta = 1$ h. Comparison between optimized charging and FIFS.

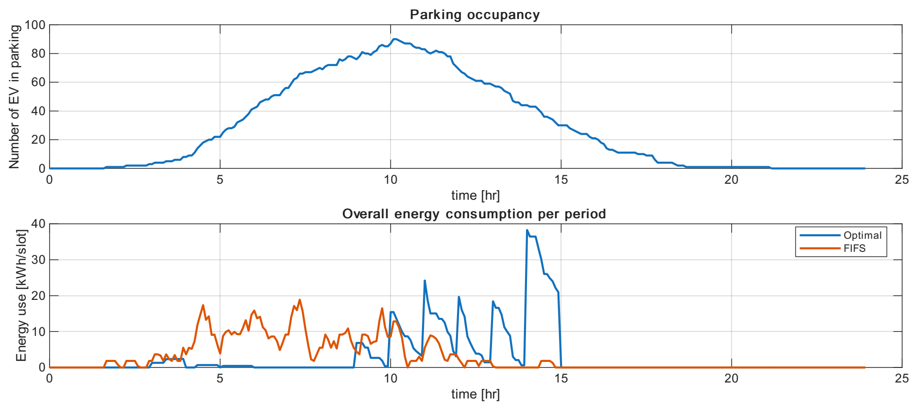

Figure 3.5: MATLAB-generated graphs of parking occupancy and energy demand for $\Delta = 5$ min. Comparison between optimized charging and FIFS.

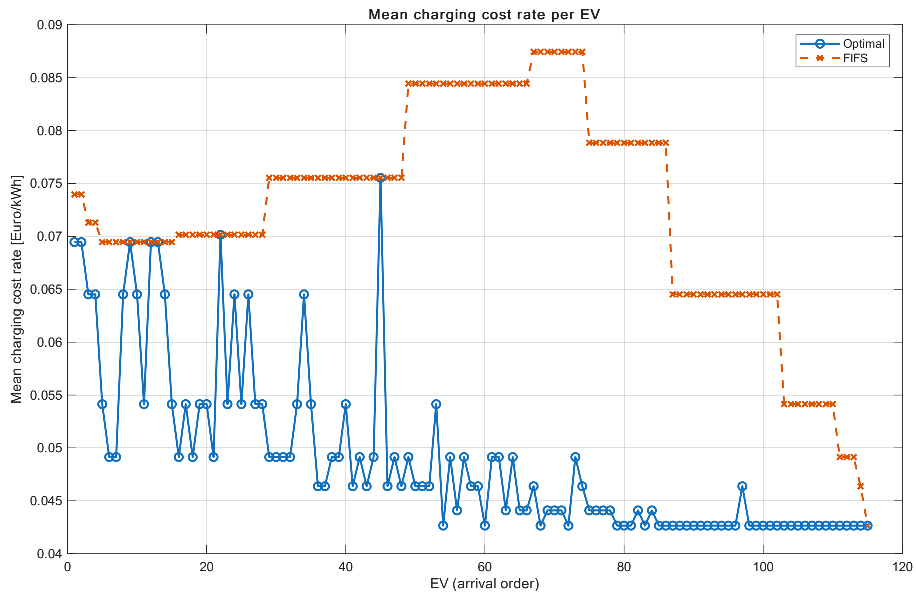

Figure 3.6: MATLAB-generated graph of the mean charging cost rate per EV, for $\Delta = 1$ h. Comparison between optimized charging and FIFS.

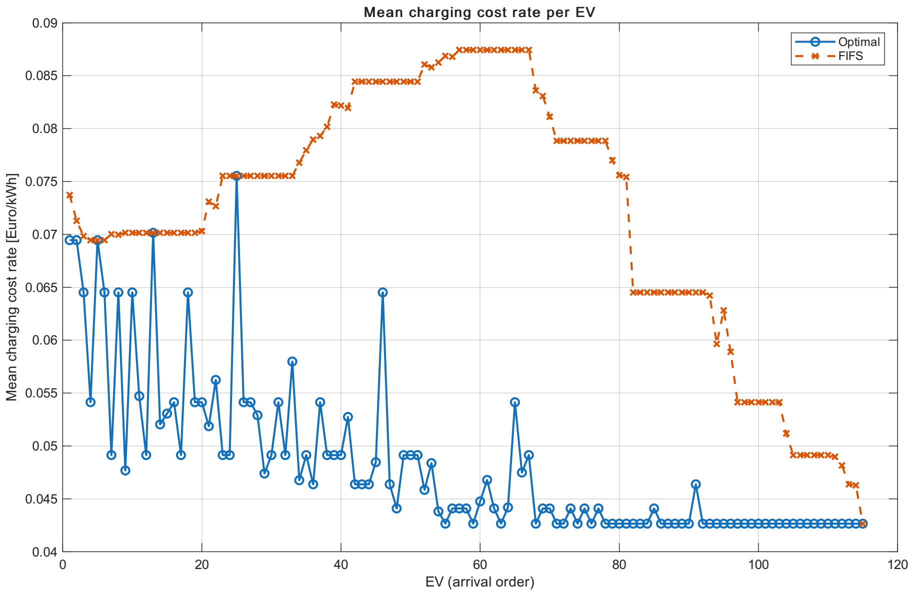

Figure 3.7: MATLAB-generated graph of the mean charging cost rate per EV, for $\Delta = 5$ min. Comparison between optimized charging and FIFS.

because a subsequent aggregation of the distribution into hourly intervals would have been necessary to upload it to the program, resulting in a purposeless task. For this reason, once the effects of the discretization were clarified and the consistency of the measurement's units verified, the hourly discretization was adopted as the standard configuration for the annual workflow.

From the physical quantities' point of view, the choice of Δ also imposes a rigorous discipline in the distinction between power and energy. The decision variable $Y(t, i)$ is the average instantaneous power allocated to the vehicle i at time step t, expressed in kW. The energy delivered at the time step t is given by the sum of the powers allocated multiplied by the duration of the slot, that is:

$$E(t) = \sum_i Y(t, i)\,\Delta. \tag{3.1}$$

When $\Delta = 1$ h, the numerical values of average power and energy per interval coincide, but they still represent different physical quantities. This clarification was essential for correctly interpreting the results.

3.3.2 Synthetic generation of vehicle behavior

For each day simulated, the model generates a synthetic set of EV behaviors. Arrival times were initially sampled through a Beta distribution with parameters $\alpha = 5.52$

and $\beta = 12$, able to concentrate arrivals during the middle of the day. This choice was adopted from the reference formulation of Calafiore and Ambrosino in their cohort-based optimization model [2] and helps avoid an unrealistic uniform distribution. However, a critical issue emerged during the course of the work: when configured this way, the distribution can result in arrivals that are too early - in some simulations, as early as the first hours of the night - and therefore a value of $\alpha = 8$ was adopted, shifting the arrivals in the morning slightly forward in time, resembling a more office-day attitude of the distribution. The comparison between the two distributions is displayed in Figure 3.8.

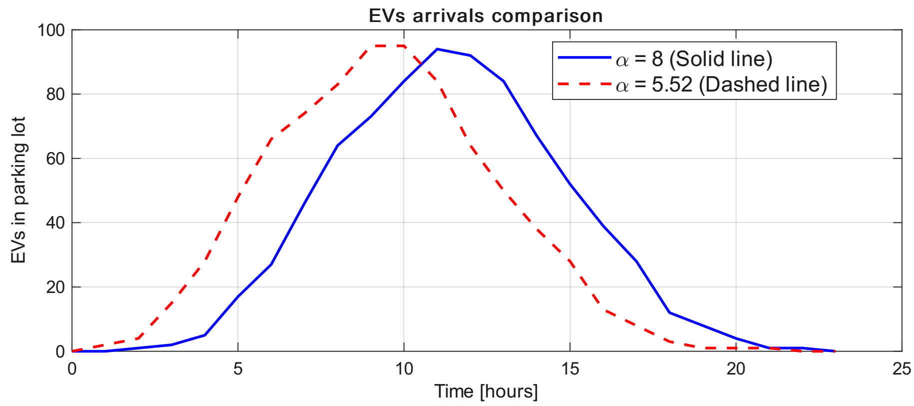

Figure 3.8: MATLAB-generated graph comparing different alpha-values for the Beta distribution.

The parking durations were generated using a normal distribution with a mean of 6 hours and a standard deviation of 1 hour, appropriately truncated to avoid unreasonable values. The combination of arrivals and stops defines the time window within which each vehicle can be recharged. Both the normal distribution and the charging window of EVs are graphed in Figures 3.9 and 3.10. It is important to note that neither the arrivals nor the stops are treated as continuous variables, but as discrete time step indexes. This implies, for example, that a stop of duration dur_T does not automatically correspond to dur_T hours, unless the factor Δ is specified.

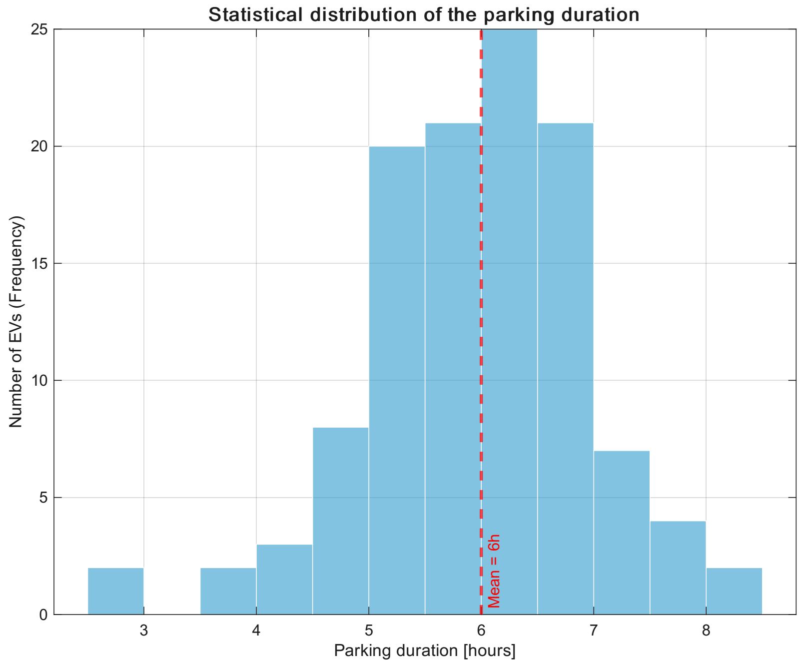

Figure 3.9: MATLAB-generated graph of the statistical distribution of EVs' parking duration.

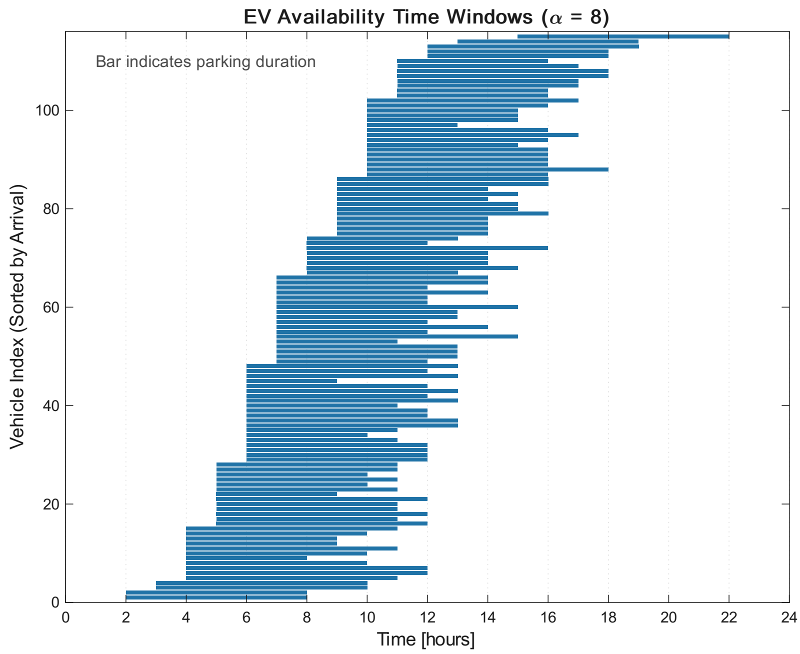

Figure 3.10: MATLAB-generated graph of the EVs' available charging window.

One of the most delicate aspects of the work was precisely the transition from discrete duration to physical duration. The initially adopted formula for the theoretically maximum deliverable energy to a vehicle during its stop was of the form:

$$\bar{L} = \bar{p} \cdot (d_i - a_i). \tag{3.2}$$

This notation is correct only if $(d_i - a_i)$ is already expressed in hours, but in the code, it represents the number of discrete intervals. In the absence of the factor Δ, the model was inconsistent: the same vehicle could have requested different quantities of energy according to the time discretization chosen. The correction of this point represented a crucial point and led to the physical coherent form:

$$\bar{L} = \bar{p} \cdot (d_i - a_i + 1) \cdot \Delta, \tag{3.3}$$

in the case of inclusive indexing.

Once the theoretical maximum energy has been defined, the model does not assume that every vehicle will always ask for a complete recharge at the maximum rate for the entire duration of the stop. A modeling decision derived from reference studies [1, 2] was to set the individual demand below the theoretical maximum - for example, using a ratio such as $\bar{L}_i = \bar{L}_i/4$ in the preliminary phase, and subsequently rescale the demands in such a way that the daily aggregate demand would be consistent with the fixed target value for the case study, later explained in Section 3.3.4.

3.3.3 Availability matrix and inclusive indexing

The availability matrix $A(t, i)$ is the link between the synthetic behavior of the vehicles and the power allocation problem. It assumes a value of 1 when the vehicle is parked in the interval t, and 0 in the opposite case. From an implementation perspective, A's consistency directly depends on how the arrival and departure times are defined.

During the development, it became necessary to explicitly clarify that the encoding used in the model follows an inclusive convention: if a vehicle arrives at time a_i and departs at time d_i, then it is available to recharge in all included slots from a_i to d_i. It follows that, if the duration of the stop in the slot is indicated with dur_T, the consistent definition of the departure is:

$$d_i = a_i + dur_T - 1. \tag{3.4}$$

A different definition, such as $d_i = a_i + dur_T$, in fact generates an error of an additional interval and leads to an overestimation of availability and the maximum theoretical energy that can be supplied.

The reconstruction of A is important not only for the validity of the availability constraint in the optimized formulation, but also for the physical interpretation of the problem. By ordering the vehicles according to their arrival, the visualization of the availability matrix generally shows a “descendant” structure, with an initial concentration of units in the upper-left quadrant that gradually shifts to the right. This representation can be observed in Table 3.1 and in Figure 3.11, and it is useful for visually understanding the degree of overlap among vehicles present at each hour and for interpreting the occupancy peaks of the parking lot.

Table 3.1: Sample of the sorted availability matrix A, showing the diagonal cascade structure of vehicle presence (1 for present, 0 for absent).

Time Interval	**EV 1**	**EV 2**	**EV 3**	**EV 4**	**EV 5**	**EV 6**	**EV 7**	**EV 8**	**EV 9**	**EV 10**	...
00:00 – 01:00	0	0	0	0	0	0	0	0	0	0	...
01:00 – 02:00	0	0	0	0	0	0	0	0	0	0	...
02:00 – 03:00	1	0	0	0	0	0	0	0	0	0	...
03:00 – 04:00	1	1	0	0	0	0	0	0	0	0	...
04:00 – 05:00	1	1	1	1	1	0	0	0	0	0	...
05:00 – 06:00	1	1	1	1	1	1	1	1	1	1	...
06:00 – 07:00	1	1	1	1	1	1	1	1	1	1	...
07:00 – 08:00	1	1	1	1	1	1	1	1	1	1	...
08:00 – 09:00	1	1	1	1	1	1	1	1	1	1	...
09:00 – 10:00	0	1	1	1	1	1	1	1	1	1	...
10:00 – 11:00	0	0	1	1	1	1	1	1	0	1	...
11:00 – 12:00	0	0	1	0	1	1	1	1	0	1	...
12:00 – 13:00	0	0	0	0	0	1	0	1	0	0	...
13:00 – 14:00	0	0	0	0	0	1	0	1	0	0	...
⋮	⋮	⋮	⋮	⋮	⋮	⋮	⋮	⋮	⋮	⋮	⋱

Another aspect that emerged during the study concerns the distinction between vehicles present and vehicles actively charging. Matrix A exclusively describes physical presence, but does not imply that all the available vehicles are actually receiving power at the same time. In some situations, the maximum parking lot occupancy can reach levels in the tens of vehicles at the same time, while the number of vehicles actively served at that given moment remains much lower. This discrepancy between occupancy and active charging was a key factor in interpreting the results, since a high number of vehicles simultaneously present in the parking lot did not necessarily correspond to an equally high charging load. For this reason, the availability matrix A had to be interpreted together with the allocated-power variable $Y(t, i)$ and the station capacity constraint.

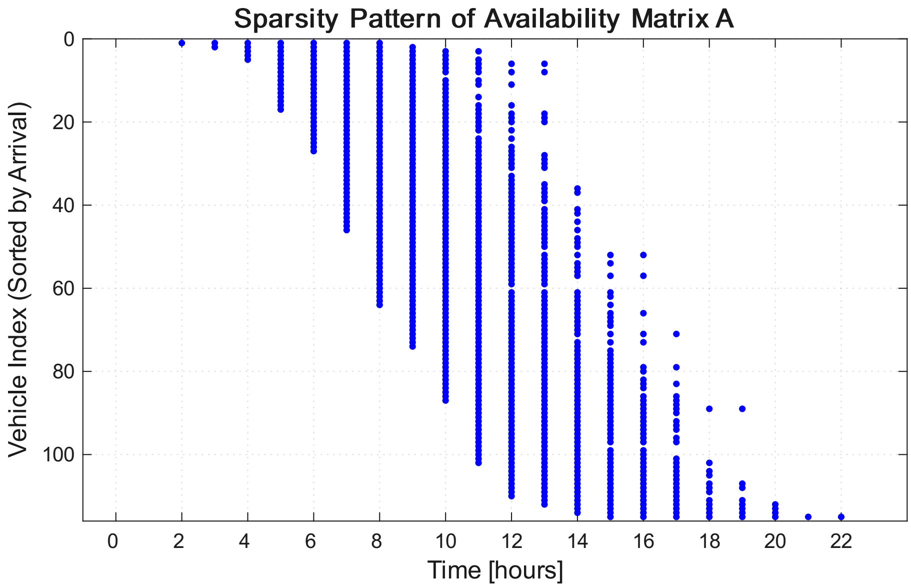

Figure 3.11: MATLAB-generated graph of the availability matrix A, where dots represent the presence of vehicles.

3.3.4 Energy demand's calibration for the case of La Gomera

Once the general structure of the EV behavior had been defined, the next step was to anchor the model to a realistic order of magnitude for the case of La Gomera. Initially, the reference used was the 115 electric vehicles present on the island in the considered year of 2023 and an average daily consumption of 7.42 kWh/day per vehicle. These values come from statistical observations and hypotheses on the kilometers traveled displayed in the *Anuario energético de Canarias 2023* and the *Plan de Transición Energética de Canarias*, produced by the Canarian government and its institutions [10, 11]: they are not meant to be intended as a direct measure of the real behavior of each user, but rather as a calibration constraint on the overall demand's scale. For the reader's convenience, the reference tables containing the mentioned data are reproduced in Table 3.2 and Table 3.3.

The daily energy target is therefore approximately 853 kWh/day. In the model, individual requests L_i are initially determined based on permanency and power limit, but are then scaled so that the total sum matches the daily target. This step is important because it separates two levels of the problem: on one hand, the relative shape of demand among vehicles, influenced by parking duration; on the other, the overall aggregate energy level, fixed by the calibration based on the case study.

This approach makes the model more transparent. The Beta distribution of the arrivals and the Normal distribution of the stops are no longer presented as an exact

Table 3.2: Evolution of the n° of electric vehicles in circulation in the Canary Islands, by island.

Year	**Gran Canaria**	**Tenerife**	**Lanzarote**	**Fuerteventura**	**La Palma**	**La Gomera**	**El Hierro**	**Canarias**	**Δ%**
2012	63	56	11	7	21	0	3	161	
2013	92	93	17	14	20	1	3	240	49,1%
2014	135	142	47	19	15	3	4	365	52,1%
2015	184	187	77	26	20	6	9	509	39,5%
2016	237	268	96	39	21	9	11	681	33,8%
2017	331	351	126	54	27	11	10	910	33,6%
2018	553	466	142	122	36	11	16	1.346	47,9%
2019	1.036	687	170	139	50	12	38	2.132	58,4%
2020	1.758	1.056	243	179	78	29	40	3.383	58,7%
2021	2.601	1.756	417	251	137	57	57	5.276	56,0%
2022	4.013	2.741	643	395	241	89	82	8.204	55,5%
2023	5.624	4.205	939	511	366	115	114	11.874	44,7%
Percentage distribution									
2023	47,4%	35,4%	7,9%	4,3%	3,1%	0,97%	0,96%	100%	
Increase compared to 2022									
23/22	40,1%	53,4%	46,0%	29,4%	51,9%	29,2%	39,0%	44,7%	

Units: $n°$ of electric vehicles.
- Includes mopeds.
- Does not include trailers and semi -trailers or special vehicles

Source: *ISTAC (Instituto Canario de Estadística)* based on data from *Dirección General de Tráfico (DGT)*, as reported in [11].

Table 3.3: Charging time based on charger power.

Charging Type	**Power**	**Distance**	**Average Daily Consumption**	**EV Capacity**	**Charging Time for Daily Consumption**	**Full-charge Time**
Slow Charging	3.6 kW	50 km/day	7.42 kWh/day	30 kWh	2 hours	8 hours
	7 kW				1 hour	4 hours
Semi-fast Charging	11 kW				40 min	3 hours
	22 kW				20 min	80 min
Fast Charging	55 kW				10 min	30 min

Source: *Plan de Transición Energética de Canarias - PTECan* [10].

statistical reconstruction of vehicle use on La Gomera, but rather as a reasonable simplification. The consistency with the case study is ensured primarily by the scale of total demand and, in a subsequent phase, by the temporal modulation on an annual basis.

Parallel to the demand's calibration, an initial aggregate infrastructural choice was introduced. In an early stage, C_t was fixed around 1.25 MW to represent a total charging capacity distributed on the island, while $\bar{p}$ was assumed equal to 22 kW per vehicle, corresponding to a typical value for a popular industrial alternating current (AC) charging port. These values were taken similarly to the reference work [1], and it is important to specify that, in order to simplify the model, power allocation, waiting time, and port availability are performed as a one, analogous charging station. In intuitive terms, this configuration is equivalent to approximately 56 theoretical ports of 22 kW, despite remaining within a continuous formulation that does not impose a discrete nature of the charging points.

3.4 A comparison of charging strategies

3.4.1 Benchmark First-In-First-Served

The first charging policy considered is a FIFS, adopted as a benchmark. The idea is simple: the vehicles are put in a queue according to their order of arrival and, following the queue, they receive power without taking into consideration the energy prices. This logic, while not optimal from an economic point of view, represents an intuitive and easily justifiable baseline: it is the closest version to a service that is not smart but well-organized.

In early implementations, the FIFS logic was closely linked to a discrete interpretation of the infrastructure. The maximum number of simultaneously rechargeable vehicles was assumed to be equal to the ratio (C_p/t) rounded to the closest lower natural number, as if the system were made up of a fixed number of ports that all delivered at the maximum rate. This choice produced reasonable behavior in a "bay-based" interpretation, but introduced a significant asymmetry compared to the optimized model, which instead allowed for a continuous sharing of the total power.

The problem became clearly evident in tests with $\Delta = 1$ h. In the presence of vehicles with modest residual demands, the discrete version of FIFS could assign reduced power for an entire hour to a vehicle about to finish without reallocating the remaining capacity to other vehicles in line. This led to wasted capacity within the hourly time slot and generated situations where the optimized model saturated C_t, while the FIFS model settled on much lower aggregate power values, despite still having several unfulfilled vehicles.

In order to make a more equal comparison, a variation of the FIFS model with power-sharing was developed. In this formulation, the priority order remains based on arrival, but the energy available in the time step, equal to $C_t \cdot \Delta$, is distributed in sequence to the vehicles in the queue, both respecting the individual power limit $\bar{p}$ and the residual energy requested by the vehicle. If a vehicle meets its charging needs before exhausting the hour's energy budget, the residual share is immediately allocated to the next vehicle. In this way, the FIFS rule is preserved, but the infrastructure uses all the available capacity when the queue is sufficiently long.

This choice has two methodological implications. First, it makes the comparison with the optimized model more accurate, because both strategies operate under the same abstraction of continuous capacity. Secondly, it clarifies that the FIFS benchmark does not necessarily correspond to a strictly discrete station, but rather to a priority policy insensitive to prices. Therefore, the distinguishing feature is not the fact that FIFS uses less power in general, but that it uses it without a temporal optimization and with a rigid allocation criterion.

3.4.2 Optimized model of smart charging

The second strategy is a smart charging policy formulated as a linear programming problem. For each simulation horizon, the model determines how much power to allocate to each vehicle at each time step, with the objective of minimizing charging costs subject to availability and capacity constraints. In general terms, the decision variable $Y(t, i)$ represents the power allocated to vehicle i at time step t.

More formally, let e_i denote the unmet energy demand associated with vehicle i. The optimization problem can then be written as:

$$\min_{Y,e} \left(\sum_{t=1}^{T} \pi_t \sum_{i=1}^{N} Y(t, i)\, \Delta + \gamma \sum_{i=1}^{N} e_i \right), \tag{3.5}$$

subject to:

$$\sum_{i=1}^{N} Y(t,i) \leq C_t \;, \qquad \forall t = 1,\ldots,T \;; \tag{3.6}$$

$$0 \leq Y(t,i) \leq \bar{p}\, A(t,i) \;, \qquad \forall t = 1,\ldots,T,\; \forall i = 1,\ldots,N \;; \tag{3.7}$$

$$\sum_{t=1}^{T} Y(t,i)\, \Delta + e_i = L_i \;, \qquad \forall i = 1,\ldots,N \;; \tag{3.8}$$

$$e_i \geq 0 \;, \qquad \forall i = 1,\ldots,N \;. \tag{3.9}$$

where π_t is the electricity price at time step t, Δ is the duration of the time step, C_t is the total charging capacity available at time step t, $\bar{p}$ is the maximum charging power that can be assigned to a single vehicle, $A(t,i)$ is the availability matrix, and L_i is the energy demand associated with vehicle i.

The first constraint limits the total charging power by the station capacity. The second ensures that a vehicle can only be charged while it is present and that its charging power never exceeds the individual upper bound. The third imposes the energy balance for each vehicle, while allowing unmet demand through the slack variable e_i. This formulation was preferred over an inequality-based energy constraint in order to avoid over-delivery in the presence of zero or negative electricity prices.

The objective function combines two terms. The first one is the energetic cost, obtained by multiplying the energy recharged at each interval by the corresponding energy price. The second is a penalty for the unmatched demand, introduced to prevent the model from artificially reducing the cost by simply waiving to serve part of the demand. This penalty is governed by parameter γ, expressed in EUR/kWh of energy not delivered.

One of the most important steps in developing the model involves the management of the vehicle's overall energy constraint. In a preliminary formulation, the demand L_i was treated as a simple lower bound: the cumulative energy delivered had to be at least equal to L_i minus a slack variable e_i. This approach proved problematic when the real-time price profile included hours with zero or negative prices. In such cases, the model might have been inclined to supply more energy than required, because the surplus did not increase the cost or might even have reduced it. To fix this distortion, the constraint was reformulated as an equality with slack: the total energy supplied to the vehicle must be exactly equal to:

$$\sum_{t=1}^{T} Y(t,i)\,\Delta + e_i = L_i\ . \tag{3.10}$$

In this way, the model maintains the ability to fail to fully satisfy the demand, paying a penalty, but it cannot “invent” additional artificial demand.

In addition, the meaning of γ deserves a specific clarification. In the annual simulation, γ was chosen as the highest price observed in the annual series, so as to have a constant penalty, sufficiently high to prevent the system from not delivering energy when it was able to serve it. It is important to note that the cost labeled as ”annual cost” in the results solely corresponds to the energy cost and does not include the penalty term. The penalty enters the objective function of the optimization problem, but for interpretive purposes, it was kept distinct from the actual energy cost to make the comparison with the FIFS benchmark more readable. To understand the fundamental operational and economic differences between the two strategies, a representative 24-hour comparison is presented in Figures 3.12 and 3.13.

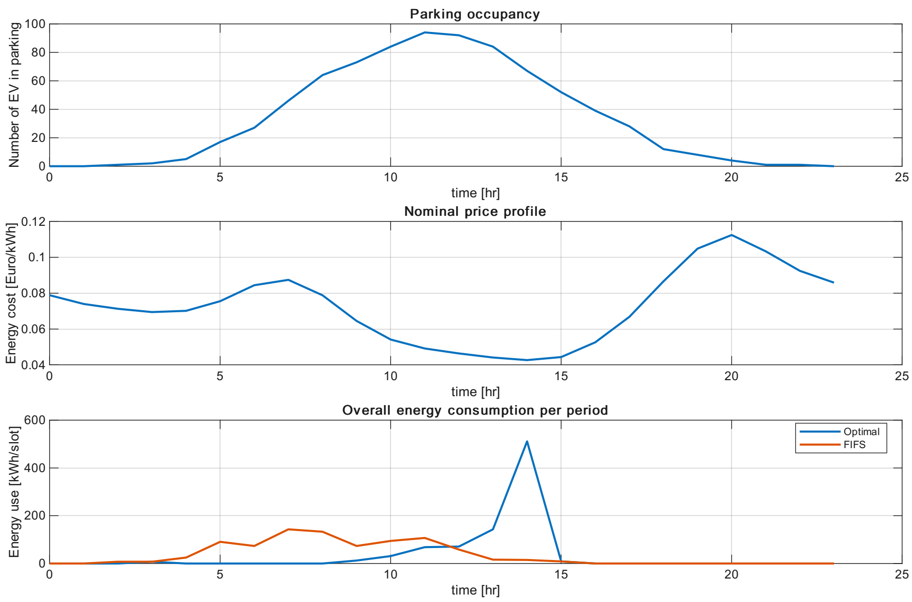

Figure 3.12: MATLAB-generated graph of parking occupancy, daily average energy price, and energy consumption for both FIFS and Optimal charging strategies. As can be seen, the Optimal model shifts demand to lower-price hours.

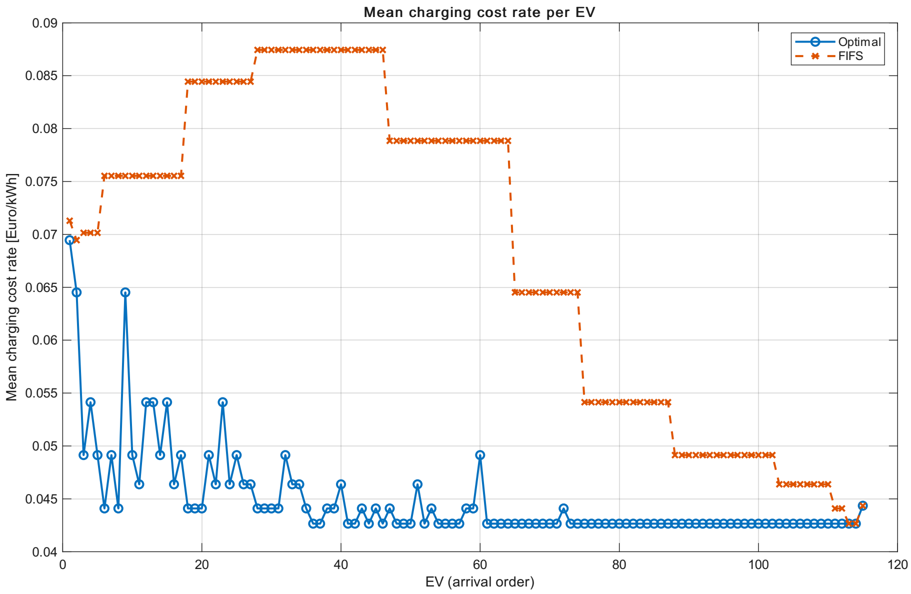

Figure 3.13: MATLAB-generated graph comparing the mean charging cost rate per EV for both FIFS and Optimal strategies. Notably, the average charging cost under the Optimal strategy decreases relative to the FIFS baseline as the daily vehicle load increases, highlighting the economic efficiency of the optimization at larger scales.

To provide a precise numerical quantification of the economic benefits visually shown in the previous figures, Table 3.4 summarizes the charging performance and costs across representative simulated scenarios. As the fleet size and C_t increase proportionally, the optimization model consistently guarantees a lower average cost per MWh, returning a steady percentage saving of approximately 25% compared to the FIFS baseline, while delivering the exact same amount of total energy.

Table 3.4: Detailed numerical results of the annual simulations: comparison between FIFS and OPT strategies across different EV fleet sizes.

EVs	**Ports**	C_t [kW]	**Energy FIFS** [MWh]	**Energy OPT** [MWh]	**Cost FIFS** [EUR]	**Cost OPT** [EUR]	**Avg Cost FIFS** [EUR/MWh]	**Avg Cost OPT** [EUR/MWh]	**Savings** [%]
150	30	660	407	407	27,985	21,089	68.70	51.77	25.0
750	150	3,300	2,037	2,037	139,929	105,399	68.70	51.75	25.0
1,500	300	6,600	4,074	4,074	279,667	210,805	68.65	51.75	25.0
2,250	450	9,900	6,110	6,110	419,536	316,242	68.66	51.76	25.0
3,750	750	16,500	10,184	10,184	699,180	527,009	68.66	51.75	25.0
7,500	1,500	33,000	20,368	20,368	1,398,480	1,054,035	68.66	51.75	25.0
11,250	2,250	49,500	30,552	30,552	2,097,436	1,581,022	68.65	51.75	25.0
15,000	3,000	66,000	40,736	40,736	2,796,967	2,107,940	68.66	51.75	25.0

3.4.3 Interpretation of power, energy, cost, and dissatisfaction

A significant portion of the work was dedicated to clarifying the physical and accounting implications of the model's main outputs. The first misunderstanding to be resolved concerned the relationship between power and energy. As already observed, $Y(t,i)$ is a power; the energy delivered to the vehicle i during the time step t is therefore given by:

$$E(t,i) = Y(t,i) \cdot \Delta\,. \tag{3.11}$$

When $\Delta = 1\text{h}$, the distinction may seem numerically irrelevant, but it becomes essential when moving to finer discretizations and for a consistent interpretation of the curves.

The second misunderstanding concerned the cost. In the annual simulations, the annual cost associated with a charging policy is calculated by summing the product of price and energy in each time interval. This is the actual energy cost. Instead, the dissatisfaction is a separate indicator that measures the energy not supplied relative to the target demand. The objective function of the optimized model combines the two terms, but for analytical purposes, it was useful to keep them separate, so as to understand whether a low cost is due to the actual advantage of the scheduling or to the fact that part of the demand was not met.

This distinction is particularly important in the sizing study presented at the end of the chapter. An excessively low capacity C_t may produce a low annual cost simply because the system delivers less energy than is needed. Instead, a capacity sufficient to meet all the demand can allow further cost reductions, not by increasing the energy supplied, but by shifting it to cheaper hours. In this sense, the relationship between cost, served ratio, and dissatisfaction is one of the central interpretive elements of the chapter.

3.5 Integration and processing of electricity prices

3.5.1 From the average daily profile to real hourly prices

In the initial phase of development, the model used an average daily electricity price profile. In practice, an historical hourly time series was rearranged into a $24 \times D$ matrix, where D represents the number of observed days, and the average for each hour of the day was then calculated. The result was a "typical day" consisting of 24 prices, repeated identically for every day of the annual simulation. This approach has the advantage of simplicity and allows for the separation of the structural effect of the prices from the daily fluctuations, but it flattens the actual market variability.

In the next step, the workflow was updated to use the actual hourly series of Spain's electricity prices, read from the structured Excel file in the Ember dataset [9].

This change had a substantial impact on the behavior of the model. When using an average daily profile, the optimized solution tends to distribute the charging according to a relatively regular and repetitive logic. Instead, when adopting the actual hourly prices, the model is subject to days with significant price fluctuations, including hours with very low, zero, or even negative prices. Under these conditions, the advantage of smart recharging emerges clearly, and the optimized daily demand profiles become more variable and better aligned with the actual market conditions. The macroscopic impact of this transition over a long-term horizon will be visually demonstrated in Section 3.6, once the annual simulation framework is introduced.

The decision to work with Coordinated Universal Time (UTC) was important to avoid ambiguities related to time changes and daylight saving time. This technical detail is crucial when building an annual simulation that produces consistent hourly vectors and can serve as input for further models.

3.5.2 Handling of zero or negative prices

The use of real prices revealed a methodological issue that was not apparent in the preliminary phase using an average profile: the presence of hours with zero or negative prices. From a market perspective, these hours are plausible; from the model's perspective, however, they immediately highlight any weakness in the formulation of the energy constraint.

If the energy required by the vehicle is treated as a simple lower bound, the model might be inclined to deliver additional energy during hours when the price is zero or negative, because this would not worsen, or may even improve, the objective function. From a physical standpoint, this solution is unacceptable: the vehicle does not have an infinite demand, and the model must not become an "artificial energy absorber".

The reformulation of the constraint as an equality with slack solved this issue. Once this correction is introduced, the model preserves the ability to choose when to charge, but it cannot alter the total energy requested. This passage is methodologically relevant because it shows how the adoption of real data, which is richer and more variable, not only results in a descriptive improvement of the model but also serves as a robustness test of the formulation.

3.6 Annual extension of the model

3.6.1 From the daily simulation to the annual simulation

Once the model's behavior was validated on a daily basis, the following step was to build an annual workflow. This passage was achieved by refactoring the code into two main components: a daily simulator and an annual wrapper. The daily simulator takes the seed, the daily price vector, and the parameters of the problem as inputs and returns the hourly energy profiles, cost and dissatisfaction for the two charging strategies. The annual wrapper reads the entire price series once, divides it into daily blocks of 24 hours, and calls the simulator for each day.

This refactoring yielded several benefits. First, it made the workflow more organized: one function for the day, one for the year, a launcher for the scenario's parameters. Second, it simplified the export of results, allowing an easy aggregation of the outputs into hourly and daily tables. Third, it facilitated the model's extension to parametric studies, allowing C_t, N, $\bar{p}$, and other inputs to be modified without having to manually edit the internal code.

The annual results are typically exported to an Excel file containing two sheets: an `Hourly` sheet, with one row for each hour of the year, and a `Daily` sheet, with one row for each day.

To illustrate the output of the annual simulation and visually confirm the behavioral shifts anticipated in Section 3.5, a comparison between two annual simulations with different pricing scenarios is provided. Figure 3.14 shows the full annual simulation comparing the FIFS and optimized charging strategies under constant average daily prices versus real variable hourly prices, as explained in Section 3.5. Figure 3.15 provides a detailed view zoomed in on the first week for both pricing scenarios. While the first simulation (average prices) shows a steadier charging pattern, where variations are solely due to the stochastic behavior of vehicles, the second scenario (variable prices) clearly displays more dynamic and pronounced peaks, as the optimization model actively shifts the load to exploit real-time market fluctuations.

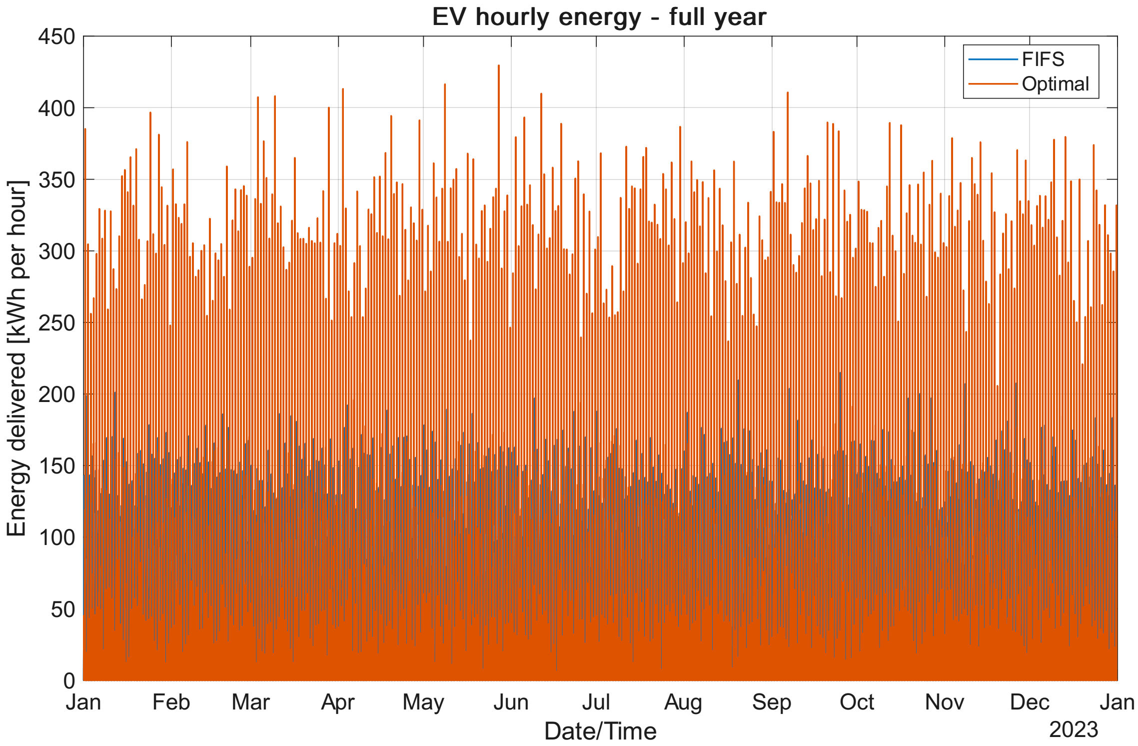

(a) Average daily prices

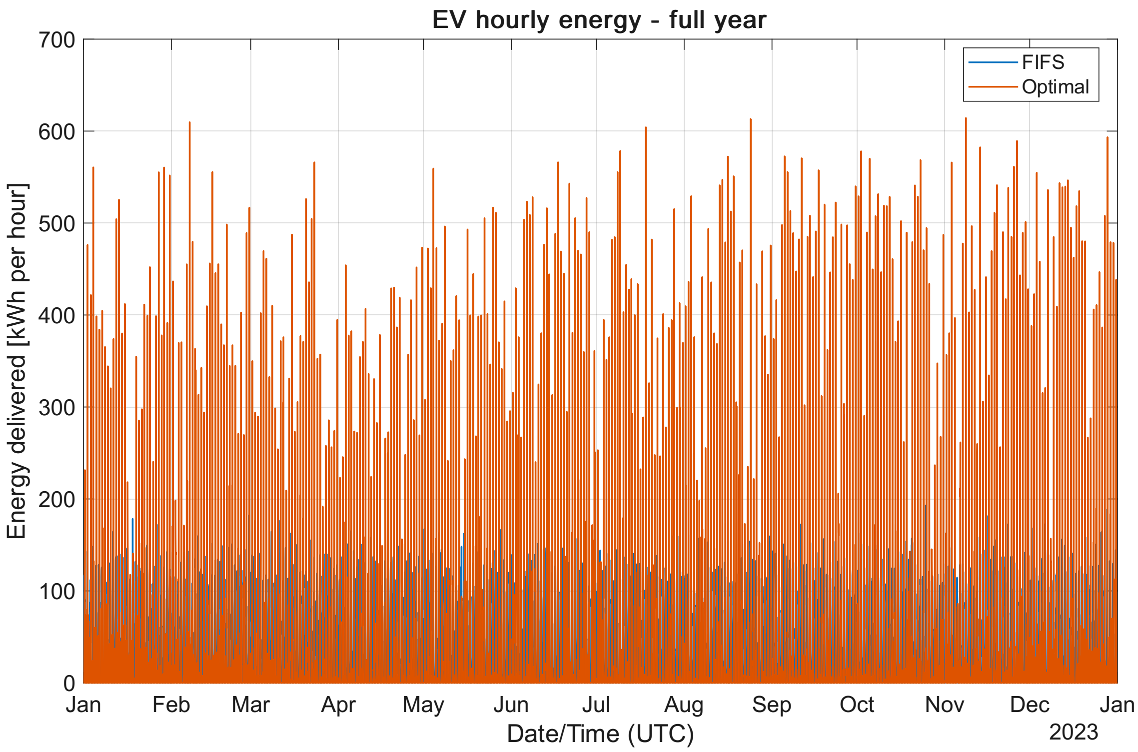

(b) Real variable hourly prices

Figure 3.14: MATLAB-generated graph of the annual charging profile comparing the FIFS and optimized strategies. (a) Scenario using constant average daily prices. (b) Scenario using real variable hourly prices.

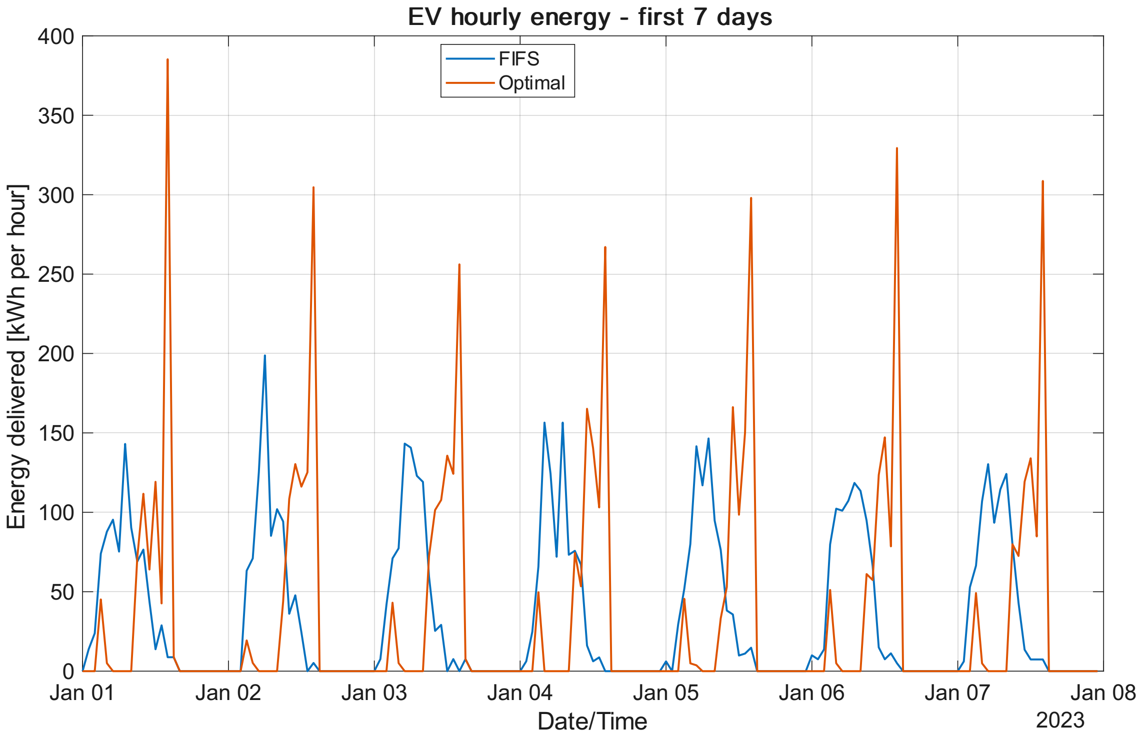

(a) Average daily prices

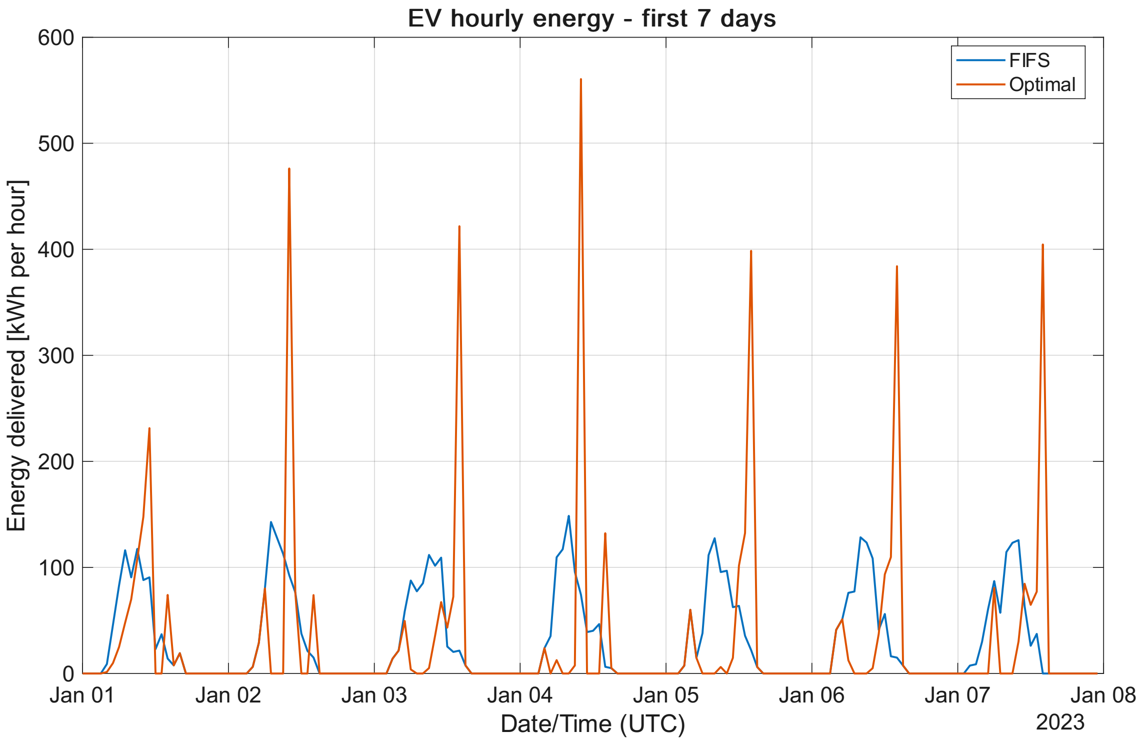

(b) Real variable hourly prices

Figure 3.15: MATLAB-generated graph of the first week of the annual charging profile comparing the FIFS and optimized strategies. (a) Scenario using constant average daily prices. (b) Scenario using real variable hourly prices.

3.6.2 Weekly and monthly seasonality of EV demand

One limitation of the initial calibration was the assumption of a constant average demand of 7.42 kWh/day per vehicle. To better reflect the context of La Gomera, the annual simulation was progressively refined by adding two levels of demand modulation: a distinction between weekdays and weekends, and monthly seasonal coefficients.

For the first level, it was initially assumed that the demand on weekends represented 85% of the demand on weekdays. However, this proportion was not directly applied to the final energy values, because the goal was to maintain unchanged the annual average demand of 7.42 kWh/day per vehicle. For this reason, the two daily levels were rescaled by imposing that the weekly average remained equal to the target value. Let x denote the daily demand on weekdays; the weekend demand was set to $0.85x$, and the value of x was derived from the equation:

$$\frac{5x + 2(0.85\,x)}{7} = 7.42. \tag{3.12}$$

From this applied condition, 7.75 kWh/day for weekdays and 6.59 kWh/day for weekends are obtained, equivalent, in terms of distance covered, to approximately 52.24 km/day and 44.4 km/day, respectively. This mechanism was implemented by passing a parameter `Eveh_day_target_kWh`, specific for each day, to the simulator.

For the second level, twelve monthly coefficients were introduced to adjust demand throughout the year based on the expected demand of the case study. The raw coefficients were combined with the week factors and subsequently normalized over the number of simulated days, in order to precisely preserve the annual average of 7.42 kWh/day. This step is essential: without normalization, the introduction of seasonality would alter the total energy demanded, whereas the model's intention is only to redistribute it over time.

The combination of these two levels of modulation allows for a more realistic annual EV demand, while remaining within a synthetic model. Daily vehicle recharging continues to be generated artificially, but its magnitude varies consistently with the type of day and month of the year. The applied modulation coefficients are summarized in Table 3.5.

Table 3.5: Demand modulation coefficients: monthly seasonality and weekly reduction.

Monthly Coefficients						
Month	Jan	Feb	Mar	Apr	May	Jun
Value	1.10	1.05	1.00	0.95	0.85	0.90
Month	Jul	Aug	Sep	Oct	Nov	Dec
Value	1.15	1.20	0.95	1.00	1.05	1.15

Weekly Coefficients	
Day Type	**Value**
Weekday (Monday to Friday)	1.00
Weekend (Saturday and Sunday)	0.85

3.6.3 Calendar year, leap year, and the April-March period

To ensure the model remained useful also for the integration with the energy system model employed (which will be discussed later), special attention was paid to the length of the annual simulation. The energy system model requires hourly vectors consisting of 8784 elements, corresponding to 366 days. To meet this requirement even in non-leap years, the code was equipped with an option that extends the annual vector by adding the first 24 hours of January 1st of the following year.

In addition to the "calendar year" mode, the option to simulate a shifted yearly time window, for example, from April 1st 2023, to March 31st, 2024, was implemented. This choice is relevant for the present study because it allows the simulation period of the EV recharge to be aligned with the reference period used in the energy study of La Gomera, which begins with the operational start-up of the new wind farm. From an implementation standpoint, this choice required appropriately anchoring the dates and associating the monthly coefficients with the simulation's actual start date, thereby avoiding errors that would have treated, for example, April as if it were January.

The introduction of the April-March window strengthened the consistency of the entire workflow, allowing for the generation of annual EV profiles already aligned with the subsequent system energy model.

To visually illustrate the combined effect of these temporal adjustments, Figures 3.16 and 3.17 show the daily energy demand across the April-March simulation window, comparing the effects of the seasonality coefficients. While the unmodulated baseline maintains a relatively flat and consistent profile throughout the year, the adjusted profile clearly exhibits more pronounced seasonal trends and weekly variations, while always maintaining the exact same total energy output in both cases.

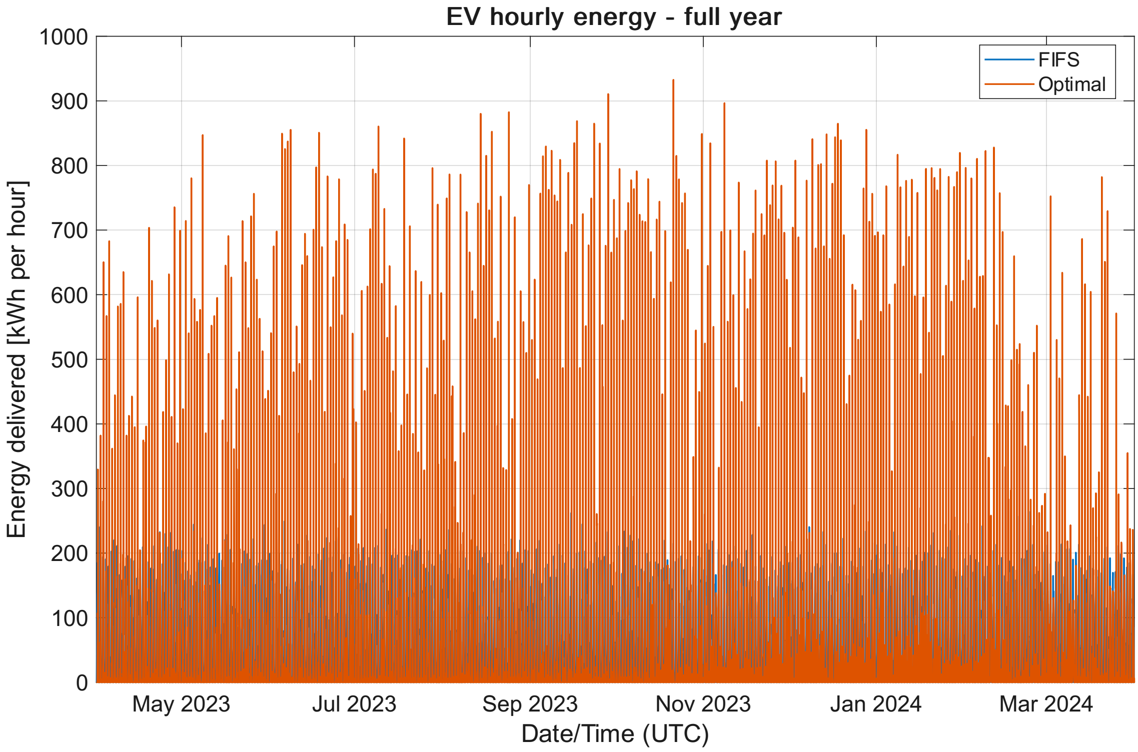

(a) Unmodulated profile

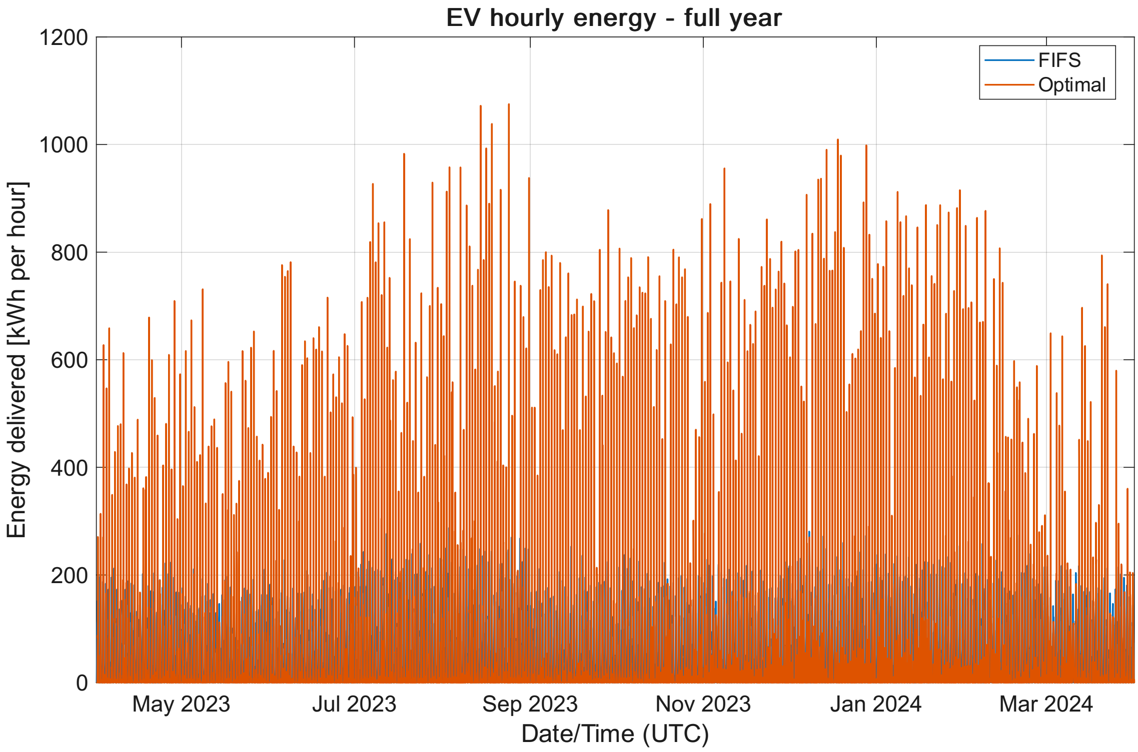

(b) Adjusted profile

Figure 3.16: MATLAB-generated graph of the full annual simulation of the energy demand spanning the April-March window. (a) The standard scenario without temporal adjustments. (b) The modified scenario illustrating the effect of the monthly and weekly seasonality coefficients.

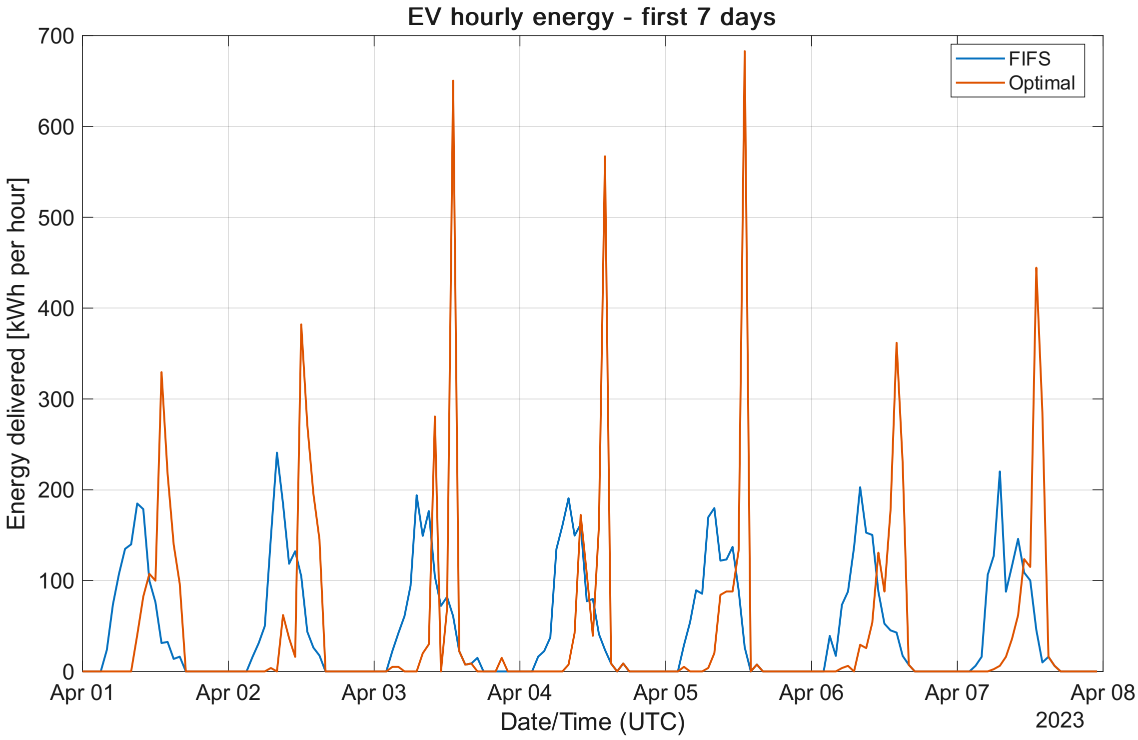

(a) Unmodulated profile

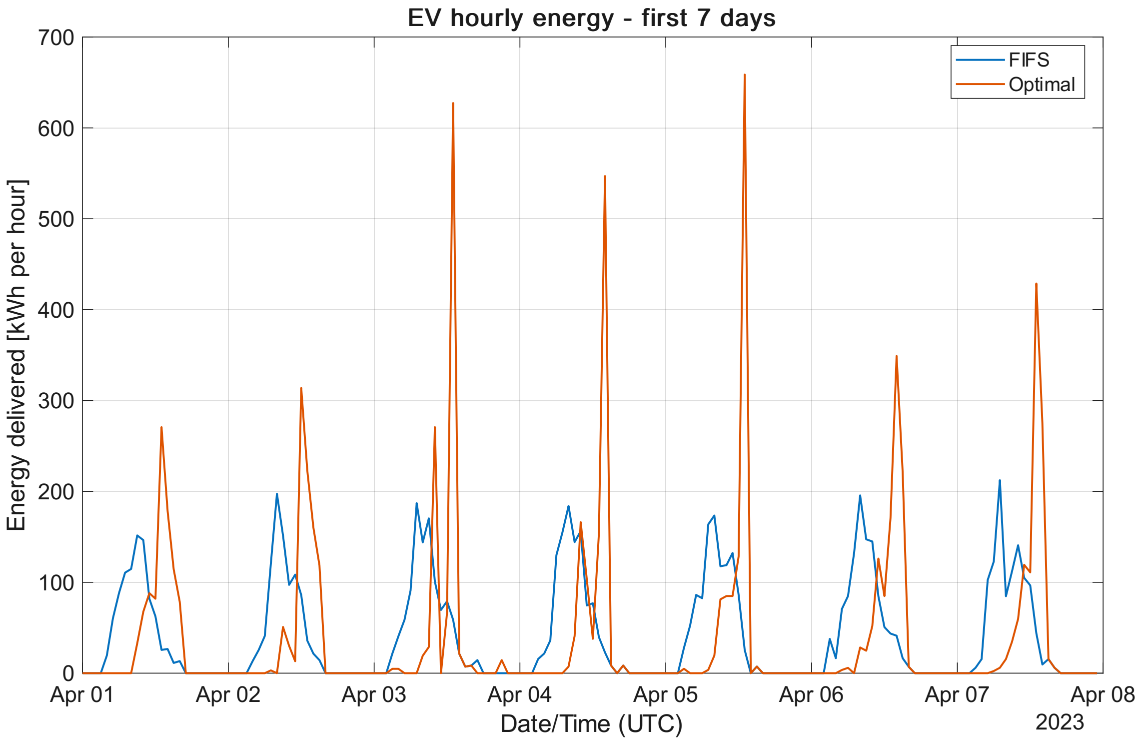

(b) Adjusted profile

Figure 3.17: MATLAB-generated graph of the first-week view of the annual energy demand. (a) The standard scenario without temporal adjustments. (b) The adjusted profile showing the short-term fluctuations introduced by the weekend reduction factor.

3.6.4 Exportation, naming, and reproducibility

As the complexity of the workflow increased, a more rigorous management of the generated files became necessary. To this end, the annual wrapper was converted into a parametric function, called by an external launcher. The output files were given explicit names containing timestamps, scenario parameters, and tags for the solver used (e.g., LP or CVX (Convex optimization package)). A writable `latest` file was also maintained for quick testing, alongside timestamped files for permanent archiving.

A second feature involved the export of single-column vectors to facilitate the transition to the energy system model. In addition to the real energy profiles, normalized versions ranging from 0 to 1 were also introduced, useful for shape comparisons between scenarios and for certain post-processing needs. These changes do not alter the physical model but make the entire workflow more traceable and easier to reuse.

3.7 Computational aspects and scalability

3.7.1 Computational bottleneck with CVX

The first prototype of the optimized model was implemented on CVX. This choice facilitated the initial development phase, as it allowed us to formulate the linear problem in a highly readable way and to quickly verify its correctness. However, as we moved on to annual simulations and larger values of N, CVX proved to be the main computational bottleneck.

The reason is structural. Every day, the optimized problem contains approximately $T \times N$ variables, plus the slack variables. With $\Delta = 1$ h and $T = 24$, the daily problem remains manageable for modest values of N, but becomes very demanding when N increases by orders of magnitude and when the solver is repeated 365 or 366 times. Under these conditions, the modeling overhead of CVX becomes dominant.

3.7.2 Switching from CVX to `linprog`

To overcome this limitation, the optimized model was reformulated equivalently using `linprog` directly. The idea was not to change the logic of the problem, but to exactly preserve its structure, objective, and constraints, removing only the overhead of the CVX layer. The result was a substantial improvement in scalability. The main annual aggregates, total energy supplied, total cost, and dissatisfaction, remain unchanged within the numerical tolerance.

As shown in Figures 3.18 and 3.19, the annual and first-week charging profiles highlight the practical differences between the two solvers. While the total energy delivered, the overall costs, and the peak boundaries are identical, the shape of the load profile changes. CVX tends to spread the charging process more evenly over the available low-price hours. In contrast, `linprog` exploits the available capacity to deliver the demanded energy as quickly as possible, resulting in a higher number of narrower, more pronounced power peaks. This variation is a common result of how different algorithmic solvers handle multiple equivalent optimal solutions, ultimately confirming that while the energy allocation logic differs, the physical constraints and the final optimized targets are perfectly respected in both cases.

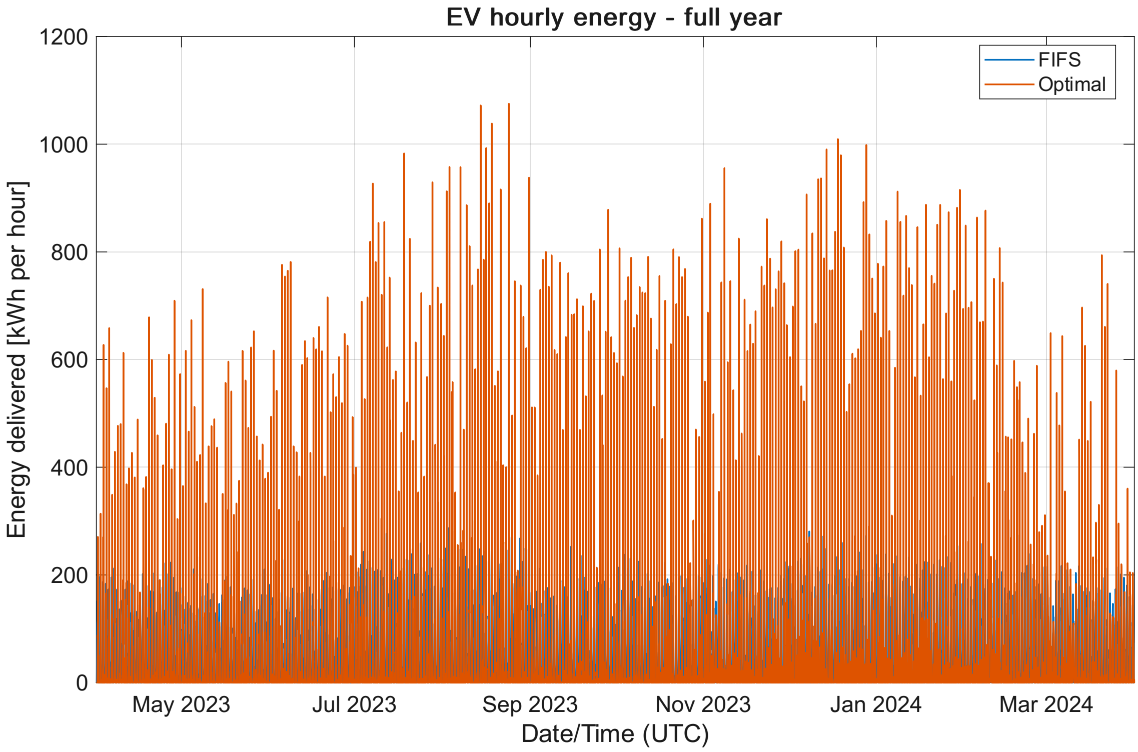

(a) CVX solver

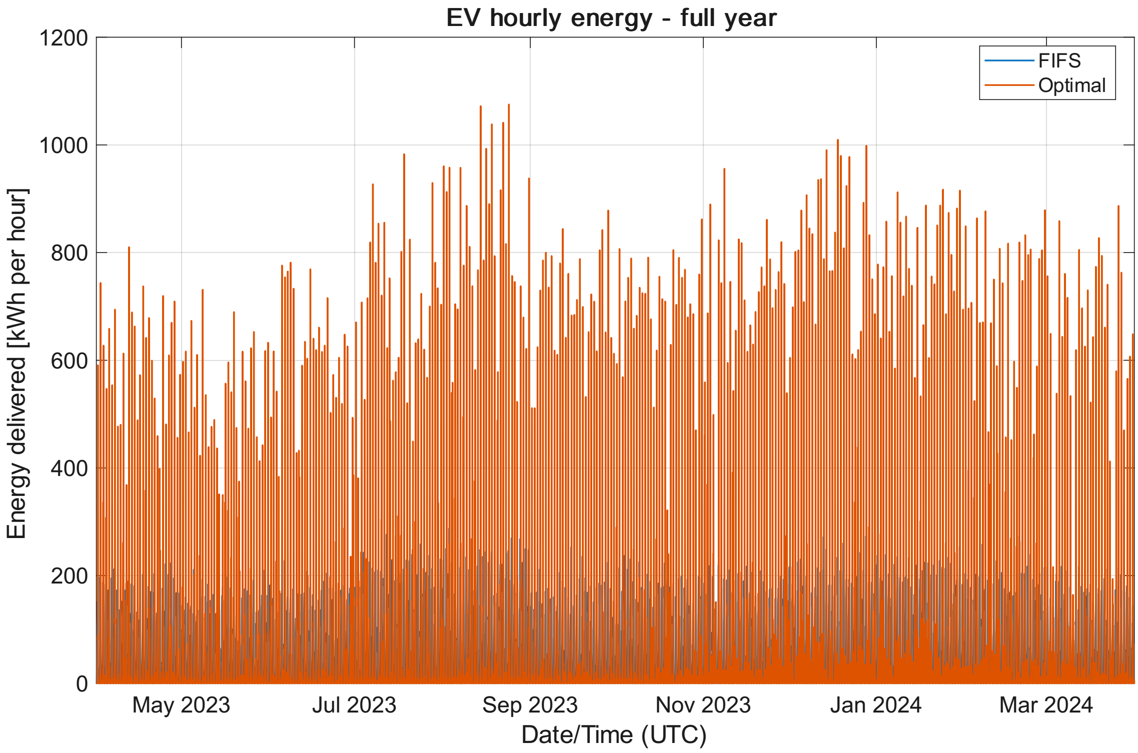

(b) `linprog` solver

Figure 3.18: MATLAB-generated graph of the full annual comparison of the optimized charging profile. (a) Profile using the CVX solver. (b) Profile using the `linprog` solver.

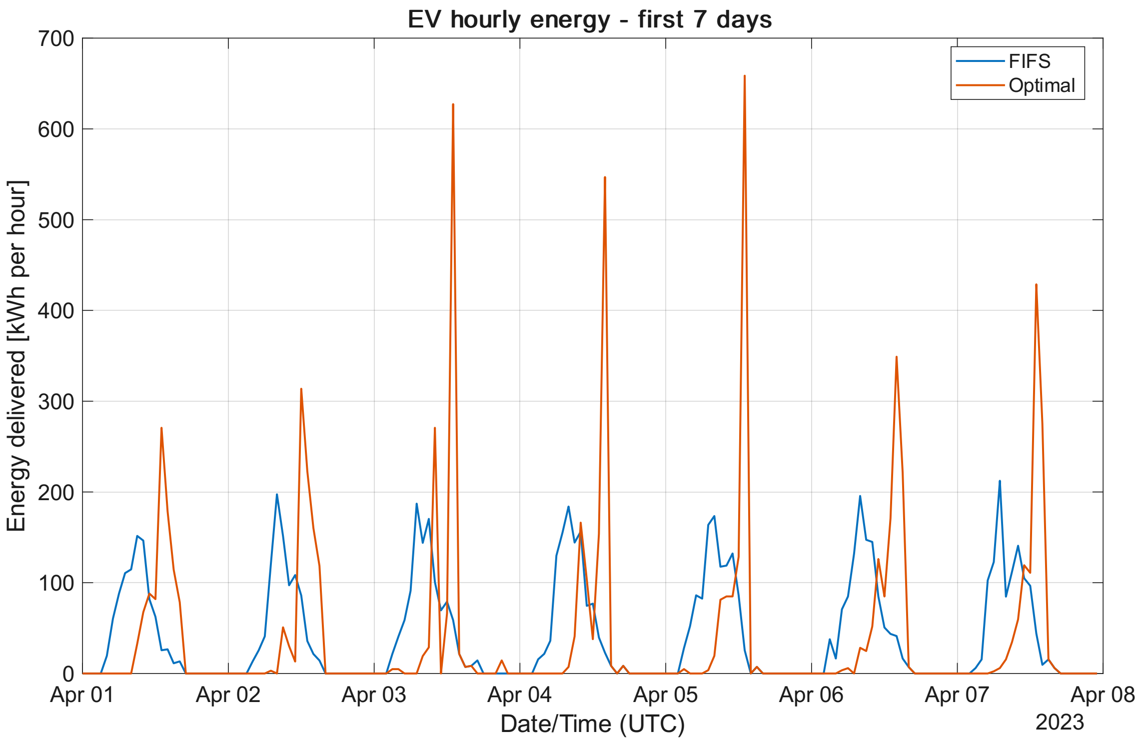

(a) CVX solver

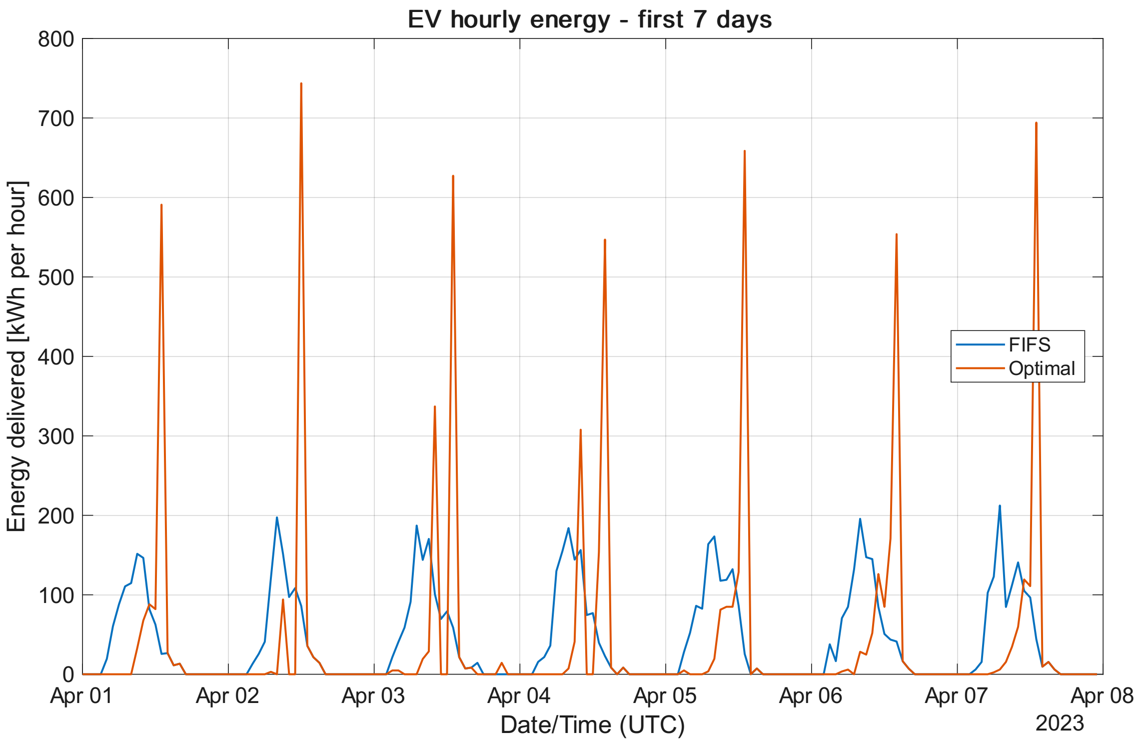

(b) `linprog` solver

Figure 3.19: MATLAB-generated graph of the first-week view of the annual load distribution. (a) Profile using the CVX solver. (b) Profile using the `linprog` solver.

3.7.3 Proportionality and near-scale-invariance test

Once the annual workflow was stabilized, scaling tests were conducted in which the number of vehicles and the available capacity were increased by the same factor, for example, $\times 10$, $\times 25$, $\times 50$, and $\times 100$. For all scenarios, the available infrastructure capacity was deliberately constrained by setting the number of charging ports equal to 10% of the total vehicle fleet. The total energy scaling ratios and the relative proportionality errors are summarized in Table 3.6. The goal was not only to verify the computational robustness of the code, but also to observe whether the shape of the optimized charging profile remained essentially unchanged as the system scaled up while maintaining a similar ratio between demand and capacity (the capacity utilization factors for both strategies are compared in Table 3.7, as well as in Figure 3.20 and Figure 3.21).

Table 3.6: Total energy scaling ratio and relative proportionality error compared to the base case.

Scenario	**Ideal Factor**	**Total Energy Ratio**		**Relative Error**	
		OPT	**FIFS**	**OPT**	**FIFS**
x10	10	10.0000	10.0000	0.142	0.239
x25	25	25.0000	25.0000	0.142	0.234
x50	50	50.0000	50.0000	0.143	0.232
x75	75	75.0000	75.0000	0.138	0.231
x100	100	100.0000	100.0000	0.143	0.230

Table 3.7: Infrastructure capacity utilization factor (E/C_t): mean values and peak percentiles.

Scenario	**OPT Strategy**			**FIFS Strategy**		
	Mean	**p95**	**p99**	**Mean**	**p95**	**p99**
Base	0.1405	1.0000	1.0000	0.1405	0.5290	0.6584
x10	0.1405	1.0000	1.0000	0.1405	0.5037	0.5807
x25	0.1405	1.0000	1.0000	0.1405	0.5023	0.5793
x50	0.1405	1.0000	1.0000	0.1405	0.5037	0.5783
x75	0.1405	1.0000	1.0000	0.1405	0.5013	0.5805
x100	0.1405	1.0000	1.0000	0.1405	0.5022	0.5783

This specific sizing choice explains the macroscopic behavior observed in the utilization charts: given the constrained infrastructure, the optimized strategy frequently reaches full saturation during peak demand periods, fully exploiting the power limits to efficiently shift the load. Despite this saturation, the results showed that the

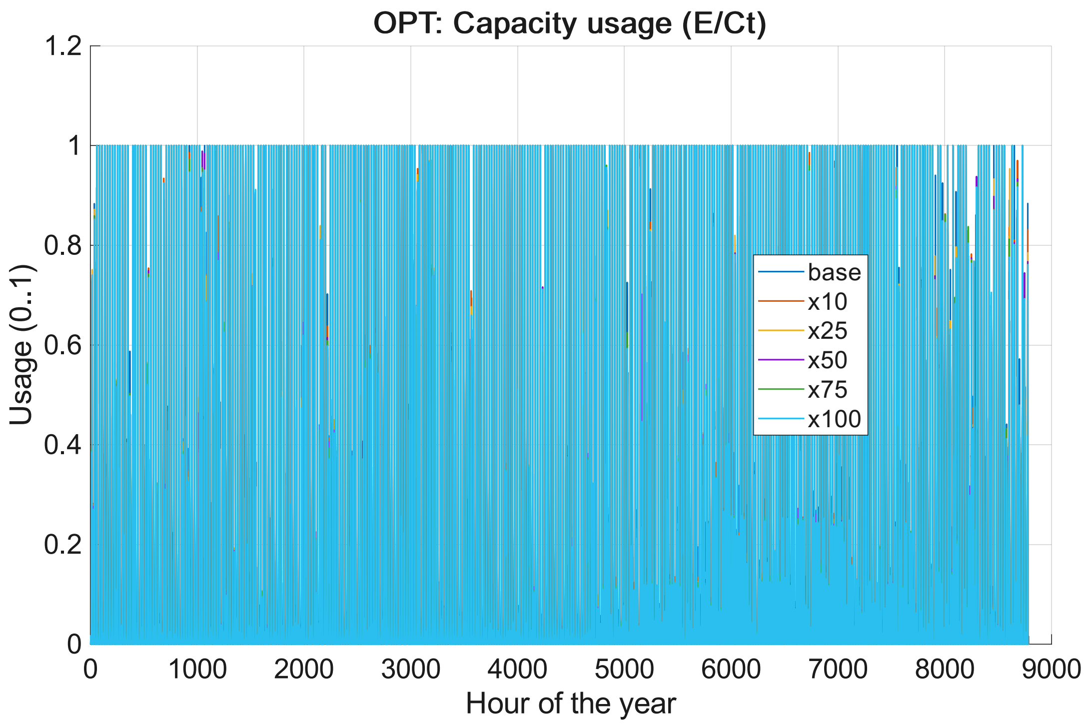

(a) Full annual profile

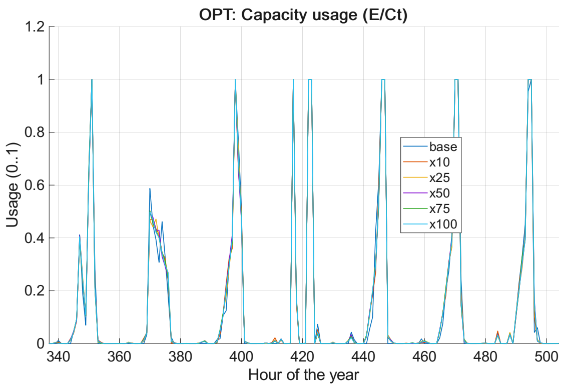

(b) Weekly view

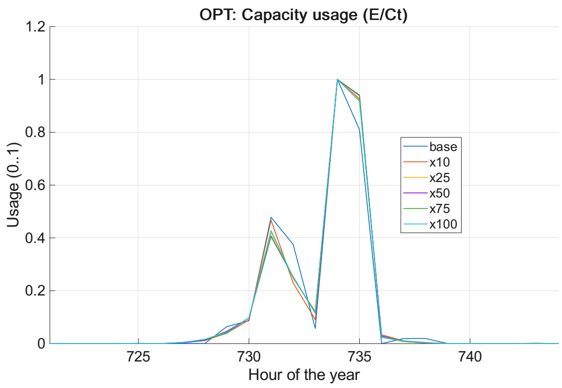

(c) 24-hour detailed view

Figure 3.20: MATLAB-generated graphs displaying the infrastructure capacity utilization factor (E/C_t) for the OPT strategy across different scaling scenarios: (a) Full annual simulation, (b) Weekly view, and (c) 24-hour detailed view. The full annual profile is included primarily to illustrate the macroscopic trend of infrastructure saturation and power limit, although the chart itself is highly condensed (simulations run with charging ports being 10% of the number of EVs). The detailed views confirm that the optimized profile scales robustly, maintaining a regular load-shifting pattern.

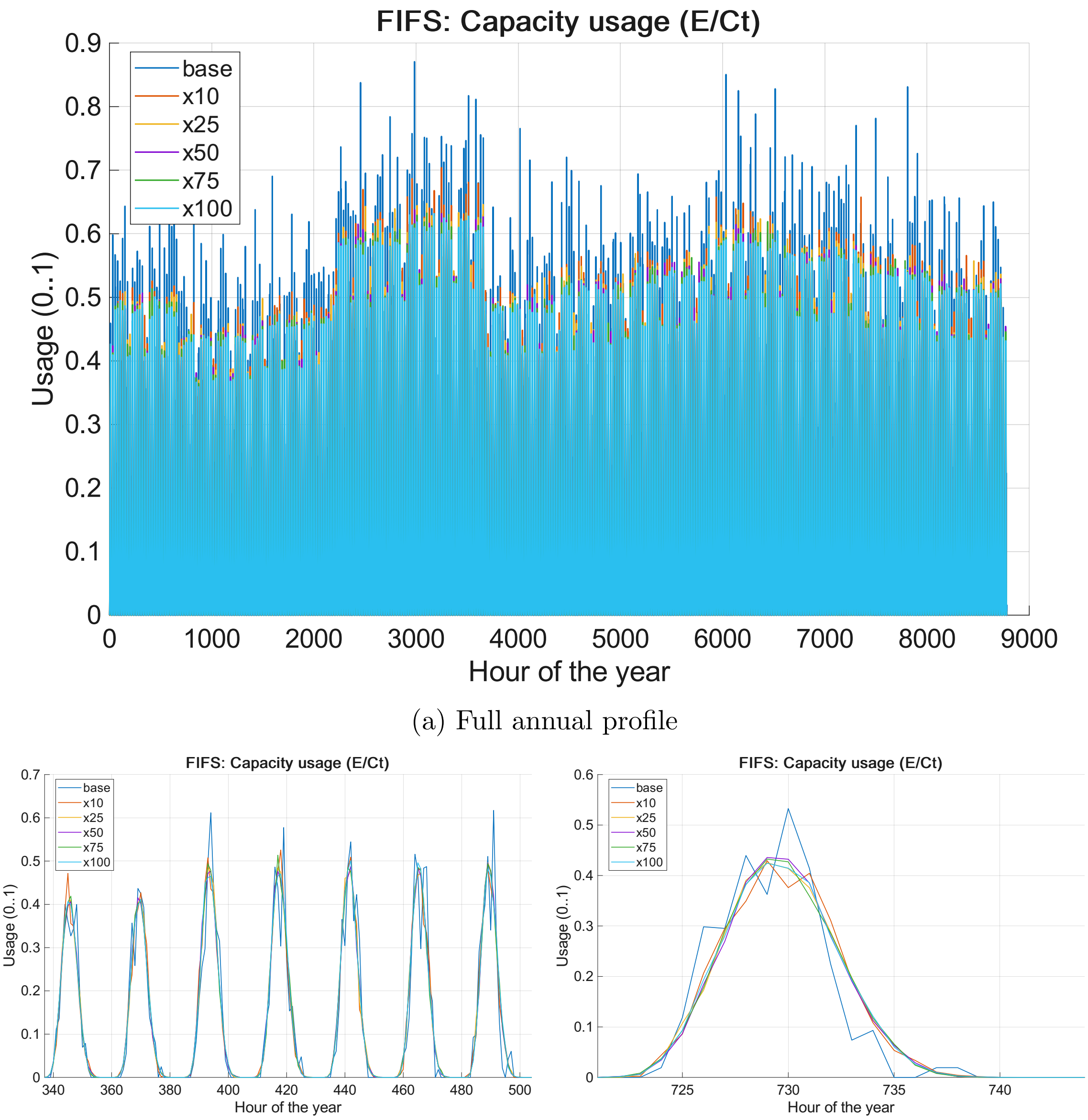

(a) Full annual profile

(b) Weekly view

(c) 24-hour detailed view

Figure 3.21: MATLAB-generated graphs displaying the infrastructure capacity utilization factor (E/C_t) for the FIFS baseline across different scaling scenarios: (a) Full annual simulation, (b) Weekly view, and (c) 24-hour detailed view. Unlike the optimized strategy, the FIFS baseline results in higher power peaks, showing a greater dependency on immediate charging dynamics.

optimized profile, once normalized relative to its sum or its maximum, tends to remain nearly invariant in shape as the scale changes (Figure 3.22). This strong correlation is quantitatively confirmed by the shape metrics presented in Table 3.8. In other words, when both the number of vehicles and the capacity are increased simultaneously, the optimized demand maintains a similar temporal pattern. The FIFS baseline, on the other hand, proved to be more sensitive to queue dynamics, showing less regularity and greater dependence on granularity and the service order, as seen in Figure 3.23.

Table 3.8: Comparison of load profile shapes (Shape metrics) against the base case.

Scenario	**OPT Strategy**			**FIFS Strategy**		
	Corr.	**RMSE**	**Max Diff**	**Corr.**	**RMSE**	**Max Diff**
x10	0.9876	3.75e-05	0.000721	0.9545	4.52e-05	0.000327
x25	0.9875	3.76e-05	0.000719	0.9564	4.43e-05	0.000274
x50	0.9874	3.77e-05	0.000721	0.9570	4.40e-05	0.000284
x75	0.9883	3.64e-05	0.000721	0.9573	4.38e-05	0.000288
x100	0.9874	3.76e-05	0.000721	0.9576	4.37e-05	0.000292

These results should not be interpreted as a universal rule, but rather as a useful guideline for justifying the subsequent sizing study. If the optimized profile is nearly invariant in shape, then the key design issue is not so much the temporal shape of the curve as the capacity level required to guarantee a given level of service and a certain annual cost.

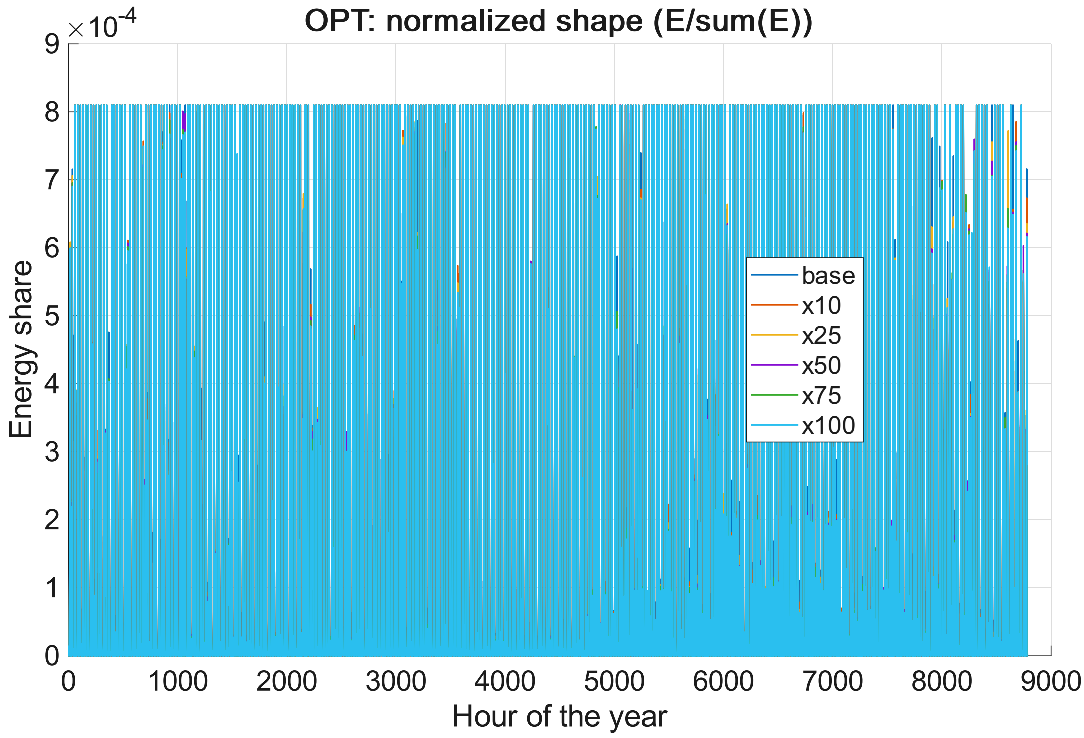

(a) Full annual profile

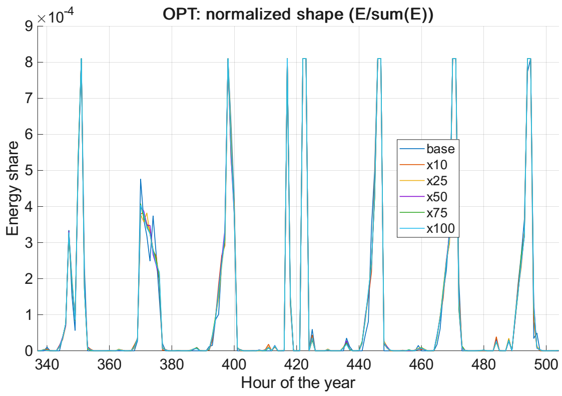

(b) Weekly view

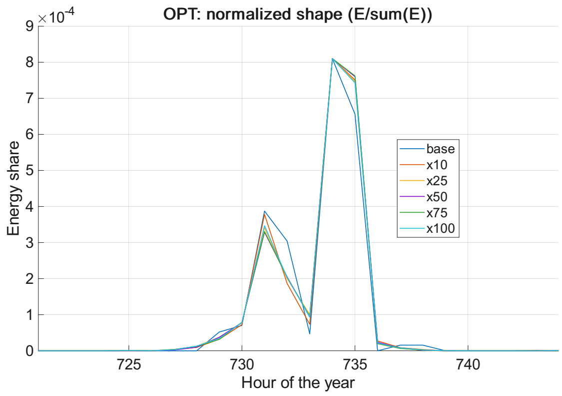

(c) 24-hour detailed view

Figure 3.22: MATLAB-generated graphs displaying the normalized load profile shape ($E/\sum E$) for the OPT strategy across different scaling scenarios: (a) Full annual simulation, (b) Weekly view, and (c) 24-hour detailed view. The annual profile shows the macroscopic distribution of demand. The perfect overlap of the curves in the detailed weekly and daily charts confirms that the optimized profile remains essentially invariant in shape as the system scales up.

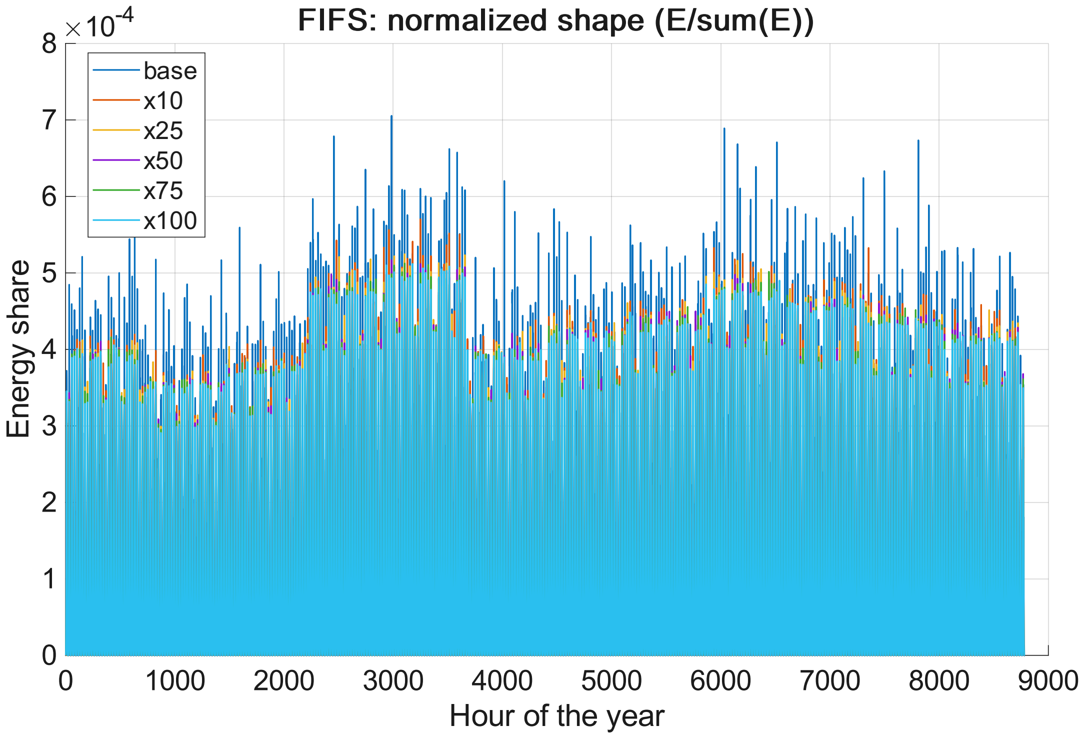

(a) Full annual profile

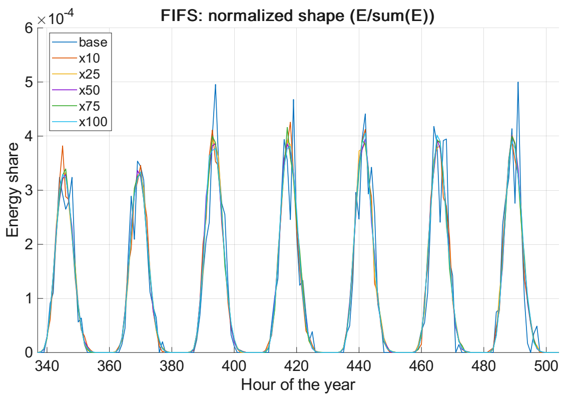

(b) Weekly view

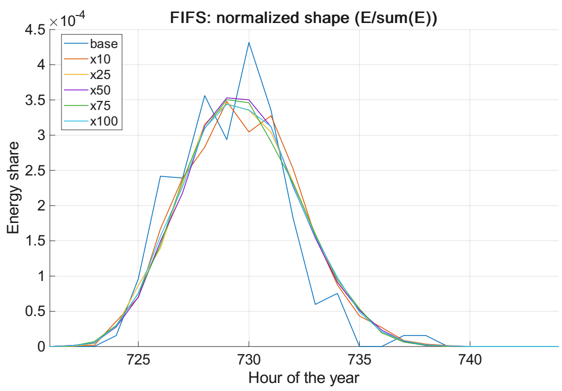

(c) 24-hour detailed view

Figure 3.23: MATLAB-generated graphs displaying the normalized load profile shape ($E/\sum E$) for the FIFS baseline across different scaling scenarios: (a) Full annual simulation, (b) Weekly view, and (c) 24-hour detailed view. The visible discrepancies show a lower degree of curve overlap compared to the OPT strategy, indicating higher sensitivity to scaling and queue dynamics.

3.8 Sizing study of the charging infrastructure

3.8.1 Project questions and scenario variables

After the annual model was defined and the main robustness and performance issues resolved, the focus naturally shifted to a sizing study of the charging infrastructure. The underlying idea was that, given the adopted calibration and the real price profiles, the aggregated capacity C_t might be oversized in many cases. Therefore, we asked ourselves two main questions.

The first concerns the level of service: for a given number of vehicles N, how much capacity C_t is needed to achieve a served ratio sufficiently close to one? The second concerns marginal returns: once near-complete service is guaranteed, how much further can the annual cost of charging be reduced by increasing C_t even more? In other words, is there a threshold beyond which additional capacity yields economical benefits that are too small to justify a further expansion of the infrastructure?

To answer these questions, grid simulations were constructed for pairs of (N, n_{ports}), where n_{ports} represents a design parameter interpreted as the equivalent number of charging ports of 22 kW, and:

$$C_t = \bar{p} \times n_{\text{ports}} \,. \tag{3.13}$$

Initially, the grid was defined in absolute values; subsequently, to avoid insignificant combinations at very different values of N, the list of values was expressed as a percentage of N, for example, 5%, 8%, 10%, 12%, etc.

3.8.2 Sizing metric

For each annual grid simulation, several metrics were collected. The most straightforward is the served ratio, which is the ratio between the annual supplied energy and the annual demanded energy. In addition to this, the following further metrics were calculated: the annual cost of optimized charging, the average cost per kWh supplied, the annual dissatisfaction, the so-called "social cost" defined as the energy cost plus the penalty γ multiplied by the dissatisfaction, and indicators of the capacity utilization, such as the average load factor and the 95th percentile of utilization.

Having these metrics available simultaneously provides a more comprehensive understanding of the results. An infrastructure that is too small may appear "cost-effective" if one looks only at the annual cost, but it is inadequate if the served ratio falls below the acceptable threshold. A very large infrastructure, on the other hand, may not increase the amount of energy delivered but can reduce costs by enabling a more effective shift towards low-price hours. The utilization metrics also help determine whether the installed capacity is being heavily utilized or remains largely underutilized.

3.8.3 Early-stopping rule for "cost-effective" sizing

To avoid overly long and uninformative sweeps, an early-stopping rule based on diminishing marginal gains was introduced. For each N, the values of n_{ports} are tested in ascending order. Once a service level considered acceptable is reached, for example, `served_ratio` ≥ 0.99, the relative improvement in energy cost between two consecutive capacities is measured. If this improvement falls below a predetermined threshold, chosen at 1%, the search is halted, and the previous point is considered a good approximation of the "cost-effective" sizing.

This rule should not be interpreted as a criterion for achieving a complete economic optimum. It does not explicitly account for investment costs or fixed infrastructure costs, and therefore does not yield a true economic optimum. However, in the context of this study, it serves as a reasonable engineering criterion to avoid evident oversizing and to identify the portion of the curve where additional benefits become very small.

The introduction of this heuristic is methodologically important because it makes explicit the distinction between technical feasibility and marginal benefit. The point at which the served ratio becomes approximately one does not necessarily coincide with the point at which the annual cost stops decreasing. In fact, there is an intermediate range in which the energy output remains constant, but the greater flexibility of C_t still allows for some additional savings by shifting the recharge to the most favorable hours. Beyond this interval, the residual benefits become increasingly modest.

3.8.4 Results and interpretation of the sizing study

The sizing study was conducted by evaluating different EV penetration scenarios, up to 100% of the total registered vehicle fleet in La Gomera (approximately 15 000 vehicles [10]). The results of the grid search showed a stable pattern across the simulated fleet sizes, characterized by three distinct operational regimes. First, undersizing the C_t capacity leads to served ratios below the unit and to non-negligible levels of dissatisfaction. Under these conditions, the annual cost may appear artificially low, but only because the system is not supplying all the demanded energy.

Second, once a sufficient capacity to ensure a served ratio close to one is reached, the annual energy delivered no longer increases substantially. However, the annual cost may continue to decrease, because the increased available capacity allows for an ever-greater portion of charging to be concentrated during the cheapest hours. This is precisely the section of the curve where the early-stopping rule applies.

Finally, a third regime emerges, in which further increases in C_t do not significantly change either the energy output or the annual cost. It is in this regime that the capacity appears oversized from the perspective of operational flexibility alone. The results, therefore, suggest that the sizing study should not be viewed as a problem of "maximizing capacity", but rather as a problem of finding a point where service, energy cost, and infrastructure complexity reach a reasonable compromise. The transition between these three regimes is illustrated in Figure 3.24, which plots the total annual optimized charging cost against the installed capacity C_t. The optimal compromise corresponds to the "knee" of these curves.

To provide a generalized sizing rule, the results were normalized and are shown in Figures 3.25 and 3.26. As expected, the normalization shows consistent behavior across all fleet scales: the optimal compromise invariably falls around an 8% port-to-EV ratio. Beyond this threshold, the curves flatten, with the optimized charging cost stabilizing around 170 €/yr per vehicle. This empirical evidence validates the adoption of an 8% port-to-EV ratio as a robust heuristic for the infrastructure design. Table 3.9 summarizes the optimal configurations extracted by the algorithm using the 1% marginal improvement early-stopping rule, confirming the stability of this ratio across the simulated scenarios.

Another important point concerns the choice of the candidate grid. If the values of C_t are tested with steps that are too large, the marginal improvement observed might reflect the artificial structure of the grid rather than the real geometry of the problem. For this reason, a robust procedure should consist of first executing a coarse sweep and then, eventually, refining the area around the point where the curve shows its "knee".

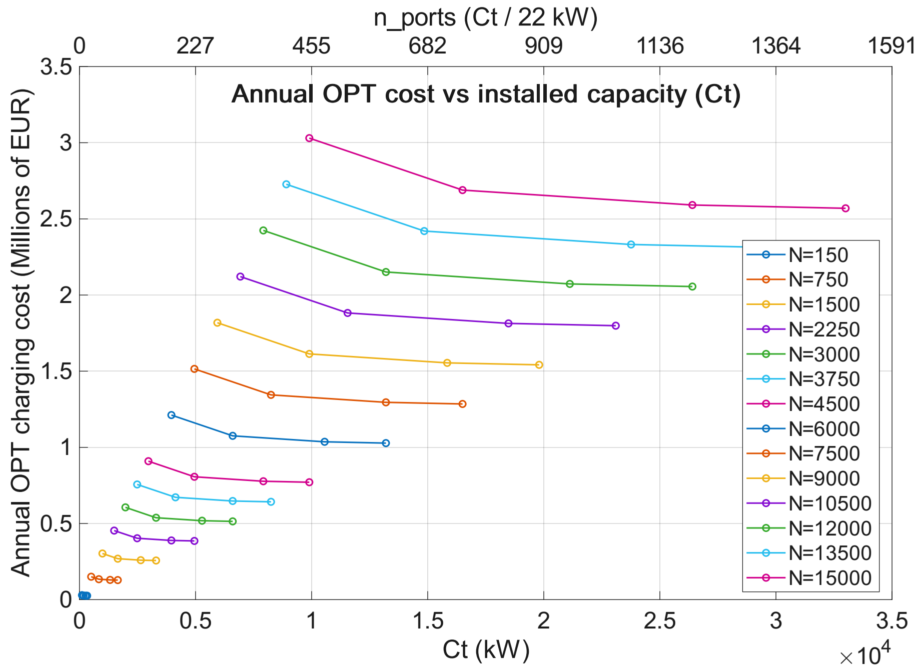

Figure 3.24: MATLAB-generated graph of the total annual optimized charging cost against the installed capacity C_t. The L-shape curves highlight the transition between undersized and oversized regimes.

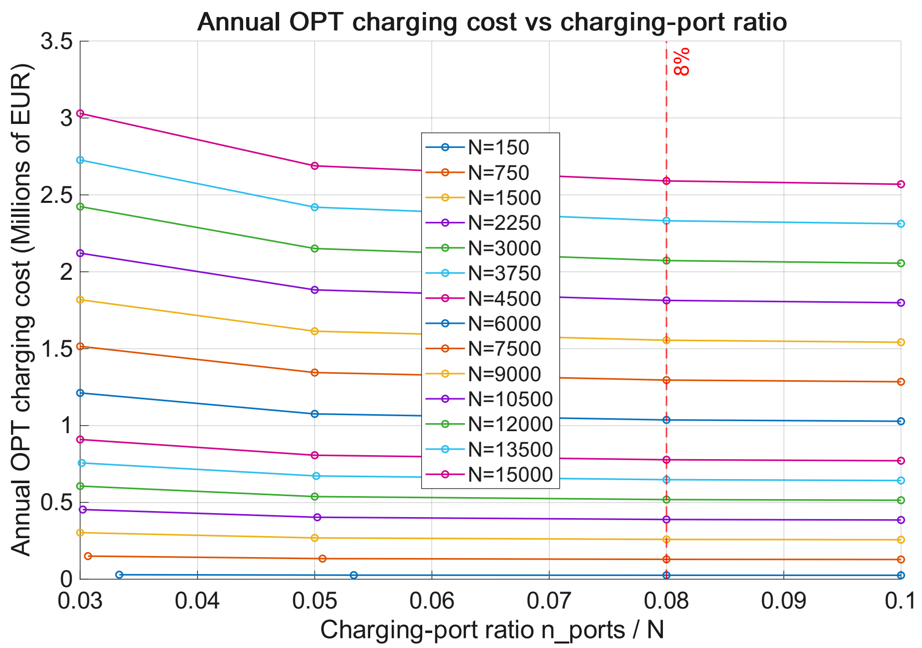

Figure 3.25: MATLAB-generated graph of the total annual optimized charging cost versus the charging-port ratio.

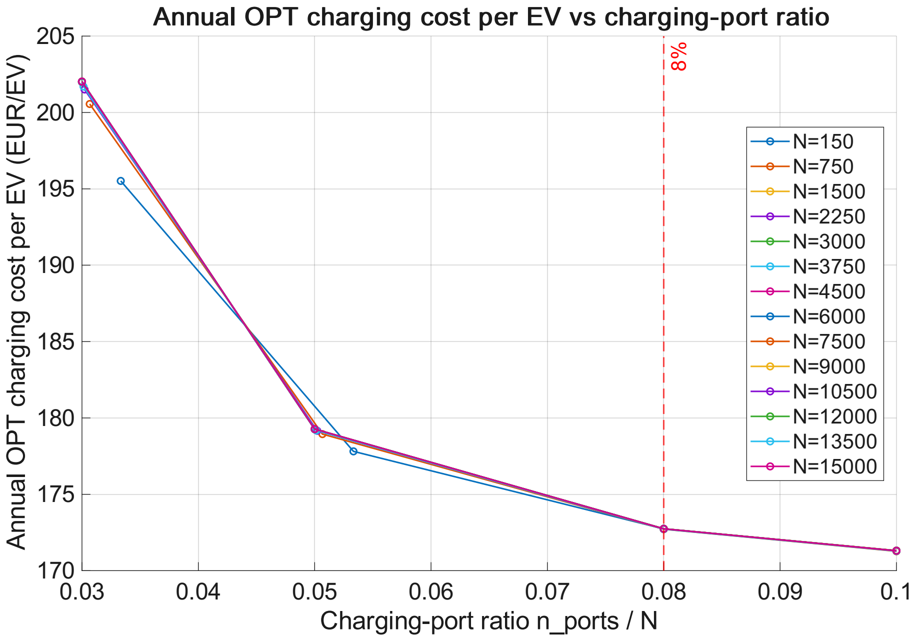

Figure 3.26: MATLAB-generated graph of the annual optimized charging cost per electric vehicle versus the charging-port ratio.

Table 3.9: Cost-effective infrastructure sizing and computational performance extracted via the 1% early-stopping rule for the year 2023.

Fleet N (Penetr.)	**Opt. Ports**	**Ratio (%)**	C_t **(kW)**	**Annual Opt. Cost (€)**	**Cost/EV (€/yr)**	**Runtime (min)**
150 (1%)	12	8.0	264	25,910	172.73	0.1
750 (5%)	60	8.0	1,320	129,536	172.72	0.2
1,500 (10%)	120	8.0	2,640	259,118	172.75	0.6
2,250 (15%)	180	8.0	3,960	388,649	172.73	1.1
3,000 (20%)	240	8.0	5,280	518,227	172.74	1.8
3,750 (25%)	300	8.0	6,600	647,695	172.72	2.6
4,500 (30%)	360	8.0	7,920	777,332	172.74	3.6
6,000 (40%)	480	8.0	10,560	1,036,402	172.73	5.9
7,500 (50%)	600	8.0	13,200	1,295,578	172.74	8.9
9,000 (60%)	720	8.0	15,840	1,554,629	172.74	12.4
10,500 (70%)	840	8.0	18,480	1,813,793	172.74	16.5
12,000 (80%)	960	8.0	21,120	2,072,963	172.75	21.2
13,500 (90%)	1,080	8.0	23,760	2,331,933	172.74	26.4
15,000 (100%)	1,200	8.0	26,400	2,591,128	172.74	32.3

Beyond the economic analysis, the grid search also provided valuable insights into the computational scalability of the model. Figures 3.27a, 3.27b, and 3.27c report the execution times required to solve the annual optimization across different combinations of N and C_t. As expected, the runtime increases non-linearly with the size of the fleet, but remains manageable thanks to the `linprog` formulation, validating the tool's applicability for more extensive parametric analyses.

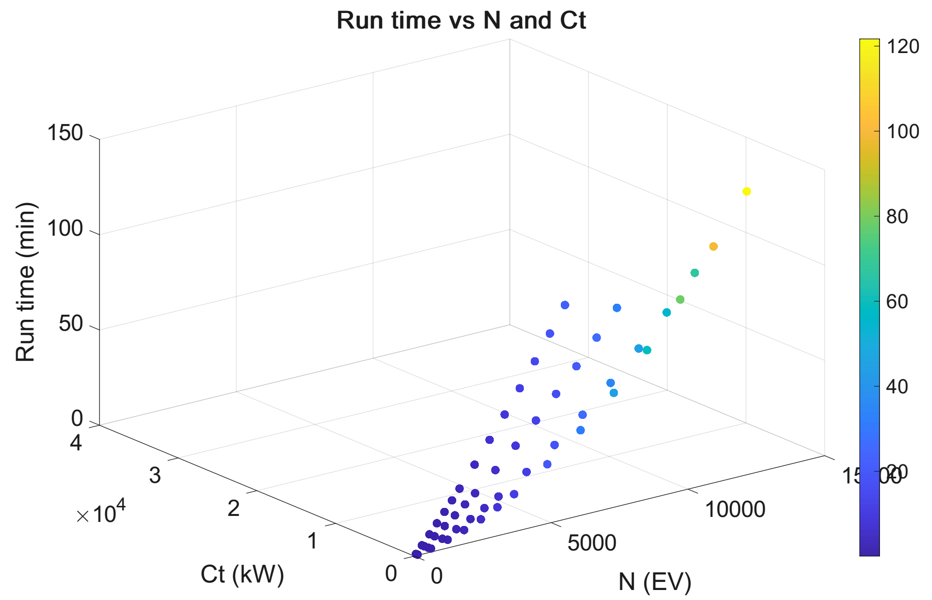

(a) Execution time vs N and C_t

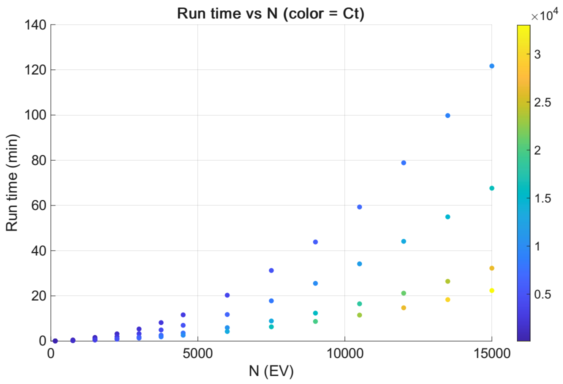

(b) Execution time vs Fleet size (N)

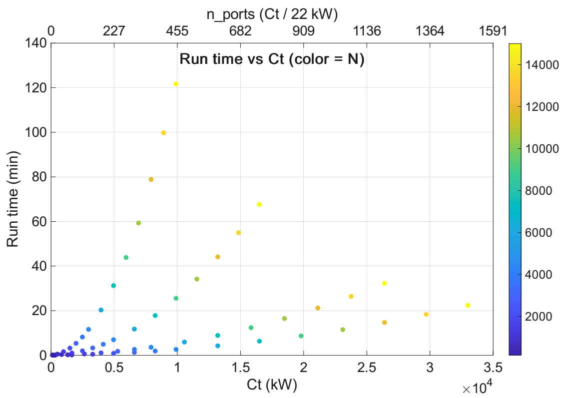

(c) Execution time vs Installed capacity (C_t)

Figure 3.27: MATLAB-generated graph of the computational scalability of the sizing sweep. The grid shows how the runtime scales with the parameters of the simulation.

3.9 Methodological discussion and limitations of the model

The model developed in this chapter was designed with a specific purpose in mind: to generate annual EV charging profiles that are consistent with price signals and capacity constraints, and that can serve as a basis for subsequent system analyses. From this perspective, the choice of an aggregated infrastructure with continuous capacity sharing, the use of synthetic arrivals and stops, and the anchoring of the daily demand to a target average value represent intentional trade-offs between realism, controllability, and computational cost.

These trade-offs also entail certain limitations. The model does not impose an integer number of vehicles connected simultaneously; therefore, it may overestimate the operational flexibility in contexts where the actual number of charging ports is limited, and fine-grained power sharing is not possible. Furthermore, the synthetic generation of EV behaviors does not constitute an empirical estimate of the mobility profile of La Gomera, but rather a simplified probabilistic framework calibrated to the overall energy scale. Finally, the presented sizing study in this chapter considers only the energy costs and does not include infrastructure investment, maintenance, or reinvestment costs. These observations are illustrated in Figure 3.28, positioning the developed model along the continuum of modeling approaches.

The mentioned limitations do not invalidate the model, but rather correctly define its scope of application. Its purpose is not to replace a real-time dispatch model or a detailed simulation of an individual station, but to provide a planning tool capable of quantifying, with methodological consistency, the potential for time-shifting EV demand and of generating annual charging profiles for use at the system level.

3.10 Conclusions of the chapter

This chapter outlined the development process of the smart charging model created in MATLAB for the case study of La Gomera. The work began with a daily prototype designed to compare a FIFS benchmark strategy with an optimized strategy based on linear programming, and subsequently evolved into a parametric, reproducible annual workflow that is sufficiently efficient to support scenario analysis and infrastructure sizing studies.

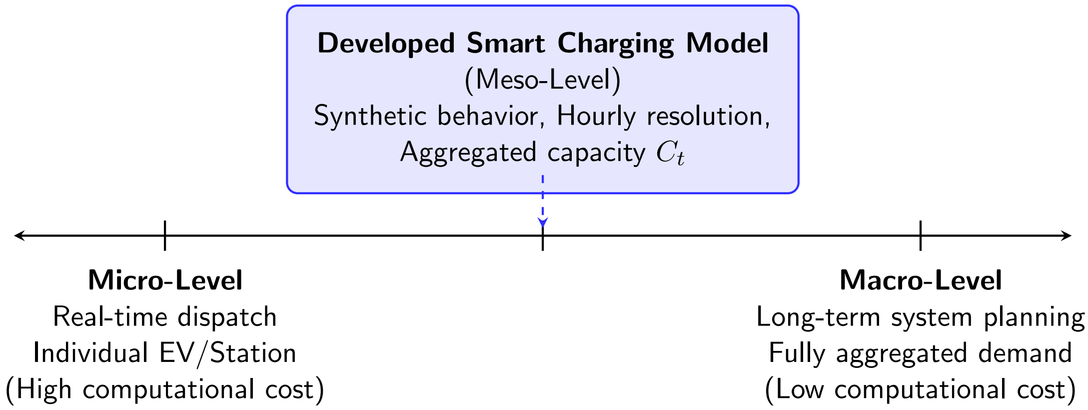

Figure 3.28: Positioning of the developed smart charging model along the continuum between operational micro-detail and macro-level system planning.

From a methodological standpoint, the most important findings of this chapter concern not only the final formulation of the problem, but also the clarifications that became necessary along the way: the proper handling of the temporal discretization, the distinction between power and energy, the consistency of the availability matrix, the need to prevent over-delivery in the presence of zero or negative prices, the separation between energy cost and dissatisfaction, and the establishment of a fair comparison between the heuristic baseline and the optimized model.

From an applied perspective, the chapter demonstrates that smart charging primarily functions as a mechanism for temporal reallocation of the demand, capable of reducing charging costs while maintaining the same total energy delivered, provided that sufficient capacity is available. In addition, it showed that the infrastructure design problem is not limited to achieving a level of service close to the unit, but also includes the issue of marginal returns on additional capacity, which can be effectively studied using parametric sweeps and early-stopping heuristics.

The final outcome of this chapter is therefore twofold. On the one hand, it provides a comprehensive description of the charging model on which the micro/meso component of the study is based. On the other hand, it provides the tools necessary for the next step of the thesis: the integration of the annual EV charging profiles into the energy system model of La Gomera, which is the subject of the following chapter. This integration framework is conceptually summarized in Figure 3.29. In this sense, this chapter serves as a bridge between the level of local demand management and the level of system analysis.

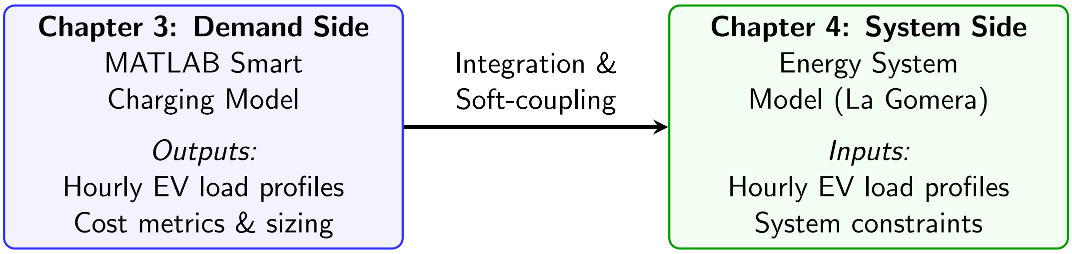

Figure 3.29: Conceptual bridge depicting the integration of the local demand management model developed in this chapter into the broader energy system analysis of the following chapter.

Chapter 4

Simulation of the model on EnergyPLAN

After developing the smart charging model described in the previous chapter, the next step in the project involved integrating it into a broader energy system model developed using EnergyPLAN. The goal of this phase was not only to use EnergyPLAN as a simulation tool, but also to build a coherent workflow that would allow the annual charging profiles for the electric vehicles generated in MATLAB to be correctly transferred into the case study of La Gomera.

The charging model developed in MATLAB allows us to describe how the EV demand can be distributed over time based on capacity constraints and price signals. However, on its own, it is not sufficient to asses the effect of this demand on the island's energy system. To analyze how charging affects the balance between generation and demand, the use of conventional fuels, emissions, and the overall behavior of the system, it is necessary to move to a higher level of simulation.

For this reason, EnergyPLAN was adopted and used as an annual simulation environment for the energy system of La Gomera. In this context, the EV demand is not treated as a simple annual aggregate value, but rather as an external hourly profile to be integrated into the model. This choice is consistent with the thesis' approach, as it allows for maintaining the link between the temporal detail obtained with the smart charging model and the system analysis conducted at the annual level.

A second relevant aspect concerns the fact that simulating a few isolated cases would not have been sufficient. A key part of the work was, in fact, dedicated to building an automated execution environment, in which MATLAB prepares the inputs, calls EnergyPLAN, collects the results, and organizes them in a format suitable for subsequent analysis. This workflow is visualized in Figure 4.1.

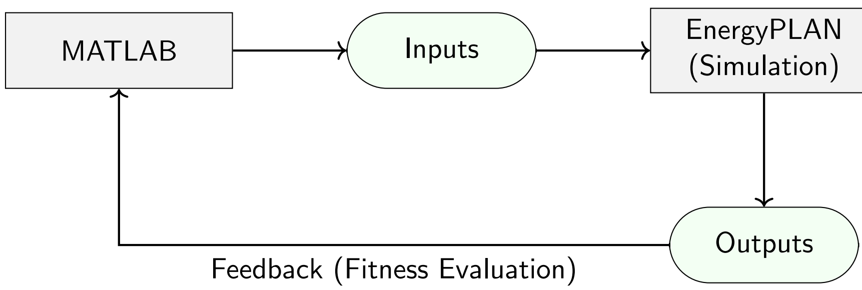

Figure 4.1: Simulation workflow and data exchange loop.

4.1 Energy system model purpose and chapter structure

In the specific case of this thesis, the integration phase in EnergyPLAN served a dual purpose. On the one hand, it helped build a reliable simulator for the case of La Gomera, in which the EV charging profile could be introduced consistently with the annual budgets of the transport sector. On the other hand, it constituted a baseline for a subsequent multi-objective optimization analysis, in which different combinations of renewable capacities and EV penetration were compared in order to minimize the mismatch (root-mean-squared error) between RES production and system's demand, and CO_2 emissions.

The chapter is organized as follows: Section 4.2 provides an overview of EnergyPLAN and introduces the validated La Gomera reference model. Section 4.3 describes the code architecture and the execution environment, detailing the workflow logic. Section 4.4 focuses on the model inputs, explaining the generation and transfer of the EV profiles, and the scaling of EV penetration to ensure absolute transport-energy consistency. Section 4.5 introduces the multi-objective exploration, outlining the optimization problem formulation, the genetic algorithm implementation, and the Pareto post-processing. Finally, Section 4.6 concludes the chapter with a methodological discussion.

4.2 Overview of EnergyPLAN and the La Gomera reference model

To comprehensively evaluate the impact of electric vehicle charging strategies on the island's energy balance, the simulator required a robust computational core. For this purpose, EnergyPLAN was selected. EnergyPLAN is a deterministic, input-output simulation freeware that allows for the analysis of regional and national energy systems with an hourly resolution [14]. It is widely recognized in the literature as a powerful tool to emulate the complex interactions across various energy sectors, including electricity, heating, cooling, industry, and transport [14]. By simulating the energy balances hour by hour, EnergyPLAN facilitates the identification of synergies among different sectors and allows for the precise evaluation of key environmental and technical indicators, such as fuel consumption, CO_2 emissions, and the temporal mismatch between renewable energy production and system demand [14].

A fundamental premise of this chapter is that the comprehensive energy system model of La Gomera was not built from scratch. Rather, the simulation relies on a robust and previously validated reference model developed in recent literature [14, 15]. These foundational studies successfully modeled the island's stationary energy demands, civil and industrial consumptions, and conventional generation constraints [14, 15]. Furthermore, the baseline model has been rigorously calibrated and validated against real-world operational data provided by the local transmission system operator (Red Eléctrica de España) and regional statistical institutes [14, 15].

By adopting this pre-existing and validated model as a baseline, the specific contribution of this thesis safely focuses on dynamically overwriting the parameters related to the transport sector and the renewable capacities. This approach ensures that the evaluation of the EV smart charging scenarios is grounded in a highly accurate and scientifically validated representation of the insular energy system.

4.3 Code architecture and execution environments

4.3.1 Problem setting and role of EnergyPLAN

The problem addressed in this chapter can be formulated simply: given an externally generated annual hourly EV charging profile, how can it be integrated into EnergyPLAN in a manner consistent with the energy system of La Gomera?

The answer requires two conditions. The first is that the EV profile is transferred in the correct format, respecting the internal logic of EnergyPLAN. The second is that this profile is consistent with the annual budgets of the transport sector. In fact, it is not enough to introduce an hourly demand distribution; it is also necessary to consistently update the annual values for electricity, diesel, and gasoline associated with mobility.

In this thesis, EnergyPLAN is therefore used as an annual energy system simulator, while MATLAB serves as an intermediate layer of input control and preparation. Conceptually, MATLAB defines and prepares the scenario, while EnergyPLAN returns the overall energy behavior. This distinction is important because it clarifies that the level of charging optimization and the level of system simulation do not coincide, but remain two distinct and complementary levels.

From a methodological standpoint, the integration of the EV profile into EnergyPLAN should not be viewed as a mere technical step, but as an essential part of the thesis' contribution. Indeed, it is precisely this integration that makes it possible to link the smart charging demand management with the assessment of the insular system as a whole.

4.3.2 Code architecture and workflow logic

The simulations in this study were performed utilizing the publicly available MATLAB Toolbox for EnergyPLAN (MaT4EnergyPLAN), developed by Cabrera et al. [13]. This tool allows for the seamless execution of EnergyPLAN via MATLAB, bridging the energy system analysis capabilities of the software with the computational and data management advantages of the MATLAB environment [13]. To make the overall workflow readable and easy to manage, the code is intrinsically organized into multiple layers, avoiding a monolithic structure, as shown in Figure 4.2.

At the first level is the La Gomera simulator launch script, used to define the design vector and test individual scenarios. In energy system modeling, the design vector is a mathematical array where each element corresponds to a specific decision variable, such as the installed capacities of various renewable technologies or the energy storage size [14, 15]. Essentially, it uniquely defines a potential configuration of the overall system to be evaluated by the simulator [14, 15]. In this thesis, the script's design vector was incorporated with EV penetration as an active decision variable alongside the aforementioned renewable capacities and storage.

At the second level is the main wrapper, implemented in the function `Simulator_wrapper_LaGomera`. This component plays a central role in the workflow, as it translates scenario parameters into inputs compatible with EnergyPLAN. In practice, the wrapper prepares the work folder, writes the necessary hourly profiles, selects the model reference file, constructs the set of parameters to be passed to the MATLAB toolbox, and organizes the outputs' paths.

The third level consists of a bridge function that actually calls EnergyPLAN and reads the results, identified in the project as `EnergyPLAN_GA_WWOPS`. This level interacts directly with the software executable by means of the toolbox cited above [13], and returns to MATLAB the annual and hourly variables necessary for the rest of the workflow.

The optimization procedure based on `gamultiobj` is then integrated onto these three levels, repeatedly calling the wrapper to explore different combinations of renewable capacity and EV penetration (*i.e.*, each corresponding to an individual of the genetic algorithm). Conceptually, genetic algorithms are metaheuristic search methods inspired by the principles of natural selection and evolution. They operate by initializing a population of candidate solutions and iteratively evolving them across generations, which makes them highly effective at identifying optimal or near-optimal trade-offs in complex mathematical problems.

The separation between these three architectural levels makes the code more manageable. In particular, it allows for a clear distinction between scenario definition, input preparation, and the actual execution of the simulation. This greatly facilitates debugging, as each error can be traced back to a specific level of the workflow.

4.4 Model inputs and transport-energy consistency

4.4.1 Generation, normalization, and transfer of annual EV profiles

Before they could be integrated into EnergyPLAN, the EV profiles had to be generated in MATLAB in a format consistent with the simulation's annual horizon. To this end, the annual code developed in the previous phase of the work was reorganized into a function that could be called from a separate script, in order to achieve

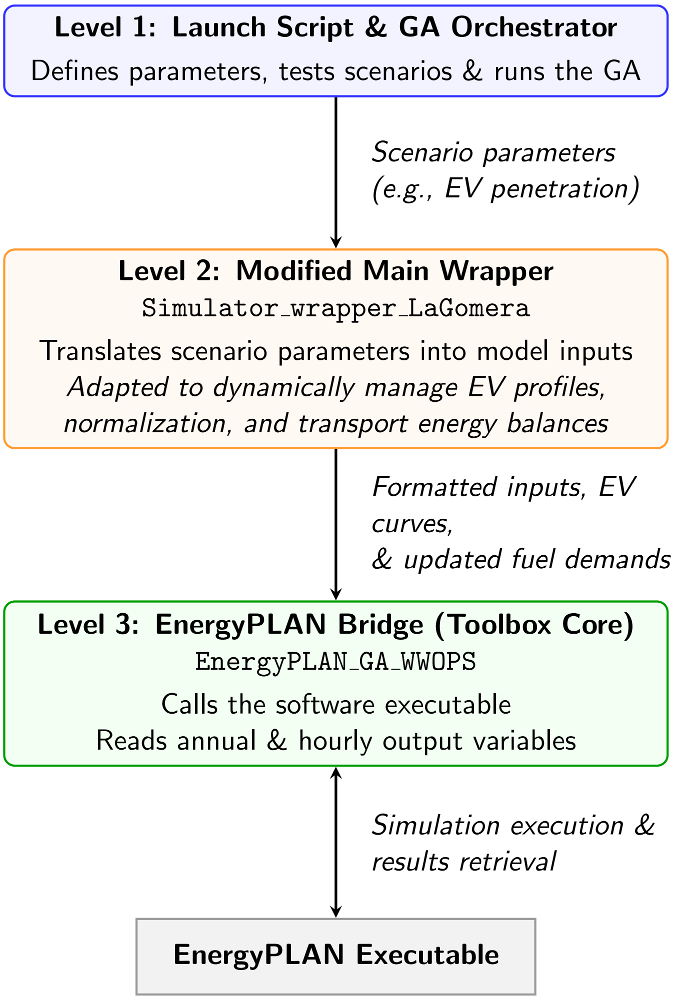

Figure 4.2: Three-layered architecture of the simulation workflow.

a more structured, reusable workflow, suitable for exporting results.

The annual model generates, for each charging strategy considered, a complete hourly vector covering the entire year. Specifically, two main profiles are available: one associated with the FIFS logic and one associated with the optimized strategy. In addition to the hourly vectors, the code also constructs daily aggregates, exports the results to Excel files, and saves the main outputs in a MATLAB structure, making them easily accessible in subsequent phases.

For the purposes of EnergyPLAN, however, having the absolute hourly energy values was not sufficient. The software requires a temporal distribution that is consistent with its internal structure. For this reason, the absolute annual profiles were combined with normalized versions, obtained by dividing each value by the annual maximum of the corresponding profile. As illustrated in Figure 4.3, this transformation alters only the vertical scale of the signal, resulting in a vector ranging from 0 to 1 that preserves the temporal shape of EV demand, but no longer directly represents the absolute energy. This distinction is important because the normalized profile defines the temporal distribution, while the total annual value is passed to EnergyPLAN via the transport sector parameters.

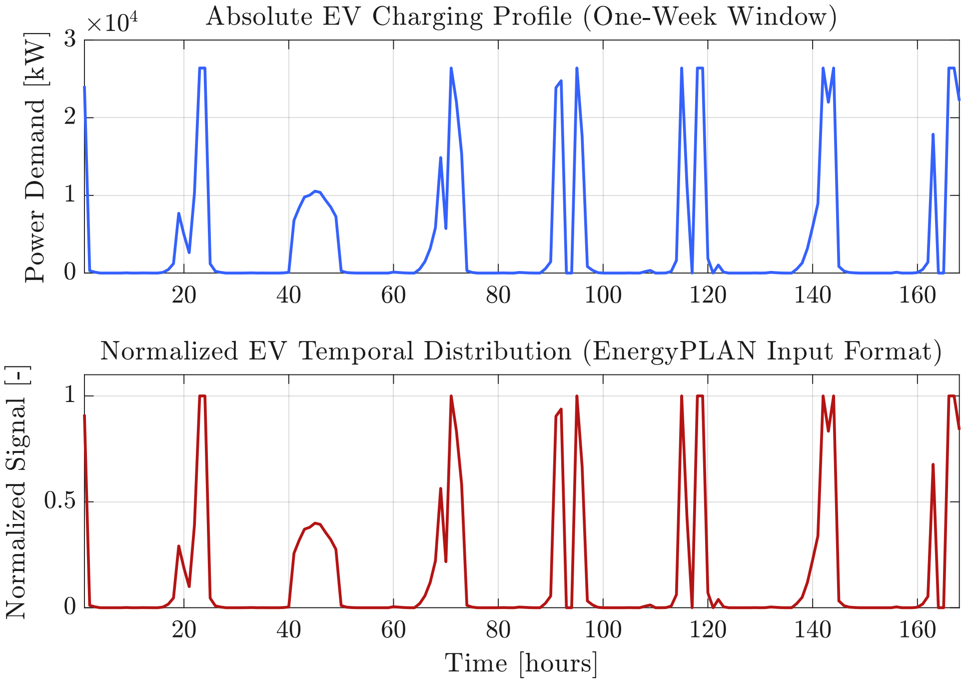

Figure 4.3: MATLAB-generated graph comparing the absolute EV charging profile in kW (top) and the normalized temporal distribution passed as input to EnergyPLAN (bottom).

From an operational standpoint, the normalized EV profile is written to a text file and then read by the EnergyPLAN wrapper. The file is read using a function such as `readmatrix`, which imports the vector and verifies its formal consistency. One of the most important checks concerns the length of the vector: in the specific case of the model used, the simulation required a file with 8784 values, consistent with a leap year. This control was treated as an integral part of the validation of the inputs, since even a minimal misalignment between the number of hours and the temporal structure of the simulation can compromise the correct functioning of the model.

In summary, the normalization of profiles and their transfer into a format compatible with EnergyPLAN serve as the operational bridge between the EV model developed in MATLAB and the system-level energy simulation.

4.4.2 Implementation of EV penetration and transport-energy consistency

A central focus of the work was how EV penetration was incorporated into EnergyPLAN. This variable could not be treated as a simple abstract parameter, but had to be made consistent with both the hourly charging profile and the annual values of the transport sector.

In the implemented workflow, the overall design vector is formally defined as an array $\mathbf{x} \in \mathbb{R}^7$. Consistent with the system configuration of the reference models [14, 15], the first six components of the vector dictate the renewable energy and storage capacities. Consequently, the EV penetration is integrated as the seventh component of this vector, referred to in the MATLAB environment as `x(7)`. In an initial formulation, this variable was treated as a selector for a discrete set of levels: 10%, 25%, 50%, 75%, and 100%. Each level corresponds to an annual hourly charging profile previously generated by the smart charging model.

From an operational standpoint, the value of the decision variable x_7 (implemented in the code as `x(7)`) is converted into an electric share, $EV_{\text{share}} = x_7/100$. Assuming 15 000 vehicles in the full penetration scenario, the number of electric vehicles associated with each scenario is then calculated as a proportion of this reference fleet. This value is subsequently used to select the corresponding annual profile and to construct the annual consumption data to be passed to EnergyPLAN.

The profile itself is imported into EnergyPLAN. However, this step alone is not sufficient. In addition to the temporal distribution, EnergyPLAN also requires consistent annual values for electricity and conventional fuels used in the transport sector. For this reason, the wrapper also calculates the annual electricity consumption associated with EVs based on the assumed average daily consumption, and consistently reduces the residual share of diesel as electric vehicle penetration increases.

The baseline assumption adopted in this study was 7.42 kWh/day per vehicle. At full penetration, corresponding to 15 000 vehicles and a 366-day year, the annual EV consumption was therefore calculated as:

$$E_{\text{EV,ann}} = \frac{7.42 \cdot N_{\text{veh}} \cdot 366}{10^6} \text{ GWh/y.} \tag{4.1}$$

This calculated value is then compared by the modified wrapper with the sum of the unnormalized annual profile, interpreted as annual energy, in order to verify the complete overall consistency of the transfer. At the same time, the residual annual consumption of diesel and gasoline is reduced in proportion to the share of non-electrified transport. In this thesis, these calculations and the reference transport energy values are directly derived from the validated La Gomera baseline models developed in recent literature [14, 15]. This ensures that the hourly charging profile and the annual transport balances remain strictly consistent with both the simulated scenarios and the consolidated energy framework of the island.Table 4.1 summarizes the exact scaling of vehicles, electrical demand, and fossil fuel reduction for the five simulated penetration scenarios, displaying the overall transport-energy consistency of the workflow.

Table 4.1: Transport sector energy balance scaling according to the investigated EV penetration levels.

EV Penetration	**Number of EVs**	**EV Electricity [GWh/y]**	**Residual Diesel [GWh/y]**	**Residual Gasoline [GWh/y]**
0% (Baseline)	0	0.00	83.32	64.74
10%	1 500	4.07	74.99	58.27
25%	3 750	10.18	62.49	48.56
50%	7 500	20.37	41.66	32.37
75%	11 250	30.55	20.83	16.19
100%	15 000	40.74	0.00	0.00

The consistency between the hourly profile and the annual quantity is one of the most methodologically important aspects of the entire workflow. Without this double check, the EV profile integrated into EnergyPLAN would risk representing an hourly demand that is formally correct but energetically inconsistent with the transport system considered.

4.5 Multi-objective scenario exploration via Genetic Algorithm

4.5.1 Definition of objectives and multi-objective formulation

Once the simulator was stabilized for individual scenarios, the workflow was extended to a multi-objective exploration. Following the mathematical framework established in recent EnergyPLAN-based optimization studies [15], the problem was formulated as a minimization problem aiming to simultaneously reduce the total annual CO_2 emissions and the energy generation-demand mismatch. The problem can be formally expressed as:

$$\min_{\mathbf{x} \in \mathcal{X}} \quad \mathbf{f}(\mathbf{x}) = \begin{bmatrix} CO_2(\mathbf{x}) \\ \phi(\mathbf{x}) \end{bmatrix} \tag{4.2}$$

subject to the boundary constraints of the design space $\mathcal{X}$:

$$\mathbf{x}_L \leq \mathbf{x} \leq \mathbf{x}_U \tag{4.3}$$

where $\mathbf{x} \in \mathbb{R}^7$ is the design vector containing the decision variables (i.e., the installed capacities of the different renewable technologies, storage capacity, and the EV penetration level), while $\mathbf{x}_L$ and $\mathbf{x}_U$ represent their respective lower and upper bounds.

The first objective function, $CO_2(\mathbf{x})$, quantifies the total annual carbon dioxide emissions of the energy system. The second objective function, $\phi(\mathbf{x})$, is defined as the Root Mean Squared Error between the annual time history of the total renewable energy production $\mathbf{E}_{RES} \in \mathbb{R}^{N_h}$ and the total annual electricity demand $\mathbf{D}_e \in \mathbb{R}^{N_h}$. This indicator, expressed in [MWh], is mathematically formulated as:

$$\phi(\mathbf{x}) = \sqrt{\frac{||\mathbf{E}_{RES}(\mathbf{x}) - \mathbf{D}_e(\mathbf{x})||^2}{N_h}} = \sqrt{\frac{1}{N_h} \sum_{h=1}^{N_h} \left(E_{RES}^h(\mathbf{x}) - D_e^h(\mathbf{x}) \right)^2} \tag{4.4}$$

where $|| \cdot ||$ indicates the Euclidean norm of the vector, N_h is the number of hours in the simulated year, E_{RES}^h is the total renewable energy generation at hour h, and D_e^h is the total electricity demand at hour h.

The indicator ϕ was used as a synthetic measure to evaluate how effectively the local renewable mix aligns with the energy demand. Lower values indicate a better match between the two quantities. CO_2 emissions, on the other hand, represent the environmental dimension of the problem and reflect the residual role of conventional generation in the system.

Unlike other recent studies conducted by the research group, in which the island's energy storage capacity was treated as an active decision variable [15], this study maintains a fixed battery storage level. This constant storage assumption relies on the system configuration and reference values established in [14]. Consequently, the multi-objective analysis focuses exclusively on two main objectives: mismatch (ϕ) and total CO_2 emissions. This choice makes the resulting Pareto front more readable and the interpretation of the trade-offs significantly clearer. The main variables explored by the optimization are therefore limited to the renewable installed capacities, specifically onshore wind, solar photovoltaic, and offshore wind. EV penetration was treated in two ways: as a fixed scenario, producing a Pareto front for each level, or as a discrete variable of the problem, allowing the genetic algorithm to select the most favorable EV level in the different regions of the objective space. A summary of the setup of the mathematical optimization problem is displayed in Table 4.2. Fixed system parameters, such as the 45 MWh battery storage, are directly defined in the model.

Table 4.2: Mathematical formulation of the multi-objective optimization model, summarizing the objective functions, decision variables, fixed parameters, and dynamic energy balances.

Model Component	**Symbol**	**Description, Domain, and Units**
		Objective Functions
Objective 1 (System Mismatch)	$\Phi_{\text{RMSE}}(\mathbf{x})$	Root Mean Squared Error of energy mismatch [MWh](to be minimized)
Objective 2 (Emissions)	$E_{\text{CO2}}(\mathbf{x})$	Total CO_2 Emissions [kt/y] (to be minimized)
		Decision Variables Vector ($\mathbf{x} \in \mathbb{R}^7$)
Onshore Wind Capacity	x_{WT}	Integer variable [MW] (Range: $[12, 50]$, Step: 1 MW)
Offshore Wind Capacity	x_{OWT}	Integer variable [MW] (Range: $[0, 50]$, Step: 1 MW)
Solar PV Capacity	x_{PV}	Integer variable [MW] (Range: $[0, 50]$, Step: 1 MW)
EV Penetration (Index 7)	x_7	Discrete variable [%] ($x_7 \in \{0, 10, 25, 50, 75, 100\}$)
		Fixed System Parameters
Battery Storage	E_{BESS}	45 MWh (Fixed reference capacity)
		Dynamic System Balances (dependent on x_7)
EV Electrical Demand	$E_{\text{EV,ann}}$	$15\,000 \cdot 7.42 \cdot 366 \cdot (x_7/100)$ [kWh/y] $\rightarrow$ [GWh/y]
Residual Diesel	$E_{\text{DSL,res}}$	$83.32 \cdot (1 - x_7/100)$ [GWh/y]
Residual Gasoline	$E_{\text{GSL,res}}$	$64.74 \cdot (1 - x_7/100)$ [GWh/y]

4.5.2 Genetic algorithm implementation

The automatic exploration of the multi-objective scenarios was implemented utilizing MATLAB's `gamultiobj` function. As detailed in recent literature concerning the optimization of the La Gomera energy system [14, 15], this built-in solver is based on a controlled elitist NSGA-II. As highlighted in these studies, this approach is particularly well-suited for solving complex, non-linear energy system design problems. It introduces a fast non-dominated sorting procedure and a crowding-distance metric to promote solution diversity, while its elitist strategy minimizes the risk of the optimizer getting stuck in local minima. Through the application of standard genetic operators, such as selection, crossover, and mutation, the algorithm efficiently explores the design space, progressively converging toward the optimal Pareto front.

To manage this iterative process efficiently, the final workflow is divided into three main components.

The first is an orchestrator script, which defines the parameters of the genetic algorithm, determines whether EV penetration should be treated as a fixed or variable scenario, and launches the optimization procedure. The second is the objective evaluation function (implemented in the `obj_la_gomera` script), which receives as input the decision vector from the GA, handles the mapping of the variables, calls the simulation wrapper, and mathematically returns, among the outputs, the values of the objective functions (ϕ and CO_2). The third is the save function, which stores the results of each generation and reorganizes them at the end of the run.

During the optimization, the GA evaluates each individual through this dedicated evaluation function. For scenarios with fixed EV penetration, the evaluation function receives only the renewable capacities as inputs from the GA, assigns a predetermined EV penetration value, and calls the wrapper to compute the objective functions. In the case of variable EV penetration, the EV share is treated by the GA as a fourth decision variable, which the evaluation function then maps to the discrete levels supported by the model before calling the wrapper. Renewable capacities are also treated at an operational level as integer values in 1 MW steps, obtained by rounding the continuous values proposed by the genetic algorithm. The complete iterative process of the GA is visually summarized in Figure 4.4.

4.5.3 Pareto post-processing and overlay analysis

Once the GA simulations were completed, a post-processing phase was carried out to reconstruct and visualize the Pareto fronts. For this purpose, a separate script was used, designed to read the saved `.mat` files, select the complete cloud of evaluated solutions, and calculate, a posteriori, the Pareto front over the complete set of points. Reconstructing the front starting from the entire cloud of evaluations provides a

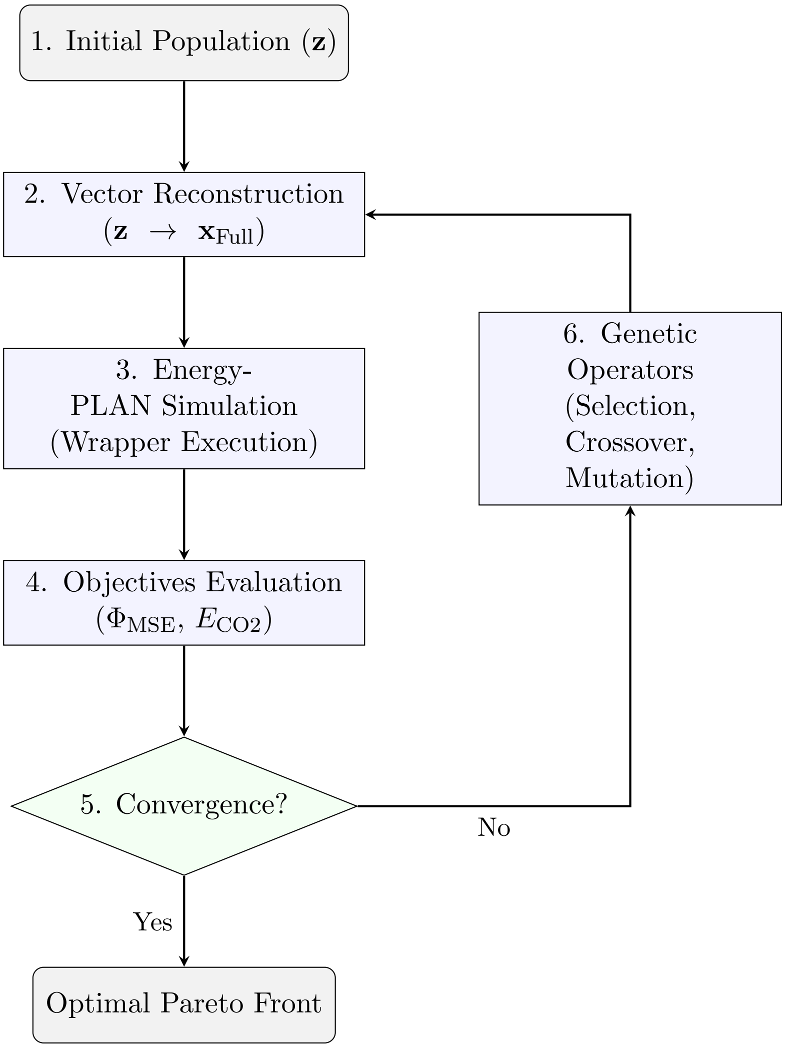

Figure 4.4: Flowchart of the multi-objective optimization loop using a genetic algorithm.

complete representation of the explored space.

The post-processing script allows for generating both cloud plots with their corresponding Pareto front and plots that only show the front. In addition, overlay plots were constructed in which the fronts corresponding to different levels of EV penetrations are compared. When EV penetration is treated as a variable, the points can be colored according to the corresponding EV level, thereby making it visible which penetration levels dominate different regions of the objective space. A detailed interpretation of these fronts is more appropriately covered in the next chapter, but it must be recalled here to underline that the post-processing does not merely visualize the GA's output: it constructs a more comprehensive interpretation that allows for comparisons across scenarios.

4.6 Methodological discussion and chapter conclusion

The work presented in this chapter shows how the smart charging model has been integrated into a system simulator such as EnergyPLAN.

From this perspective, there are three key elements in this chapter. First, the use of the MATLAB toolbox for EnergyPLAN made it possible to incorporate the EV profiles as time-series distributions consistent with the system model. Second, the wrapper-based structure allowed for a clear separation between the definition of the scenario and its translation into simulation inputs. Finally, the extension to a multi-objective procedure transformed the single-scenario simulator into a true tool for exploring the trade-off between mismatch and emissions.

It is important to emphasize that this chapter does not exhaust the scientific discussion of the results. Its primary purpose is to establish and document the method. The significance of the Pareto fronts, the role of the different levels of EV penetration, and the interpretation of the most favorable renewable energy combinations will be addressed in the next chapter. In this sense, this chapter constitutes the methodological foundation upon which the analysis of the results is based.

Chapter 5

Simulations' results and interpretation

Building upon the development of the smart charging profiles and their integration into the EnergyPLAN simulator, this chapter focuses on the final results of the multi-objective system simulation. The objective is to interpret the energy configurations obtained for the island of La Gomera, analyzing the trade-offs that emerge between the mismatch indicator (ϕ) and CO_2 emissions.

Through the use of genetic algorithms, different scenarios were evaluated to explore how the system's efficient frontier changes as renewable capacities and electric vehicle penetration vary. The question this chapter addresses is no longer merely when it is most cost-effective to charge vehicles, but rather which system configurations prove efficient when this electrified demand is incorporated into the annual energy budget of the island.

5.1 Scope, structure, and interpretation of the results

The chapter is organized to progressively analyze the system's response to transport electrification. Section 5.2 constitutes the core of the analysis, exploring the multi-objective optimization outputs. Specifically, it evaluates system performance under fixed EV scenarios, compares their hierarchical dominance, analyzes EV penetration as an active decision variable, and breaks down the resulting renewable energy mix.

Subsequently, Section 5.3 broadens the perspective by discussing the systemic implications of smart charging alongside the methodological limitations of the study. Finally, Section 5.4 summarizes the main findings of the chapter.

Before discussing the quantitative results, it is helpful to briefly clarify how the optimization outputs should be interpreted. In the graphs presented in the following sections, the "cloud" represents the entire set of configurations actually evaluated by the genetic algorithm. The broadness of this cloud illustrates how widely dispersed the simulated configurations are. The "Pareto front" (highlighted in a different color) identifies the non-dominated configurations along the boundary of that space; for these points, no other evaluated solution exists capable of simultaneously improving both objectives. Consequently, the front should not be interpreted as a single optimal solution, but as a set of efficient alternatives. Finally, the "global Pareto" set refers to the absolute non-dominated frontier constructed by simultaneously considering all the points evaluated across various scenarios.

5.2 Analysis of the results

5.2.1 Performance under fixed EV penetration scenarios

The first set of results concerns scenarios where the level of transport electrification is fixed prior to the genetic algorithm optimization. The advantage of this approach is that it allows us to isolate the effect of the renewable mix within each specific EV penetration level. To provide a comprehensive evaluation, the analysis encompasses the full spectrum of simulated penetration levels: 10%, 25%, 50%, 75%, and 100%, visually represented in Figures 5.1a to 5.1e.

For each scenario, the genetic algorithm explores combinations of renewable capacity, generating a dense cloud of evaluated configurations from which the Pareto front is extracted. A fundamental observation is that the morphological structure of the Pareto fronts remains remarkably consistent across all simulated EV levels. They all exhibit a distinct convex, L-shaped profile. This geometric similarity indicates that the core physical trade-off governing the island's energy system remains unchanged regardless of the EV fleet size: pushing the system towards near-zero emissions requires exponentially higher investments in renewable capacity, which inevitably leads to a massive increase in the demand-production mismatch (ϕ) due to overgeneration.

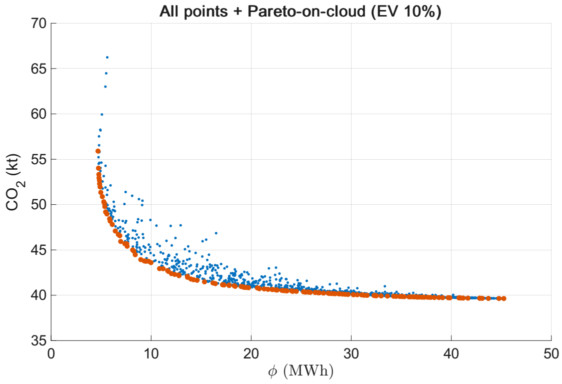

(a) 10% EV penetration

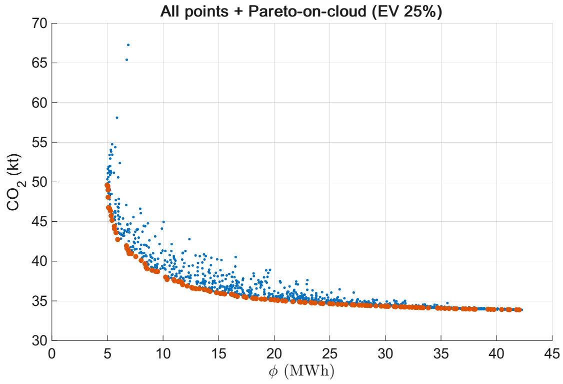

(b) 25% EV penetration

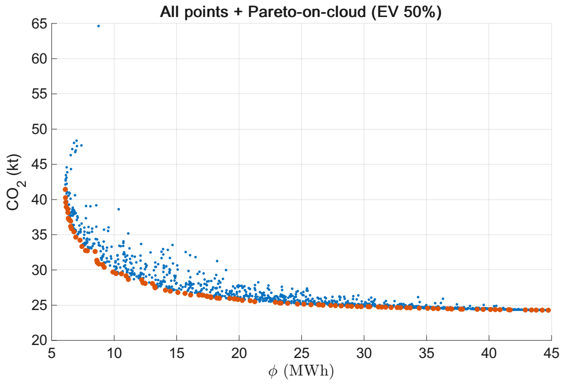

(c) 50% EV penetration

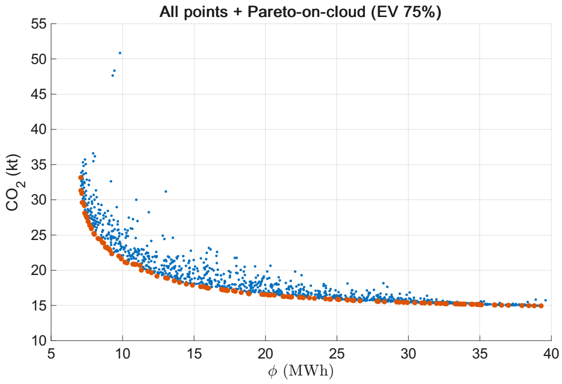

(d) 75% EV penetration

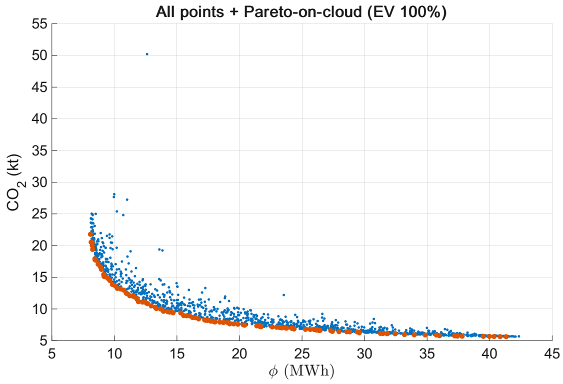

(e) 100% EV penetration

Figure 5.1: MATLAB-generated graphs showing the cloud of evaluated solutions and Pareto fronts (highlighted) across different fixed EV penetration scenarios.

However, while the shape is consistent, synthesizing the results across all levels reveals a structural shift in the absolute boundaries of the explored space. Taking the extreme cases as reference, in the 10% EV scenario (Figure 5.1a), the non-dominated solutions are bounded within a high-emission region. CO_2 values struggle to drop below the 40 kt threshold, while the mismatch reaches extreme values, up to 45 MWh. This high mismatch is a direct consequence of the algorithm exacerbating the renewable capacities in a forced attempt to lower the emissions, which are fundamentally bottlenecked by the fossil fuels still consumed by the non-electrified transport sector.

As the penetration increases progressively through the intermediate levels (Figures 5.1b to 5.1d) up to the 100% scenario (Figure 5.1e), the entire cloud of evaluated configurations shifts systematically downwards. Interestingly, the mismatch indicator ϕ at the optimal trade-off point (the "knee" of the curve) exhibits a slight rightward shift, increasing by approximately 5 MWh from the 10% to the 100% scenario. This modest increase is an expected consequence of the higher absolute electricity demand introduced by the fully electrified fleet. Nevertheless, it is primarily the CO_2 emission level that dictates the macroscopic structural difference, shifting the curves downwards. Each incremental step in EV penetration lowers the minimum achievable emissions, clearly indicating that optimizing the renewable mix alone is insufficient if the penetration level restricts the available load flexibility and keeps the fossil-fuel baseline high.

5.2.2 Cross-scenario comparison and impact of EV penetration

Comparing the different levels of EV penetration is the core of the system-level analysis. While individual fronts show the trade-off within a specific boundary, overlaying them on a single graph reveals how the overall system's efficient frontier structurally changes as the share of electrified mobility increases. The overlay comparison is not intended to automatically identify a "best" level in an absolute sense, but rather to understand in which regions of the objective space each level is competitive.

As shown in Figure 5.2, the overlay plot of all simulated cases highlights a strict hierarchical dominance. The fronts stack sequentially without intersections: the 10% EV front sits at the top (highest minimum emissions), followed downward by the 25%, 50%, and 75% fronts, culminating in the 100% EV penetration front, which strictly dominates all lower penetration scenarios across the entire objective space. By shifting from a 10% EV share to a 100% EV share, the absolute minimum achievable CO_2 emissions for the island decrease from approximately 40 kt to less than 10 kt.

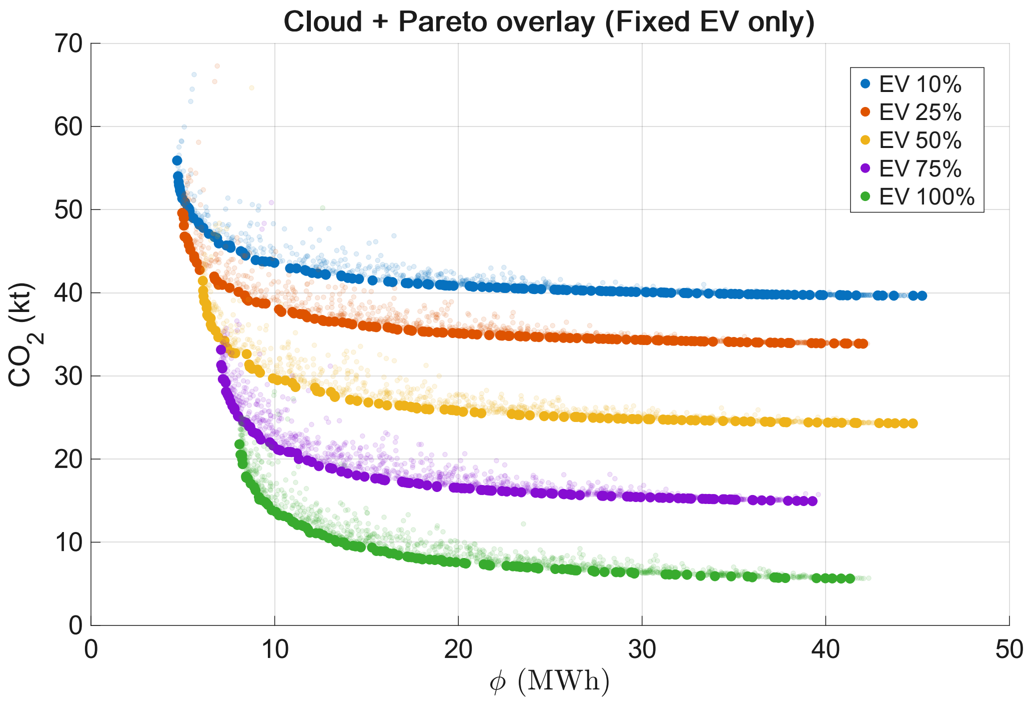

Figure 5.2: MATLAB-generated graph overlaying the Pareto-on-cloud frontiers for all fixed EV penetration scenarios, illustrating the strict hierarchical dominance of higher electrification levels.

This strict dominance is explained by the combination of two physical effects. First, achieving 100% EV penetration physically removes the consumption of diesel and gasoline from the transport sector (as modeled in Chapter 4), establishing a fundamentally lower baseline for the island's CO_2 emissions.

Second, the charging profiles integrated into the system were optimized in Chapter 3 to minimize charging costs. Because low wholesale electricity prices strongly correlate with periods of high renewable energy generation, this cost-driven strategy naturally forces the EVs to charge when there is an excess of solar or wind power.

Consequently, the 100% EV fleet does not act as a rigid, problematic load, but rather as a massive, highly flexible buffer. The genetic algorithm leverages this available flexibility to absorb renewable overgeneration, allowing the system to simultaneously reach the lowest possible emissions and minimize the generation-demand mismatch.

5.2.3 EV penetration as an active decision variable and Global Pareto analysis

To further validate the systemic role of transport electrification, a specific scenario was formulated in which EV penetration was not fixed, but rather treated as a discrete decision variable directly accessible by the genetic algorithm. In this formulation, the algorithm evaluates configurations by actively selecting the EV share from the allowed levels (10%, 25%, 50%, 75%, 100%) during the optimization run.

Figure 5.3 visualizes the results of this EV-variable simulation. The evaluated points forming the cloud and the Pareto front are colored according to the specific EV penetration level selected by the algorithm for each configuration. This visualization reveals a sophisticated behavior of the optimizer. The algorithm does not simply collapse onto a single EV level; instead, it dynamically adapts the EV penetration based on the specific region of the trade-off it is exploring. In the central and lower regions of the graph, where minimizing CO_2 is the priority, the algorithm systematically converges toward the 100% EV penetration level. However, to reach the absolute minimum mismatch (the extreme left, high-emission region of the objective space), the algorithm must select progressively lower EV penetrations, climbing up the y-axis through 75%, 50%, 25%, and finally 10%. This occurs because a smaller EV fleet inherently reduces the total energy production of the island, allowing for a tighter temporal match with the renewable generation, albeit the cost of leaving fossil-fueled vehicles on the road.

To compare the behavior of this active search with the previously discussed fixed scenarios, Figure 5.4 displays an overlay of all fixed-scenario fronts alongside the newly generated EV-variable front (represented by the light blue line). Given a sufficient number of simulations, the EV-variable scenario faithfully traces and stitches together the optimal segments of all the individual fixed profiles. It perfectly overlaps the 100% fixed scenario at the absolute optimal CO_2 boundary, and seamlessly transitions to trace the lower penetration fronts in the high-mismatch/high-emission regions. This confirms that transport electrification acts as a primary design variable: when the algorithm searches for the absolute optimum, it inherently maximizes the EV share to leverage fossil fuel reduction and load flexibility, but it mathematically acknowledges lower penetrations as the only physical pathway to absolute zero-mismatch conditions.

Finally, to establish the absolute non-dominated boundary of the entire study, a

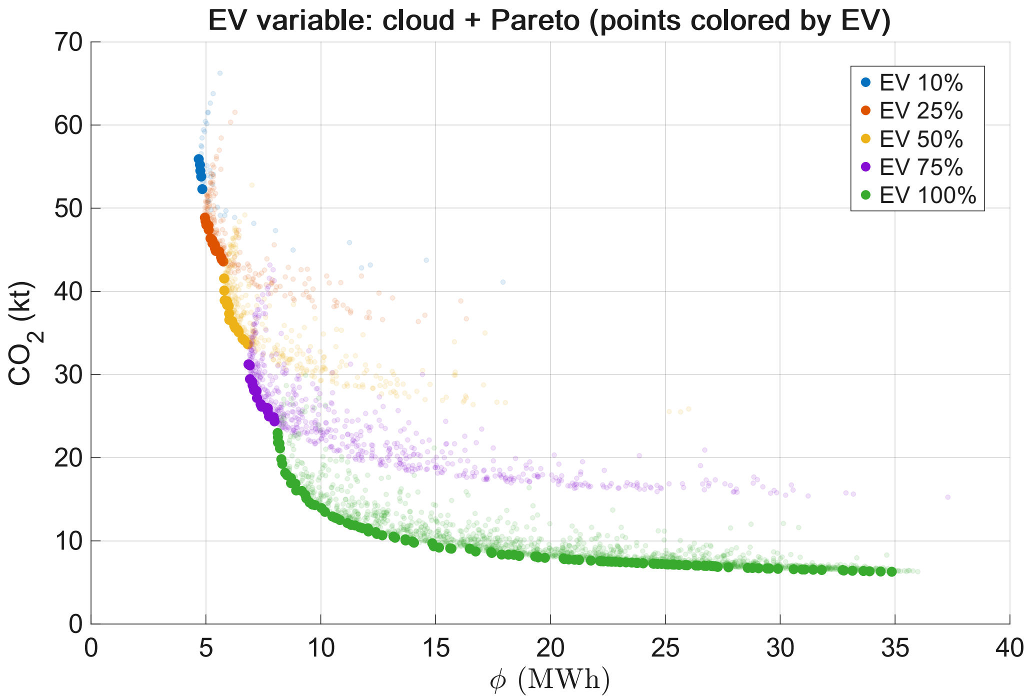

Figure 5.3: MATLAB-generated graph of the optimization cloud and Pareto front for the EV-variable scenario, with points colored by the EV penetration level actively selected by the genetic algorithm.

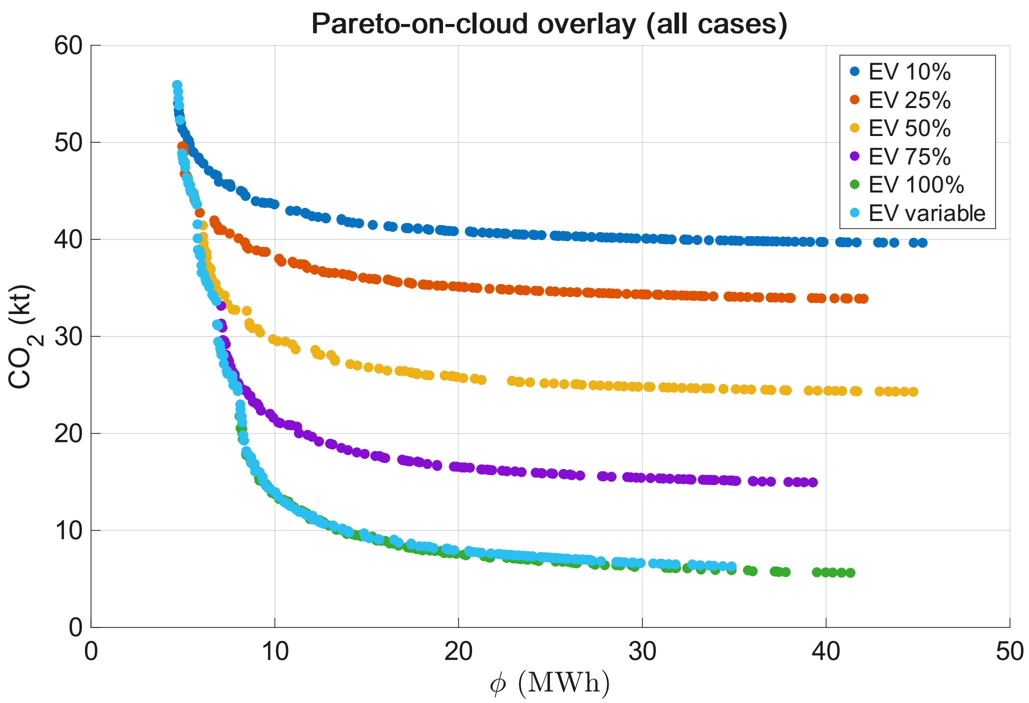

Figure 5.4: MATLAB-generated graph overlaying the Pareto fronts for all fixed EV penetration scenarios alongside the EV-variable scenario (light blue).

"Global Pareto" analysis was conducted, as shown in Figure 5.5. It is crucial to clarify the conceptual and structural difference between the EV-variable scenario and the Global Pareto analysis.

The EV-variable scenario discussed above represents a new, independent simulation run where the EV share is actively manipulated by the algorithm as a decision variable. Conversely, the Global Pareto is obtained through a post-processing extraction. It is constructed by aggregating all the individual simulations performed across all the fixed EV penetration scenarios into a single, massive point cloud. The Pareto front is then recalculated over this entire combined dataset.

This difference is methodologically important: it is not a simple visual overlay of lines on a graph, but a rigorous search for the non-dominated solutions across every single system configuration evaluated during the project. While the visual outcome is highly similar (both the EV-variable front and the Global Pareto front ultimately converge on the 100% EV configurations) the Global Pareto mathematically guarantees the identification of the absolute best trade-offs explored throughout the study. It definitively confirms that the dominance of high EV penetration is a structural, physical characteristic of the island's energy system, rather than an artifact of a single optimization run.

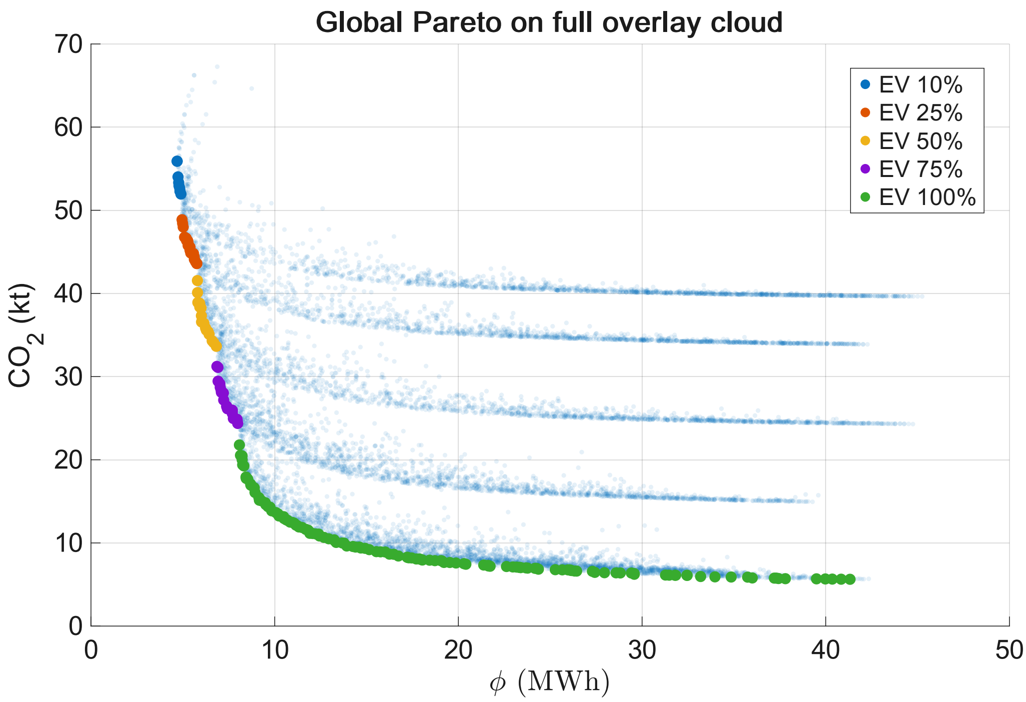

Figure 5.5: MATLAB-generated graph of the global Pareto analysis: the absolute non-dominated frontier extracted by post-processing the combined cloud of all simulations performed across the different EV penetration scenarios.

5.2.4 Renewable mix along the Pareto front

Analyzing the renewable energy mix allows us to answer questions that the (ϕ, CO_2) front alone does not clarify. For example, it allows us to observe whether solutions with low emissions require a greater share of a specific technology, whether renewable shares remain stable along the front, or whether they change significantly when moving from one region of the trade-off to another. In this sense, analyzing the composition of the mix transforms the Pareto front from an abstract numerical result into a set of interpretable energy configurations. A Pareto point does not simply represent a pair of objective values; it represents a complete physical configuration of the system.

Figure 5.6 illustrates both the absolute installed capacities (top subplot) and the relative percentage share (bottom subplot) of the renewable sources along the global Pareto front. Observing the capacity trends, distinct and well-defined technological roles emerge depending on the region of the trade-off.

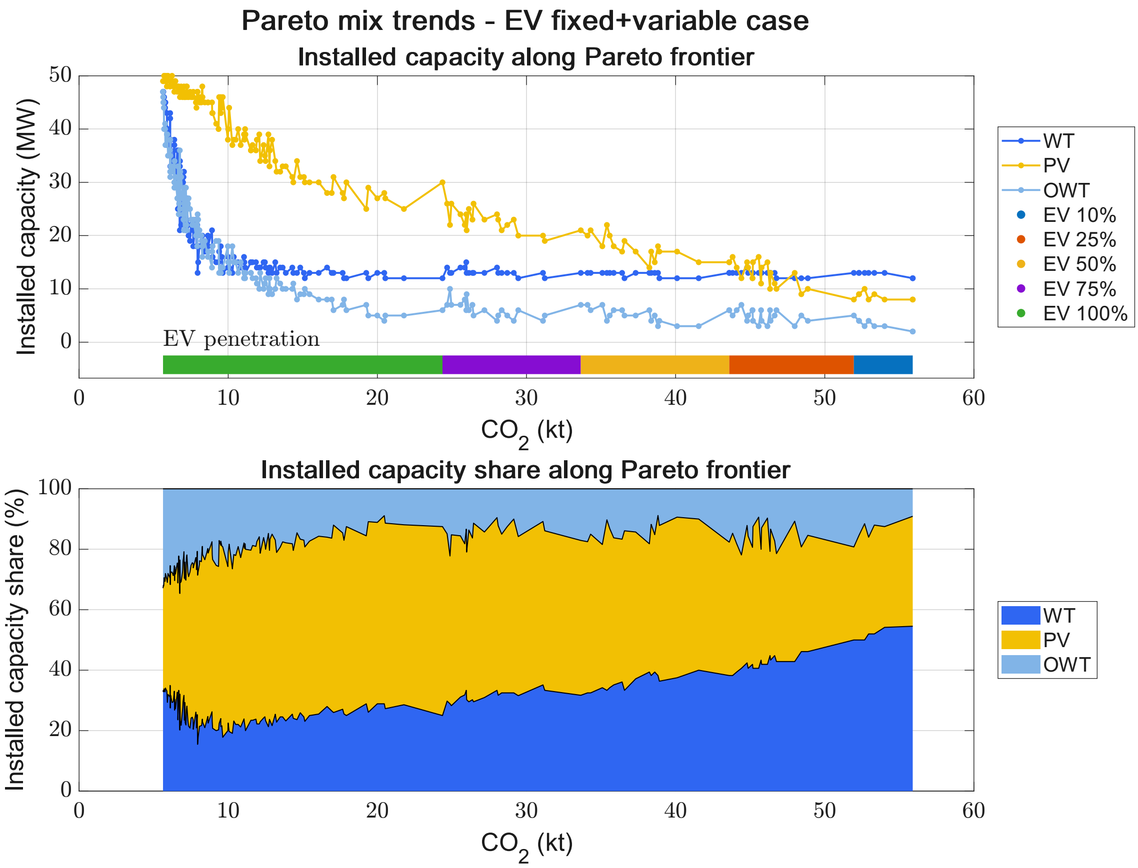

Figure 5.6: MATLAB-generated graph of the absolute installed capacity (top) and relative capacity share (bottom) of renewable technologies along the Pareto front.

In the high-emission/low-mismatch region (right side of the graph, above 40 kt of CO_2), the system relies on a moderate capacity installation. Here, Onshore Wind (WT) acts as the foundational baseload, maintaining a steady capacity of approximately 12 MW across almost the entire front. Its relative share in this region is dominant, covering roughly 50% of the installed mix, supported by a slightly lower capacity of Solar PV. Offshore wind (OWT) is almost absent in this phase, covering approximately 10% of the share, as its high deployment is not required to meet these less stringent environmental targets.

Moving into the central, intermediate region of the Pareto front (between 15 kt and 40 kt of CO_2), a massive expansion of Solar PV defines the system's architecture. The absolute capacity of PV grows steeply, fluctuating between 20 MW and 50 MW, and coming to represent the absolute majority of the system's capacity share (the wide yellow band). PV acts as the primary bulk generator for the island's daytime consumption and EV charging. However, because PV generation is strictly bound to daylight hours, relying on it to push emissions even lower causes the mismatch (ϕ) to grow rapidly, as the excess midday energy cannot be instantly absorbed.

To achieve deep decarbonization and reach the absolute minimum emissions (moving left on the graph, below 15 kt of CO_2), the required technological mix undergoes a radical shift. The capacity of Offshore Wind (OWT) experiences a sharp, exponential surge, rapidly escalating from just a few MWs to peak at the 50 MW upper bound. Interestingly, in this extreme low-emission region, all three energy sources are pushed to their maximum potential. As seen on the far left of the capacity plot, WT, PV, and OWT all converge towards the 50 MW limit, resulting in a condition where the three technologies have practically the same share (approximately 33% each). This clearly indicates that reaching absolute minimum emissions on La Gomera cannot be achieved merely by overbuilding a single source; it requires maximizing the diverse generation profiles of all available technologies to cover both diurnal and night-time loads, thereby eliminating the residual reliance on conventional diesel generators.

5.3 Discussion and limitations

5.3.1 System-level implications

The combined analysis of these results provides crucial systemic insights. Foremost, the value of the methodology developed in this thesis lies in proving that local demand management (smart charging) and island-scale energy transition are inseparable.

An increase in EV penetration is not simply an increase in electricity load, nor is it merely a reduction in transport emissions. It is both, and its ultimate effect depends on the energy system's capacity to absorb the new demand in combination with the available renewable sources. If the electrical load of 15,000 vehicles had been introduced into the system as an unmanaged, rigid demand, the temporal mismatch ϕ would have drastically penalized the high-EV scenarios. Instead, by integrating the optimized charging schedules, the EV fleet effectively functions as a distributed flexibility resource. By shifting the charging loads to match hours of abundant renewable generation, the system minimizes the need for fossil-fuel backup and curtails significantly less wind and solar energy. Therefore, EV charging must be treated structurally as a core component of the energy system, rather than as a generic additional load.

5.3.2 Limitations of the result interpretation

The interpretation of the results must be contextualized within the boundaries of the adopted workflow. First, the EV profiles integrated into EnergyPLAN derive from a synthetic model of vehicle behavior. Although this model was calibrated in terms of annual energy and constructed in a manner consistent with availability and capacity constraints, it does not represent a direct empirical measurement of driving and charging behaviors on La Gomera.

Second, the Pareto front inherently depends on the space of the variables explored. A different choice of bounds imposed on renewable capacities, or the inclusion of alternative storage technologies, could alter the geometry of the non-dominated front. Finally, this assessment evaluates technical trade-offs (mismatch vs. emissions) and operational energy costs, without incorporating a full economic investment model for the generation infrastructure. The results should therefore be viewed as a structured assessment of system behavior rather than a definitive financial forecast.

5.4 Conclusions of the chapter

This chapter demonstrated how the integration of smart EV charging profiles into the EnergyPLAN simulator allows for a comprehensive multi-objective exploration of La Gomera's energy future. The primary conclusion is that higher levels of electric vehicle penetration unequivocally improve the system's efficient frontier, thanks to the combined effect of eliminating fossil fuels in transportation and providing flexible load shifting to accommodate renewable generation.

A critical conclusion concerns the multi-objective nature of the problem. A single optimal valid solution in an absolute sense does not exist; instead, there is a set of efficient configurations defined by the trade-off between energy mismatch and CO_2. The analysis of the WT, PV, and OWT capacities along the Pareto front shows that the non-dominated points must be interpreted as complete system configurations, and not only as pairs of objective values. The Pareto front becomes interpretable only when linked to the decisional variables that generate it, proving that deep decarbonization requires a highly balanced mix, particularly leaning on offshore wind in the lowest emission scenarios.

As a whole, the chapter confirms the methodological sense of the thesis: connecting smart charging, annual EV profiles, EnergyPLAN simulation, and multi-objective optimization allows us to analyze electric mobility as an integral part of the insular energetic system. This reading prepares for the conclusive chapter, in which the main contributions of the study, the limits of the methodology, and possible future extensions will be addressed.

Chapter 6

Conclusions and future perspectives

This thesis analyzed the effects of the electrification of the transport sector on the energy systems of isolated communities, focusing on the case study of the island of La Gomera. To do so, a methodological framework was developed that linked two complementary levels of analysis: a demand management model developed in MATLAB and an energy system simulation model implemented in EnergyPLAN. The value of this integrated approach lies in its ability to link local charging profile generation with a system simulation, transforming the analysis of specific electricity demand into a systemic assessment of the island's energy transition.

At the local demand level, simulations conducted in MATLAB compared a basic FIFS strategy with a charging policy optimized using linear programming. The results confirmed that smart charging primarily acts as a mechanism for the temporal reallocation of load, capable of significantly reducing costs by shifting demand to the cheapest hours of the day, thereby mitigating peaks in renewable overproduction. Furthermore, the infrastructure sizing study highlighted that a ratio of charging ports to vehicles of approximately 8% represents the optimal trade-off between operational flexibility and cost containment.

At the system level, a multi-objective analysis has highlighted the dual role of electric mobility, which can increase electricity demand while reducing fossil fuel consumption in transportation. Although 100% EV penetration leverages the vehicle fleet as a flexible buffer to reduce absolute minimum emissions to below 10 kt, the analysis confirmed that there is no single, absolutely optimal scenario. Optimal solutions vary depending on the desired trade-off between minimizing CO_2 and reducing the energy mismatch between generation and demand.

The Pareto frontier analysis also demonstrated that efficient configurations do not rely on maximizing a single technology. Achieving the deepest levels of decarbonization requires a highly diversified and balanced mix of onshore wind, solar photovoltaics, and offshore wind to ensure system stability. In this context, the mismatch indicator (ϕ) proved its importance not as a direct economic metric, but as a measure of temporal consistency between renewable supply and demand. Overall, the methodological link between the two levels has demonstrated that the electrification of transportation must be treated structurally as a flexible and integral component of the energy transition, rather than as a mere additional and inflexible load.

Future perspectives

Despite the validity of the multiscale framework developed, the results have some inherent limitations that point to clear directions for future research.

On the demand-side modeling front, treating the island's entire charging infrastructure as a single aggregated entity represents a necessary modeling abstraction. In reality, large-scale EV adoption would likely lead to more heterogeneous charging dynamics. Therefore, future developments should move beyond this abstraction by incorporating a more granular modeling of user behavior, assessing the spatial distribution of charging stations across the territory, and utilizing real traffic data. Furthermore, a natural extension of the model would be to include a comprehensive economic analysis that also considers the infrastructure's investment and maintenance costs (CAPEX and OPEX).

Finally, from a systems analysis perspective, the geometry of the resulting Pareto frontiers is closely linked to the decision space explored and the predefined objectives. In this regard, future research could expand the GA multi-objective analysis by including the number of charging points as a variable, rather than maintaining it at the economically optimal fixed threshold identified in Chapter 3. Furthermore, future studies could analyze multiple indicators simultaneously to evaluate renewable configurations with respect to different parameters. A crucial extension would be to explicitly integrate the flexibility of storage systems into the simulations, or to integrate alternative technologies (such as V2G [19]), in order to assess grid stability in greater detail and support increasingly reliable long-term planning in island contexts.

Bibliography

[1] Calafiore, G. C., Ambrosino, L., Nguyen, K. M., Zorgati, R., Nguyen-Ngoc, D., & El Ghaoui, L. (2025). *Robust Power Scheduling for Smart Charging of Electric Vehicles.* In *2025 23rd European Control Conference (ECC).* Thessaloniki, Greece.

[2] Calafiore, G. C., & Ambrosino, L. (2025). *A Cohort-Based Optimization Model for Electric Vehicles Charging. IFAC PapersOnLine*, 59(9), 163–168.

[3] Jiménez, A., Cabrera, P., Medina, J. F., Østergaard, P. A., & Lund, H. (2024). *Smart energy system approach validated by electrical analysis for electric vehicle integration in islands. Energy Conversion and Management*, 302, 118121.

[4] Meschede, H., Child, M., & Breyer, C. (2018). *Assessment of sustainable energy system configuration for a small Canary island in 2030. Energy Conversion and Management*, 165, 363–372.

[5] Akbari-Dibavar, A., Sohrabi Tabar, V., Ghassem Zadeh, S., & Nourollahi, R. (2021). *Two-stage robust energy management of a hybrid charging station integrated with the photovoltaic system. International Journal of Hydrogen Energy*, 46, 12701–12714.

[6] Ambrosino, L., Zorgati, R., Calafiore, G., Nguyen-Ngoc, D., Nguyen, K. M., & El Ghaoui, L. (2024). *Optimizing electric vehicles charging through smart energy allocation and cost-saving.*

[7] Meschede, H., Hesselbach, J., Child, M., & Breyer, C. (2019). *On the impact of probabilistic weather data on the economically optimal design of renewable energy systems – a case study of La Gomera island. International Journal of Sustainable Energy Planning and Management*, 23, 15–26.

[8] Gracia Rosado, D. (2015). *Viabilidad técnica de la integración de generación renovable en la isla de La Gomera.* Trabajo Fin de Grado, Escuela de Ingeniería y Arquitectura, Universidad de Zaragoza.

[9] Ember. *European Wholesale Electricity Price Data.* Historical hourly Spanish wholesale day-ahead electricity prices used for the period April 2023 to March 2024. Accessed on 5 November 2025.

[10] Gobierno de Canarias, Dirección General de Energía, & Instituto Tecnológico de Canarias, S.A. (2023). *Plan de Transición Energética de Canarias (PTECan) – Versión inicial.* Las Palmas de Gran Canaria, Spain.

[11] Gobierno de Canarias, Consejería de Transición Ecológica y Energía. (2025). *Anuario Energético de Canarias 2023.*

[12] Instituto Canario de Estadística (ISTAC). *Pernoctaciones, viajeros alojados y entrados y estancia media según tipos de establecimientos turísticos, categorías y nacionalidades. Islas de Canarias por periodos.* Database.

[13] Cabrera, P., Lund, H., Thellufsen, J. Z., & Sorknæs, P. (2020). *The MATLAB Toolbox for EnergyPLAN: A tool to extend energy planning studies. Science of Computer Programming*, 191, 102405.

[14] Giorcelli, F., Cabrera, P., Paduano, B., Sirigu, S. A., & Mattiazzo, G. (2025). *Energy system co-design approach for WECs optimisation: the pendulum wave energy converter case study. Applied Energy*, 402, 126846.

[15] Giorcelli, F., De Clerck, V., & Pasta, E. (2026). *Assessing long-term metocean data variability for optimal energy system planning via static robust optimization approach. Applied Ocean Research*, 170, 105015.

[16] Iacono, I., Giorcelli, F., Spertino, F., & Cabrera, P. (2026). *From standalone to interconnected: Sector-coupled optimisation of La Gomera's renewable energy portfolio for integrated energy planning. Energy*, 345, 140249.

[17] Groppi, D., Nastasi, B., Prina, M. G., & Garcia, D. A. (2021). *The EPLANopt model for Favignana island's energy transition. Energy Conversion and Management*, 241, 114295.

[18] Rivera-Durán, Y., Berna-Escriche, C., Córdova-Chávez, Y., & Muñoz-Cobo, J.

L. (2023). *Assessment of a fully renewable generation system with storage to cost-effectively cover the electricity demand of standalone grids: The case of the Canary archipelago by 2040. Machines*, 11(1), 101.

[19] Lund, H., & Kempton, W. (2008). *Integration of renewable energy into the transport and electricity sectors through V2G. Energy Policy*, 36(9), 3578-3587.

[20] Lund, H., Thellufsen, J. Z., Østergaard, P. A., Sorknæs, P., Skov, I. R., & Mathiesen, B. V. (2021). *EnergyPLAN-advanced analysis of smart energy systems. Smart Energy*, 1, 100007.

[21] Richardson, D. B. (2013). *Electric vehicles and the electric grid: A review of modeling approaches, Impacts, and renewable energy integration. Renewable and Sustainable Energy Reviews*, 19, 247–254.

[22] Clement-Nyns, K., Haesen, E., & Driesen, J. (2010). *The impact of charging plug-in hybrid electric vehicles on a residential distribution grid. IEEE Transactions on Power Systems*, 25(1), 371–380.

[23] Sortomme, E., Hindi, M. M., MacPherson, S. D., & Venkata, S. S. (2011). *Coordinated charging of plug-in hybrid electric vehicles to minimize distribution system losses. IEEE Transactions on Smart Grid*, 2(1), 198–205.

[24] Hu, J., Morais, H., Sousa, T., & Lind, M. (2016). *Electric vehicle fleet management in smart grids: A review of services, optimization and control aspects. Renewable and Sustainable Energy Reviews*, 56, 1207–1226.

[25] Kuang, Y., Zhang, Y., Zhou, B., Li, C., Cao, Y., Li, L., & Zeng, L. (2016). *A review of renewable energy utilization in islands. Renewable and Sustainable Energy Reviews*, 59, 504–513.

[26] Mwasilu, F., Justo, J. J., Kim, E. K., Do, T. D., & Jung, J. W. (2014). *Electric vehicles and smart grid interaction: A review on vehicle to grid and renewable energy sources integration. Renewable and Sustainable Energy Reviews*, 34, 501–516.